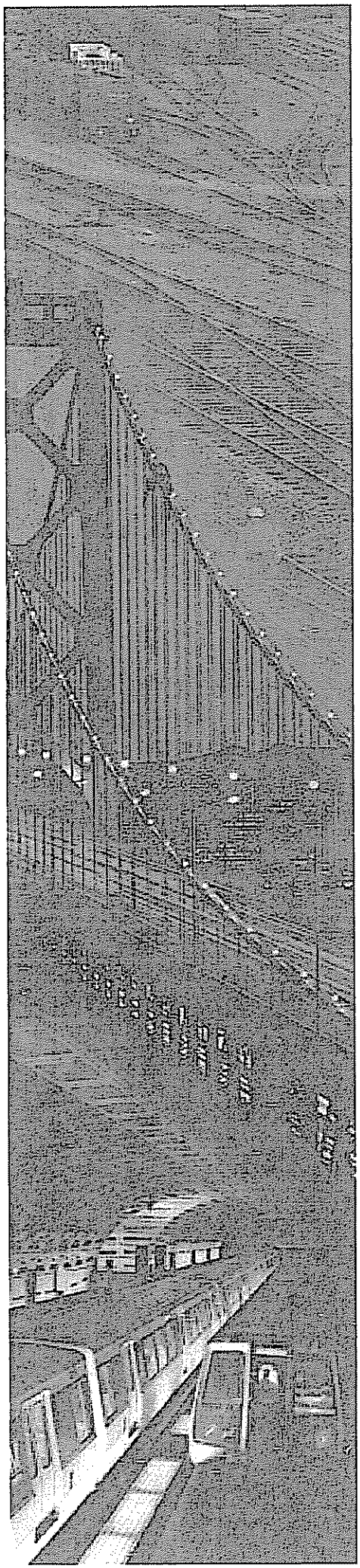

DCT 163

Design Study of Composite Sandwich Truck Tank Using a High-Order Sandwich Theory Approach

By

Jack R. Vinson
Department of Mechanical Engineering, University of Delaware

Ole T. Thomsen
Institute of Mechanical Engineering, Aalborg University

March 2003

Delaware Center for Transportation
University of Delaware
355 DuPont Hall
Newark, Delaware 19716
(302) 831-1446

The Delaware Center for Transportation is a university-wide multi-disciplinary research unit reporting to the Chair of the Department of Civil and Environmental Engineering, and is co-sponsored by the University of Delaware and the Delaware Department of Transportation.

DCT Staff

Ardeshir Faghri
Director

Jerome Lewis
Associate Director

Ellen Pletz
Assistant to the Director

Earl "Rusty" Lee
T² Program Coordinator

Matheu Carter
T² Engineer

Sandra Wolfe
Event Coordinator

DCT Policy Council

Natalie Barnhart, Co-Chair
Chief Engineer, Delaware Department of Transportation

Babatunde Ogunnaike, Co-Chair
Dean, College of Engineering

Delaware General Assembly Member
Chair, Senate Highways & Transportation Committee

Delaware General Assembly Member
Chair, House of Representatives Transportation/Land Use & Infrastructure Committee

Ajay Prasad
Professor, Department of Mechanical Engineering

Harry Shenton
Chair, Civil and Environmental Engineering

Michael Strange
Director of Planning, Delaware Department of Transportation

Ralph Reeb
Planning Division, Delaware Department of Transportation

Stephen Kingsberry
Executive Director, Delaware Transit Corporation

Shannon Marchman
Representative of the Director of the Delaware Development Office

James Johnson
Executive Director, Delaware River & Bay Authority

Holly Rybinski
Project Manager-Transportation, AECOM

Delaware Center for Transportation
University of Delaware
Newark, DE 19716
(302) 831-1446

CONTENTS

Chapter 1

INTRODUCTION

The use of sandwich structures is growing very rapidly around the world. Its many advantages, the development of new materials, and the need for high performance, low weight structures insure that sandwich construction will continue to be improved and have wider use. In the study herein, an improvement for the traditional truck tank by a sandwich structure is investigated, and parametric analysis to optimize this structure using different approaches are given and compared.

At present most if not all of the truck tanks used in the highway transportation of liquids, gases, and solids are a metallic monocoque (thin single walled) construction that acts structurally as a membrane. In general, such construction requires a large heavy keel (or a metallic undercarriage/chassis structure) to support the loaded container. Most of these tanks are either elliptical, or circular in cross-section, which is inefficient. A major improvement can be made through replacing these tanks with an advanced "boxy" tank design incorporating a fiber reinforced composite material sandwich construction. These tanks will involve four plates joined at each corner of the cross-section by a quarter of a circular shell, such that the overall width of the tank will not exceed the eight feet width limitation, and the overall height of the truck tank will not exceed the fourteen feet height limitation.

Sandwich construction typically consists of a core sandwiched between two faces, where the two faces are of a strong, stiff material and the core is a very lightweight material. In this design, the faces take most of the in-plane and bending

loads and the core acts as a spacer to hold the faces apart and to resist the transverse shear loads much the same as the web of an I-beam.

Although there are many variations on the basic form, most sandwich cores fall into four general categories shown in Figure 1.1: (1). honeycomb core, (2). foam or solid core, (3). web core and (4). truss core. This study will consider sandwiches of a foam core design. This type of sandwich construction is used extensively in the aerospace industry and is gaining popularity in the automotive and passenger rail industries.

The advantage to sandwich construction is in its superior ability to handle bending loads. For in-plane tension, compression and shear loads (not including buckling), a sandwich offers no improvement over a monocoque structure; however, when loaded in bending, for example, a sandwich with a core depth to face thickness ratio of 20 is shown [23] to have a flexural stiffness 300 times that of a monocoque of similar weight and when the sandwich is subjected to a bending moment, while the bending stresses will be 1/30 of those in the monocoque constructions. So the sandwich construction can bring about a dramatic reduction in weight when used for structures loaded in bending and provide enough flexural stiffness that hopefully will enable a truck tank to be completely self-supporting. Consequently, the traditional heavy keel structure (undercarriage/chassis) would be no longer necessary, and considerable reduction in structural weight can be achieved. The use of suitable composite materials for the sandwich faces will preclude maintenance (including painting) and salt deterioration.

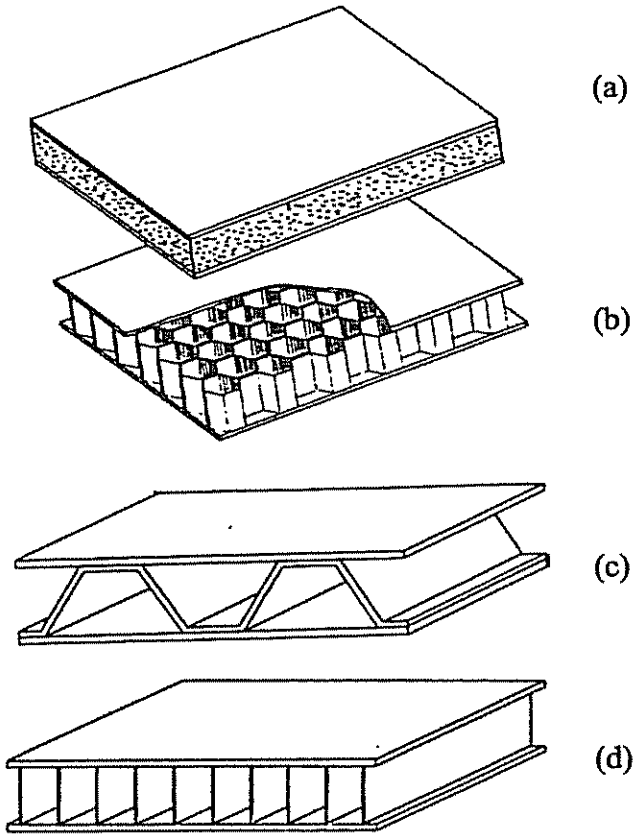

Figure 1.1 Types of Sandwich Construction

(a) foam core, (b) honeycomb core, (c) truss core, (d) web core

Most often, the two faces of a sandwich structure are identical in material and thickness, however, in special cases the faces may differ. In this study, the sandwich construction is assumed to be mid-plane asymmetric in order to suppress the bending stresses in the four corners through bending-stretching coupling (i.e. the B

matrix quantities in the stiffness matrix). This can be accomplished by having the faces of sandwich be of different thickness, and/or be of a different fiber orientation, and/or be of a different material. Thus, it will be easy to have the inner face be a material with little or no deterioration or reaction to the chemical or other attack by the load being carried, while the material of the outer face can be chosen to best withstand the outer environment. Figure 1.2 shows a schematic illustration of a self-supporting composite/sandwich shell truck tank. Such truck tanks will weigh a small fraction of the present structures, will be nearly maintenance free, and will have a lifetime much greater than the present tanks, thereby significantly reducing the cost of the truck fleet of DelDOT as well as increasing the efficiency of its operation.

Using a sandwich can also increases the natural vibration frequencies and overall buckling loads since these characteristics are a function of the bending stiffness.

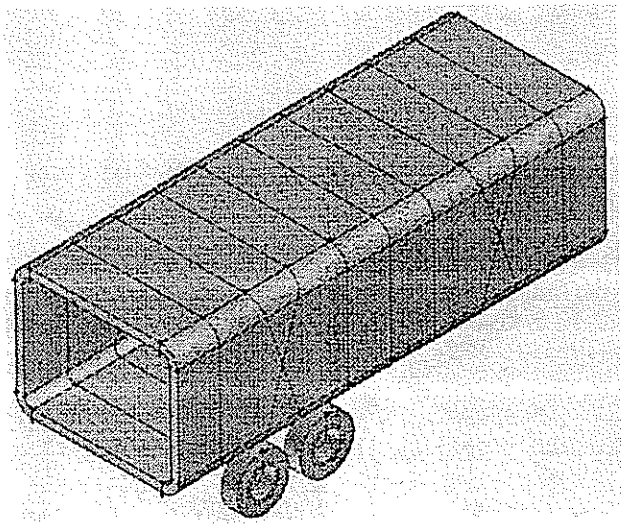

Figure 1.2 Conceptual Design of Boxy Composite/Sandwich Shell Truck Tank

1.1 Related Research

In most of the research that has been performed in the past, the sandwiches investigated were symmetrical about their mid-surface. The result is that there is no coupling between the responses to in-plane and bending loads. Asymmetric sandwiches are considerably more complicated to analyze due to their coupled behavior between in-plane and lateral responses. While in many cases a symmetric sandwich is desirable, an asymmetric sandwich is used in this study to achieve the advantages mentioned above.

A brief summary of some of the work that is related to the current research is presented below, with an emphasis on that involving an asymmetric sandwich configuration.

1.1.1 General Response Due to Simple Loading

As aircraft age, it is often necessary to repair fatigue cracks in various parts of the airframe. One of the methods used to reduce crack growth is to use a bonded composite patch. A paper published by Caisheng, Heller and Lam [5] in 1993 develops analytic solutions for an unbalanced (asymmetric) laminated panel subject to distributed shear loads on one face and an offset concentrated load at one end. This analysis could describe such a patch used to repair a fatiguing aircraft structure. The analysis assumes a plane strain condition and fiber directions of zero or ninety degrees. This configuration produces no bending/twisting or stretching/twisting coupling.

Monforton and Ibrahim [14] published a numerical solution for asymmetric composite plates using a double Fourier series expansion. It is assumed that the core is incompressible in the transverse direction and possesses no stiffness in the in-plane direction. The faces were considered to be asymmetric, cross-ply laminates with fibers in the zero and/or ninety degree direction. It was found that unlike thin plates, the coupling effects do not always reduce the stiffness of a sandwich plate. The coupling effects can cause an increase or decrease in the effective stiffness of a sandwich depending on the lay-up configuration, the material properties of the faces and core, the level of anisotropy of the face materials and the thickness of the core relative to that of the faces.

Satapathy and Vinson [16] investigated the optimization of asymmetric sandwich beams subject to a distributed lateral load and either clamped/clamped or simple/simple boundary conditions. They established a factor of merit by which different materials could be ranked in order of the weight required for an equal strength beam. It was found that the properties of Kevlar/epoxy in tension made it a good choice for the face experiencing tensile loading and the properties of carbon/epoxy in compression made it a likely choice for the compressed face.

1.1.2 Impact on An Asymmetric Sandwich

A paper published by Kwon and Fuller [13] investigated the effect of impact on the compressive failure behavior of asymmetric sandwich panels. The sandwich considered was composed of one titanium face and one glass reinforced plastic face with a Nomex honeycomb core. It was found that when the asymmetric sandwich beam was subjected to an impact on one face, the decrease in the compressive strength as a result of the damage sustained was very dependent on which

face was impacted. When the titanium face was subjected to the impact, the panel was 30% – 40% weaker.

1.1.3 Buckling and Elastic Stability

Sandwich beams in bending can experience local buckling of the face in compression. This is known as face wrinkling. Aiello and Ombres [1] investigated the critical face wrinkling loads for various face lay-ups. Since face wrinkling is a local phenomena, and the interaction between the faces is minimized for sandwiches with a large face thickness to core depth ratio, where overall asymmetry of the sandwich does not appreciably affect the face wrinkling loads. Aiello and Ombres [1] find that using a hybrid laminate made up of layers with different material properties through the thickness can increase the critical face-wrinkling load. A four-layer face was studied using a variety of stacking sequences. By using one outer layer of high stiffness composite material and three inner layers of a lower stiffness composite material next to the core, improvements in the wrinkling load are generally found when compared to a face of equal weight with all laminae made of the same material.

Vinson [22] performed a minimum weight optimization for sandwich panels with a variety of cores including foam, honeycomb, web and truss cores. This treatment takes into consideration compressive overstressing, overall buckling, face wrinkling, core shear instability, monocell dimpling (for honeycomb core), web and truss plate buckling. The optimum construction for in-plane compression and in-plane shear is determined for various boundary conditions.

Conflicting formulae have been proposed for the critical face-wrinkling load. Heath [11] derived an expression for the critical load that is dependent on the thickness of the face and that of the core in addition to the material properties. The

widely used equation developed by Hoff and Mautner [12] is dependent only on the face and core material properties but also includes a constant whose value is not agreed upon.

1.1.4 Higher Order Theories

In classical beam or plate theory, the strains are assumed to be small and the rotations are assumed to be very small, such that the higher order terms are sufficiently small that they may be neglected in order to simplify the equations. This simplification is relatively accurate for very small deflections but if the strains or rotations become too large, the geometric non-linearity becomes more important and the higher order terms are no longer negligible. Many researchers have looked at higher order theories for sandwich behavior and developed models that have a greater range of applicability.

Frostig, Baruch, Vilnay and Sheinman [9] and later Frostig and Shenhar [8], performed research on the bending of asymmetric sandwich beams that allowed for a transversely flexible core. A higher order theory was used to investigate the effect of three-point bending with pinned ends and a concentrated load in the middle of the span. Near the point load, there exist large stress concentrations and gradients and it can be seen that there is a noticeable deflection of the loaded face relative to the other face. This is an important effect to consider when investigating the effects of hard points, bulkheads, stiffeners, etc. or in the assessment of damage due to localized impact.

Shenhar, Frostig and Altus [17] further investigated sandwich beams subject to singular loading using a higher order theory that allows for asymmetric, orthotropic faces and a transversely flexible core. Stress maps and failure patterns are

generated for a beam in three-point bending. It is found that in the area near the application of the concentrated load, failure is often caused by behavior that cannot be explained by simple first order shear theories.

Bozhevolnaya and Frostig [4] developed a high-order solution for the analysis of curved sandwich panels that considers the geometric non-linearity of the deflection response. The model allows for the intermediate class of deflections so the rotations are not required to be very small. The deflections obtained with the non-linear solution show a slight attenuation when compared to a linear model. This 'stiffening spring' behavior is due to the geometric non-linearity in the problem. Of note is the fact that if the geometrically non-linear effects are ignored, the predicted deflection will be slightly greater and a linear solution is conservative when applied to a case where the maximum deflection is the primary restriction.

Frostig and Rabinovitch [10] investigated the behavior of sandwich panels that consist of a multi-skin construction and a multi-layered core layout.

Thomsen [21] developed a high-order theory for the analysis of arbitrary multiple layer plate assemblies with N high stiffness layers separated by (N-1) compliant interface layers. The theory includes the transverse flexibility of the interface layers, thus allowing the thickness of the multiple layer plate assembly to change during deformation. The theory provides a complete solution with respect to the solid laminate displacements, stress resultants and moment resultants, as well as the interface layer displacements, tansverse normal stresses and shear stresses.

A review of the papers written on the use of higher order theories for sandwich beam bending show that a simple first order shear theory is often not adequate to describe the behavior of the beam, asymmetric or not, near concentrated

loads, in the vicinity of restrictive boundary conditions, or in the presence of large transverse normal stresses.

1.1.5 Vibration

Qatu [15] studied the vibration of curved, laminated beams using a variational approach to determine the governing equations and boundary conditions. The responses to forced and free vibrations are characterized using classical beam theory for thin beams and first order shear deformation theory for moderately thick beams. The paper gives some insight as to the limitations of thin beam theory. It is found that when the fundamental natural frequency of the beam is calculated using both thick and thin beam theories, the difference is approximately 5 percent when the ratio of the beam height to length is 0.05. This is the point that is taken as the limit for the thin beam solution. As the thickness ratio increases beyond 0.05, the shear deformation plays a larger role and the difference between the theories increases noticeably.

The nonlinear oscillations of asymmetric composite beams were investigated by Singh and Rao [18] in order to better determine the natural frequencies under large deformations. The results show that the natural frequencies for asymmetric, laminated beams are lower than those predicted by linear theory when subject to small deflections and higher than the linear predictions for large amplitudes. The amplitudes are also found to be different in the positive and negative directions. Nonlinear analysis is therefore recommended for asymmetric laminates subject to dynamic loading.

1.1.6 Fatigue

Friction, fatigue and failure modes of a composite pressure vessel was presented by Wu, J.S., Zhu, X.Q. and Chen, G.L. [24]. The authors developed a new type of multiplayer wrapped composite thick-walled vessel that includes an inner cylinder and layer bearing loads by the layer friction. Also a theoretical mechanical model was established and the overall analyses were carried out and matched with experimental results.

1.2 Current Research

The effect of loading on fairly simple shapes of asymmetric sandwich construction is considered in several papers. The current research involves combining the solutions for straight beams and curved beams to analyze a more complicated shell structure. Analytical solutions are developed for constant as well as varying internal pressures, the resulting solutions are then subjected to a parametric optimization to obtain the lowest weight structure that meets the desired constraints.

The structure dealt with in this study is that of a truck tank shell that is axially asymmetric and is shown in Figure 1.3, the portion of the shell that is investigated is that which is far enough away from the ends and other restrictive supports as to be outside the shell bending boundary layer. In this region, it is assumed that all dependent variables do not vary in the shell axial direction. As a result, a two dimensional solution to a cross section can be used and the shell may be reduced to a complex set of beam problems. In the bending boundary layers, the presence of fasteners, bulkheads, variable boundary conditions, etc. will likely require the use of a finite element solution.

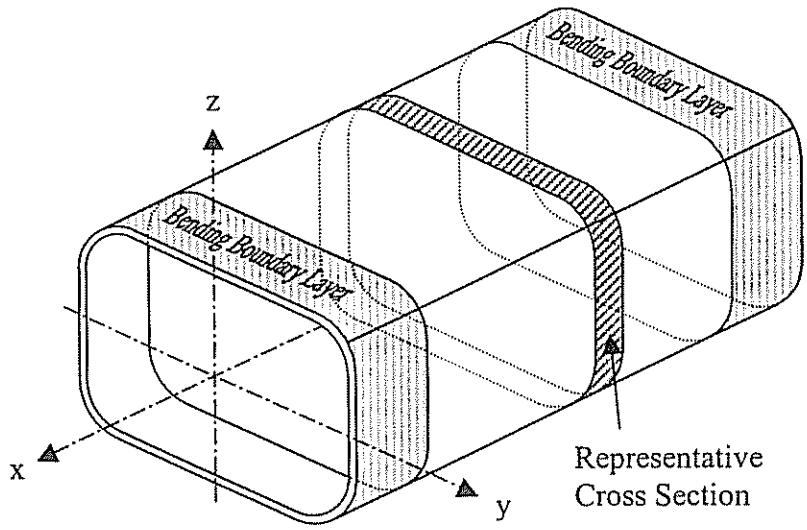

Figure 1.3 Bending Boundary Layers and a Cross Section being Analyzed

This construction is analyzed for two different situations, one filled with a gas giving a constant internal pressure, and the other filled with liquid that gives an internal pressure varying linearly with depth. This structure is geometrically symmetric about the vertical and horizontal axes, so when the constant internal pressure is under consideration, only a quarter of the cross section need to be analyzed; for the liquid internal pressure, since it is only symmetrical about the vertical axis, half of the cross section must be analyzed.

In an attempt to more efficiently utilize space inside a truck tank, it is desirable to use this cross section that is not circular. If a rectangular cross section were to be used, the resulting stress concentrations in the corners would likely result in a much heavier structure. A compromise is to use a rectangular cross section with rounded corners. The problem of constant internal pressure has been well analyzed by Forbes in his Master's thesis [26], so in the study herein, only the analysis for this

structure in the second situation is given, i.e. a linearly varying internal pressure. See Figure 1.4.

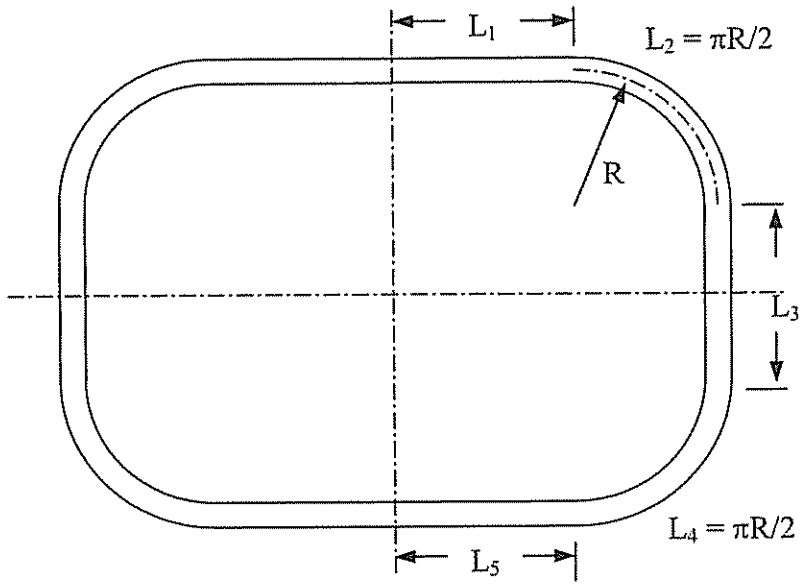

Figure 1.4 Cross Section of the Truck Tank

While the flat portions in the cross section will experience large bending loads when subject to an internal pressure, it is possible to minimize the increase in weight associated with the increased stresses by using an asymmetric sandwich. An analytic beam solution to the rectangular cross section with rounded corners will be obtained and the sandwich optimized for the lowest weight subject to various constraints. The solution will be sufficiently general to allow for an asymmetric sandwich, different materials in each face and will include the effects of transverse shear deformation.

Chapter Two will detail the problem and the development of the analytic solution. The governing equations, stress/strain and strain/displacement relationships will be developed. The loading and boundary conditions will be defined and the governing equations solved using Waterloo's Maple V software. Chapter Three will describe the Maple worksheet and its capabilities. In Chapter Four, parametric analysis will be performed on cross sections constructed from a sandwich with constant geometric and material properties. In Chapter Five, several factors that may affect the optimal structure and weight will be considered, different materials combinations will be optimized for comparison, and a preliminary study for variable geometry in the circumferential direction will be conducted.

Chapter 2

ANALYSIS OF THE PROBLEM

2.1 Basic Description

The problem of interest is that of a truck tank shell with a cross section that of a rectangle with rounded corners, it is composed of flat, plate sections at the top, bottom and on both sides, joined by circular, cylindrical shell sections at the corners.

The portion of the shell that will be investigated is that which is far enough from the ends and from any concentrated loads to consider this as a plane-strain problem in the axial direction. This shell will exhibit bending boundary layer type behavior near the ends, supports, etc. but that there will be no variation of any parameter in the axial direction outside this bending boundary layer. So the resulting problem is then a two-dimensional, plane-stress or plane-strain problem. If it is assumed that axial warping of the cross section is constrained so that plane cross sections remain plane after deformation, the problem becomes a plane-strain problem. The in-plane stress in the axial direction will vary around the cross section due to Poisson ration effects so it cannot be treated as a plane-stress problem.

The portion of interest can then be described as a thin piece taken from anywhere outside the bending boundary layers and away from any concentrated load. It is assumed that the truck tank is filled with liquid that gives internal pressure varying linearly with depth. This structure is symmetrical about the vertical and horizontal

axes, but the internal pressure is only symmetrical about the vertical axis, so half of the cross section must be analyzed. This plane-strain "slice" is taken to be of unit length in the axial direction.

Thus, the problem studied is that of a beam comprised of an upper straight horizontal section, followed by an upper curved section that covers an angle of ninety degrees, then a straight vertical section, a lower curved section covers the same angle and a lower straight horizontal section. Each of the sections is constructed as a sandwich made from a lower face, a core and an upper face. See Figure 2. 2.

The two faces are not necessarily made of the same material and do not have to be of the same thickness. It is possible to take advantage of the bending/stretching coupling resulting from the use of an asymmetric sandwich to reduce the maximum stresses experienced due to the internal pressure.

Flat sandwich plates or beams that are made with identical faces are straightforward to analyze since the responses to in-plane and lateral loads are uncoupled. Curved shells and beams, as well as flat sandwiches made with asymmetrical faces will experience coupling behavior when subjected to loading. In these cases, there will exist bending/stretching coupling behavior such that an in-plane load will produce both a lateral deflection and an in-plane displacement. Likewise, a lateral load will produce both in-plane displacement and lateral deflection. Bending/twisting, stretching/twisting, bending/shearing and stretching/shearing coupling are usually due to fiber reinforced composite faces with the fibers aligned at an angle to the principle directions of the sandwich.

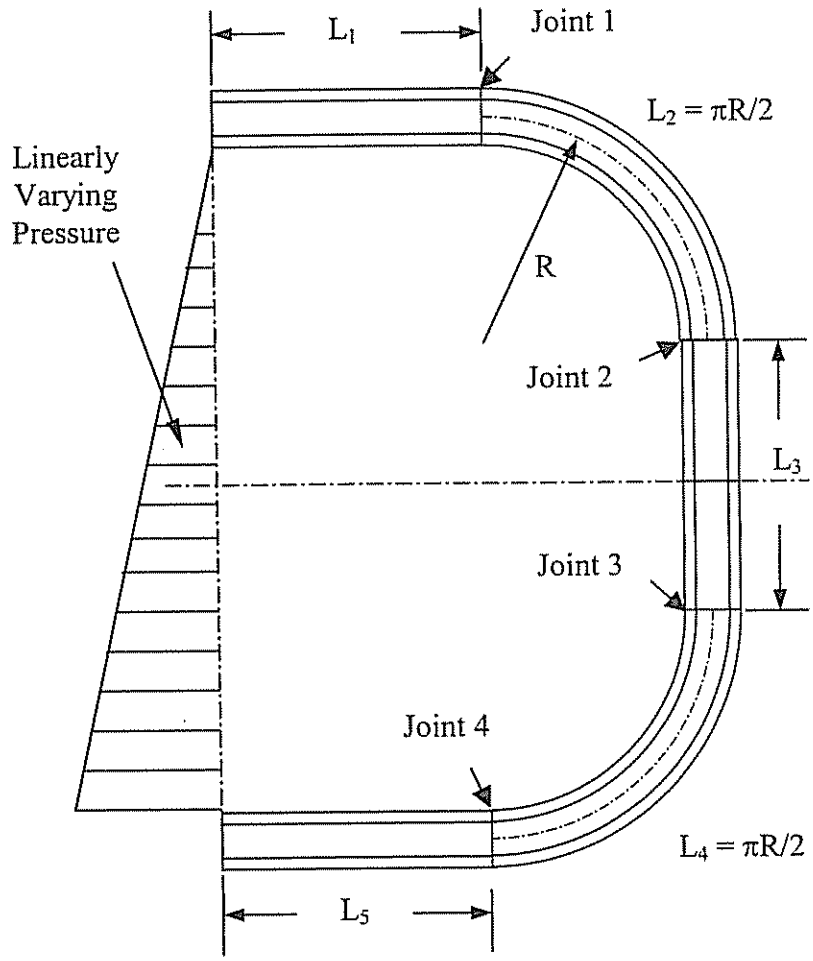

Figure 2.1 Half of Cross Section

The twisting and shearing interactions are used in structures such as wings or helicopter rotors to produce an effect known as aero-elastic tailoring. It is expected that they will not be allowed in the truck tank since they would produce undesirable effects. For example: a tank that bends upward when it is subject to positive torsion and bends downward when subject to negative torsion is likely to cause severe problems. As a result, the investigation presented here will consider sandwiches that

exhibit only bending/stretching coupling. Allowing only specially orthotropic materials (those with the material principle directions aligned with the geometric principle directions) will ensure this. Such materials could be unidirectional composites with the fibers aligned in either the axial or the 'hoop' direction, cross-ply composites with the fibers aligned in the zero and ninety degree directions, quasi-isotropic composites or isotropic metallic faces.

An asymmetric sandwich can be used to reduce deflection and/or weight in the following manner. Due to the geometry of the truck tank, the internal pressure produces both in-plane and moment resultants. By using an asymmetric sandwich, the lateral deflection caused by the bending moment can be partially offset by the coupling effects generated by the in-plane resultant. Alternately, if one face is being under-utilized; that is, if the maximum stress found in the face is less than the allowable stress, the face thickness can be reduced to save weight. Since the maximum loads in the faces will likely be different, one face will be thinner than the other resulting in an asymmetric sandwich.

Since the problem is not convenient to work with in a global coordinate system, a local coordinate system will be utilized. The coordinate system used will be an x, s, z system where x is the axial direction of the truck tank (normal to the cross section), z is the direction normal to the un-deformed mid-plane of the sandwich and s is the direction tangent to the un-deformed mid-plane of the sandwich, normal to the x and the z directions. The origin for the s coordinate is the top center of the truck tank and the origin for the z coordinate is the mid-plane of the sandwich (note that this may not be the mid-plane of the core).

For this study, the sign conventions are as the following and shown in Figure 2.2: tensile in-plane stresses are considered positive and compressive stresses are negative; a positive moment causes a concave-down curvature and a positive transverse shear stress acts in the positive z direction on a face with a normal vector in the positive s direction.

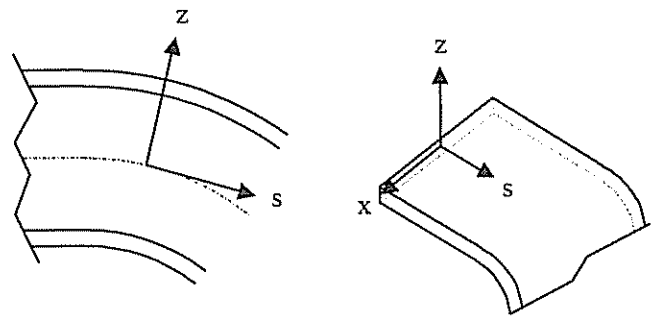

Figure 2.2 Local Coordinate System

2.2 Strain/Displacement Relations

It is assumed that the simplified structure behaves as a Timoshenko beam. A lineal element through the thickness of the sandwich, normal to the un-deformed mid-plane will undergo, at most, a translation and a rotation. The effect of transverse shear deformation will be included, so the element may not remain normal to the mid-plane after deformation. It is also assumed that there is no stretching or shrinking of the element; that is, there is no strain in the z direction and that the normal stress, σ_z is negligible. The result of the above assumptions is that the in-plane strains are linearly

distributed through the thickness of the sandwich and the displacement at any point can be related to the displacement at the mid-plane by the following relationship.

$$u(x,s,z) = u_0(x,s) + z\beta_x(x,s,z) \tag{2.1}$$

$$v(x,s,z) = v_0(x,s) + z\beta_s(x,s,z) \tag{2.2}$$

$$w(x,s,z) = w(x,s) \tag{2.3}$$

The displacements u, v and w correspond to the x, s and z directions. β is the rotation of the element from its un-deformed state. The strains at the mid-plane can be given by

$$\varepsilon_x^0(s) = \frac{\partial u_0}{\partial x} \tag{2.4}$$

$$\varepsilon_s^0(s) = \frac{\partial v_0}{\partial s} \tag{2.5}$$

$$\varepsilon_z = 0 \tag{2.6}$$

$$\varepsilon_{xs}^0 = \frac{1}{2}\left(\frac{\partial u_0}{\partial s} + \frac{\partial v_0}{\partial x}\right) \tag{2.7}$$

$$\varepsilon_{xz} = \frac{1}{2}\left(\beta_x + \frac{\partial w}{\partial x}\right) \tag{2.8}$$

$$\varepsilon_{sz} = \frac{1}{2}\left(\beta_s + \frac{\partial w}{\partial s} - \frac{v_0}{R}\right) \tag{2.9}$$

R is the radius of curvature of the structure in the s-z plane. To find ε_{sz} in a plate section, we can set R equal to infinity. The transverse shear strains do not need to be related to the mid-plane value since they are necessarily constant through thickness due to the assumption that the lineal element remains straight. Since it is assumed that no parameter varies in the x direction, all the x derivatives are zero. Although in reality there may be some warping of the cross sections, it is expected that

such warping will be small enough that the cross section can be assumed to remain plane; therefore, $\partial u_0 / \partial s = 0$.

2.3 Stress/Strain Relations and Stress Resultants

The general formula for the stress/strain relationship, ignoring hygrothermal effects and before applying the simplifications discussed above is:

$$\begin{Bmatrix} \sigma_x \\ \sigma_s \\ \sigma_z \\ \sigma_{sz} \\ \sigma_{xz} \\ \sigma_{xs} \end{Bmatrix} = \begin{bmatrix} \overline{Q}_{11} & \overline{Q}_{12} & \overline{Q}_{13} & 0 & 0 & 2\overline{Q}_{16} \\ \overline{Q}_{12} & \overline{Q}_{22} & \overline{Q}_{23} & 0 & 0 & 2\overline{Q}_{26} \\ \overline{Q}_{13} & \overline{Q}_{23} & \overline{Q}_{33} & 0 & 0 & 2\overline{Q}_{36} \\ 0 & 0 & 0 & 2\overline{Q}_{44} & 2\overline{Q}_{45} & 0 \\ 0 & 0 & 0 & 2\overline{Q}_{45} & 2\overline{Q}_{55} & 0 \\ 2\overline{Q}_{16} & 2\overline{Q}_{26} & 2\overline{Q}_{36} & 0 & 0 & 2\overline{Q}_{66} \end{bmatrix} \begin{Bmatrix} \varepsilon_x \\ \varepsilon_s \\ \varepsilon_z \\ \varepsilon_{sz} \\ \varepsilon_{xz} \\ \varepsilon_{sx} \end{Bmatrix} \tag{2.10}$$

The $\overline{Q}_{ij}$ values are the material properties, transformed as second order tensors from the principle material coordinate system to the x, s, z coordinate system.

$$\left[\overline{Q}\right] = [T]^{-1}[Q][T] \tag{2.11}$$

Where

$$Q_{11} = \frac{E_{11}}{(1 - \nu_{12}\nu_{21})} \quad Q_{22} = \frac{E_{22}}{(1 - \nu_{12}\nu_{21})} \quad Q_{12} = Q_{21} = \frac{\nu_{21}E_{11}}{(1 - \nu_{12}\nu_{21})} \tag{2.12}$$

$$Q_{44} = G_{23} \quad Q_{55} = G_{13} \quad Q_{66} = G_{12} \tag{2.13}$$

In this case, where only specially orthotropic materials are allowed:

$$\overline{Q}_{66} = Q_{66} \tag{2.14}$$

$$\overline{Q}_{16} = \overline{Q}_{26} = \overline{Q}_{36} = \overline{Q}_{45} = 0 \tag{2.15}$$

For laminae with fibers aligned in the axial direction:

$$\overline{Q}_{ii} = Q_{ii} \quad (i = 1,2 \text{ and } 4,5) \tag{2.16}$$

and for laminae with fibers aligned in the hoop direction:

$$\overline{Q}_{ii} = Q_{jj} \quad (i = 1,2 \text{ and } 4,5), (j = 2,1 \text{ and } 5,4) \tag{2.17}$$

The loading in this study is limited to an internal pressure with no torsion loads present; therefore, $\sigma_{xs} = \varepsilon_{xs} = 0$. When equation (2.10) is simplified for a specially orthotropic laminate and the assumptions made regarding the strains are applied, the stress/strain relation for this study becomes the following with the stresses written in terms of the mid-plane strains where appropriate:

$$\begin{Bmatrix} \sigma_x \\ \sigma_s \\ \sigma_{sz} \\ \sigma_{xz} \end{Bmatrix} = \begin{bmatrix} \overline{Q}_{11} & \overline{Q}_{12} & 0 & 0 \\ \overline{Q}_{12} & \overline{Q}_{22} & 0 & 0 \\ 0 & 0 & 2\overline{Q}_{44} & 0 \\ 0 & 0 & 0 & 2\overline{Q}_{55} \end{bmatrix} \begin{Bmatrix} \varepsilon_x^0 \\ \varepsilon_s^0 + z\partial\beta_s / \partial s \\ \varepsilon_{sz} \\ \varepsilon_{xz} \end{Bmatrix} \tag{2.18}$$

Since a two faces, single core sandwich can be treated as a three-layer laminate, the traditional A, B, D stiffness matrix formulation is employed. The vectorial distance from the mid-plane to the top of the kth lamina is h_k.

$$A_{ij} = \sum_{k=1}^{3} \left(\overline{Q}_{ij}\right)_k \left[h_k - h_{k-1}\right] \quad (i,j = 1,2,6) \tag{2.19}$$

$$B_{ij} = \frac{1}{2}\sum_{k=1}^{3} \left(\overline{Q}_{ij}\right)_k \left[h_k^2 - h_{k-1}^2\right] \quad (i,j = 1,2,6) \tag{2.20}$$

$$D_{ij} = \frac{1}{3}\sum_{k=1}^{3} \left(\overline{Q}_{ij}\right)_k \left[h_k^3 - h_{k-1}^3\right] \quad (i,j = 1,2,6) \tag{2.21}$$

$$A_{ij} = \frac{5}{4}\sum_{k=1}^{3} \left(\overline{Q}_{ij}\right)_k \left[h_k - h_{k-1} - \frac{4}{3}\left(h_k^3 - h_{k-1}^3\right)\frac{1}{\left(h_3 - h_0\right)^2}\right] \quad (i,j = 4,5) \tag{2.22}$$

Finally, an expression can be written for the stress and moment resultants.

$$\left[\begin{array}{c} N_x \\ N_s \\ N_{xs} \\ \hline M_x \\ M_s \\ M_{xs} \end{array}\right] = \left[\begin{array}{ccc:ccc} A_{11} & A_{12} & 2A_{16} & B_{11} & B_{12} & 2B_{16} \\ A_{12} & A_{22} & 2A_{26} & B_{12} & B_{22} & 2B_{26} \\ A_{16} & A_{26} & 2A_{66} & B_{16} & B_{26} & 2B_{66} \\ \hdashline B_{11} & B_{12} & 2B_{16} & D_{11} & D_{12} & 2D_{16} \\ B_{12} & B_{22} & 2B_{26} & D_{12} & D_{22} & 2D_{26} \\ B_{16} & B_{26} & 2B_{66} & D_{16} & D_{26} & 2D_{66} \end{array}\right] \left[\begin{array}{c} \varepsilon_x^0 \\ \varepsilon_s^0 \\ \varepsilon_{xs}^0 \\ \hline \kappa_x \\ \kappa_s \\ \kappa_{xs} \end{array}\right] \tag{2.23}$$

$$Q_x = 2\left(A_{45}\varepsilon_{sz} + A_{55}\varepsilon_{xz}\right) \quad Q_s = 2\left(A_{44}\varepsilon_{sz} + A_{45}\varepsilon_{xz}\right) \tag{2.24}$$

where the curvatures are written as

$$\kappa_x = \frac{\partial \beta_x}{\partial x} \quad \kappa_s = \frac{\partial \beta_s}{\partial s} \quad \kappa_{xs} = \frac{1}{2}\left(\frac{\partial \beta_x}{\partial s} + \frac{\partial \beta_s}{\partial x}\right) \tag{2.25}$$

From the plane strain assumption and the use of specially orthotropic materials

$$A_{45} = \beta_x = \kappa_x = \kappa_{xs} = \varepsilon_{xs}^0 = \varepsilon_{xz} = M_{xs} = N_{xs} = Q_x = \varepsilon_x = 0 \tag{2.26}$$

Since stretching/shearing coupling is not allowed, A_{16} and A_{26} must be zero. Likewise, because the bending/shearing and twisting/stretching coupling is zero, the B_{16} and B_{26} terms must be zero and the lack of bending/twisting coupling requires that D_{16} and D_{26} be zero. Using these simplifications in (2.23) and (2.24) yields:

$$\left[\begin{array}{c} N_x \\ N_s \\ \hline M_x \\ M_s \end{array}\right] = \left[\begin{array}{cc:cc} A_{11} & A_{12} & B_{11} & B_{12} \\ A_{12} & A_{22} & B_{12} & B_{22} \\ \hline B_{11} & B_{12} & D_{11} & D_{12} \\ B_{12} & B_{22} & D_{12} & D_{22} \end{array}\right] \left[\begin{array}{c} 0 \\ \varepsilon_s^0 \\ \hline 0 \\ \kappa_s \end{array}\right] \tag{2.27}$$

$$Q_s = 2A_{44}\varepsilon_{sz}$$

Now substituting the strain/displacement relations from section 2.5 into (2.27), the simplified equations for the resultants can be written in terms of the displacements

$$N_x = A_{12}\left[\frac{\partial v_0}{\partial s} + \frac{w}{R}\right] + B_{12}\frac{\partial \beta_s}{\partial s}$$

$$N_s = A_{22}\left[\frac{\partial v_0}{\partial s} + \frac{w}{R}\right] + B_{22}\frac{\partial \beta_s}{\partial s}$$

$$M_x = B_{12}\left[\frac{\partial v_0}{\partial s} + \frac{w}{R}\right] + D_{12}\frac{\partial \beta_s}{\partial s}$$

$$M_s = B_{22}\left[\frac{\partial v_0}{\partial s} + \frac{w}{R}\right] + D_{22}\frac{\partial \beta_s}{\partial s}$$

$$Q_s = A_{44}\left[\beta_s + \frac{\partial w}{\partial s} - \frac{v_0}{R}\right]$$

$$Q_x = M_{xs} = N_{xs} = 0 \qquad (2.28)$$

2.4 Governing Equations

Now the governing equations can be written in terms of the resultants. Starting with the equilibrium equations for a circular cylindrical shell in the x, s, z coordinate system, the shell equations can be reduced to those for a plate by setting R equal to ∞ as above. For equilibrium to be maintained:

$$\sum F_x = \frac{\partial N_x}{\partial x} + \frac{\partial N_{xs}}{\partial s} + q_x = 0$$

$$\sum F_s = \frac{\partial N_{xs}}{\partial x} + \frac{\partial N_s}{\partial s} + \frac{Q_s}{R} + q_s = 0$$

$$\sum F_z = \frac{\partial Q_x}{\partial x} + \frac{\partial Q_s}{\partial s} - \frac{1}{R} N_s + p(x,s) = 0 \qquad (2.29)$$

$$\sum M_{//s} = \frac{\partial M_x}{\partial x} + \frac{\partial M_{xs}}{\partial s} - (Q_x - m_x) = 0$$

$$\sum M_{//x} = \frac{\partial M_{xs}}{\partial x} + \frac{\partial M_s}{\partial s} - (Q_s - m_s) = 0$$

where q_x, q_s, m_x, and m_s are functions of the surface shear stresses and $p(x,s)$ is a distributed lateral load. Since the surface shear stresses are zero for this analysis, they will be omitted from this point on. Simplifying for the plane strain case with no surface shear stresses and a hydraulic internal pressure p, the equilibrium equations in the s, z plane can be written as

$$\frac{\partial N_s}{\partial s} + \frac{Q_s}{R} = 0 \qquad \frac{\partial M_s}{\partial s} - Q_s = 0$$

$$\frac{\partial Q_s}{\partial s} - \frac{1}{R} N_s + p = 0 \qquad (2.30)$$

Note that for constant internal pressure $p = p_0$; for liquid internal pressure $p = \rho_{liquid} g h$, where ρ_{liquid} is the mass density and g is the gravitational constant. h will be specified respectively for different sections.

In terms of the displacements, (2.30) can be written as

$$A_{22}\left[\frac{\partial^2 v_0}{\partial s^2}+\frac{1}{R}\frac{\partial w}{\partial s}\right]+B_{22}\frac{\partial^2 \beta_s}{\partial s^2}+\frac{A_{44}}{R}\left[\beta_s+\frac{\partial w}{\partial s}-\frac{v_0}{R}\right]=0$$

$$B_{22}\left[\frac{\partial^2 v_0}{\partial s^2}+\frac{1}{R}\frac{\partial w}{\partial s}\right]+D_{22}\frac{\partial^2 \beta_s}{\partial s^2}-A_{44}\left[\beta_s+\frac{\partial w}{\partial s}-\frac{v_0}{R}\right]=0 \qquad (2.31)$$

$$A_{44}\left[\frac{\partial \beta_s}{\partial s}+\frac{\partial^2 w}{\partial s^2}-\frac{1}{R}\frac{\partial v_0}{\partial s}\right]-\frac{1}{R}\left[A_{22}\left(\frac{\partial v_0}{\partial s}+\frac{w}{R}\right)+B_{22}\frac{\partial \beta_s}{\partial s}\right]+p=0$$

Equation (2.31) is the set of governing equations for a circular, cylindrically curved, laminated shell in the s, z plane, allowing for an asymmetric stacking sequence and assuming a constant strain ε_x in the x direction. The equations are in terms of three unknown functions; w, v_0, and β_s.

At this point, the assumptions used herein to obtain the governing equations will be reviewed.

- Shell cross section to be analyzed is outside the bending boundary layer.
- Plane cross sections of the shell remain plane after deformation.
- No properties except u_0 vary in the x direction.
- $\varepsilon_x = 0$.
- Euler beam behavior: a lineal element through the thickness of the sandwich, normal to the un-deformed mid-plane will undergo, at most, a translation and a rotation. This requires that $\varepsilon_z = 0$ and $\sigma_z \approx 0$.
- Small displacements and rotations.
- h << R. Love's first approximation: the thickness of the sandwich is much smaller than the radius of curvature.

- No thermal or hygrothermal effects.
- Specially orthotropic materials.
- Displacement Functions For The Sandwich Beam Using First Order Shear Deformation Theory

2.5 Displacement Functions for an Asymmetric Sandwich

The solution to the set of governing equations is obtained here by using Waterloo Maple's *Maple V, release 5* mathematical software package. All further mathematical analysis is also performed using Maple. Equation (2.31) is the set governing equations for an asymmetric, curved beam under plane strain conditions. It is a set of three differential equations in three functions of s: $w(s)$, $v_0(s)$ and $\beta_s(s)$. Since it is assumed that there is no variation in x, the system of partial differential equations becomes a system of ordinary differential equations and may be readily solved using Maple. The solutions are given respectively for the five sections.

2.5.1 Upper Horizontal Section (0<s<L1)

The beam of this section does not undergo any loading because the liquid is not pressurized. But for generality, a constant pressure $p = p_0$ is taken into account, which can be set to zero in the present case, and R is set to infinity in this section. The general solutions are:

$$w_1(s) = \frac{p_0}{24\overline{\overline{D}}} s^4 + C_{14}s^3 + C_{13}s^2 + C_{12}s + C_{11} \tag{2.32}$$

$$v_1(s) = \frac{p_0}{6\overline{\overline{B}}} s^3 + \frac{B_{22}\left(3C_{14}s^2 + 2C_{13}s + C_{12}\right)}{A_{22}} + C_{16}s + C_{15} \tag{2.33}$$

$$\beta_1(s) = -\frac{p_0}{6\overline{\overline{D}}} s^3 - \frac{p_0}{A_{44}} s - \frac{6C_{14}\overline{D}}{A_{44}} - 3C_{14}s^2 - 2C_{13}s - C_{12} \tag{2.34}$$

where $\overline{B}$ and $\overline{D}$ are the reduced stiffnesses defined by Whitney (1987) and are will be used in the following equations:

$$\overline{B} = \frac{D_{22}A_{22} - B_{22}^2}{B_{22}} \tag{2.35}$$

$$\overline{D} = \frac{D_{22}A_{22} - B_{22}^2}{A_{22}} \tag{2.36}$$

2.5.2 Upper Curved Section (L1<s<L1+L2)

In this section the pressure varies with the depth, which can be expressed as $h = R(1-\cos\theta)$, as shown in Figure 2.3, and approximately, we can use $\theta = \frac{s}{R}$, then the pressure is $p = p_0 + \rho_{liquid} gR(1-\cos\theta)$. The general solutions are:

$$
\begin{aligned}
w_2(s) = & -\frac{B_{22}}{A_{22}R}C_{22} - C_{22} + C_{23}\sin\theta - C_{24}\cos\theta + C_{25}\theta\sin\theta - C_{26}\theta\cos\theta \\
& + [\frac{2}{A_{22}R\Sigma}(B_{22}^3 - 2B_{22}^2 A_{44}R - B_{22}A_{44}D_{22}) + \frac{2D_{22}A_{44}}{\Sigma} - \frac{2D_{22}B_{22}}{R\Sigma} \\
& + \frac{B_{22}}{A_{22}R} - 1](C_{25}\cos\theta + C_{26}\sin\theta) + \frac{R^2 p_0}{A_{22}} \\
& + \rho_{liquid}gR^3\{\theta^2\cos\theta[\frac{A_{22}D_{22} - B_{22}^2}{8A_{44}\Sigma} + \frac{D_{22} + A_{22}R^2 + 2B_{22}R}{4\Sigma} \\
& + \frac{1}{8\Sigma}(\frac{4A_{44}D_{22}R}{\overline{B}} + \frac{A_{22}A_{44}R^4}{\overline{D}} + \frac{4A_{22}A_{44}R^3}{\overline{B}} + \frac{2A_{44}D_{22}R^2}{\overline{D}} \\
& + \frac{4A_{44}B_{22}R^2}{\overline{B}} + \frac{A_{44}D_{22}^2}{\overline{D}A_{22}})] - \cos\theta[\frac{3(A_{22}D_{22} - B_{22}^2)}{4A_{44}\Sigma} \\
& + \frac{13D_{22} + 6A_{22}R^2 + 19B_{22}R}{4\Sigma} + \frac{1}{4\Sigma}(\frac{29A_{44}D_{22}R}{\overline{B}} + \frac{9A_{44}D_{22}R^2}{\overline{D}} \\
& + \frac{22A_{44}B_{22}R^2}{\overline{B}} + \frac{15A_{22}A_{44}R^3}{\overline{B}} + \frac{3A_{22}A_{44}R^4}{\overline{D}} + \frac{10A_{44}D_{22}^2}{\overline{D}A_{22}})] \\
& - \theta\sin\theta[\frac{A_{22}D_{22} - B_{22}^2}{2A_{44}\Sigma} + \frac{3D_{22} + 2A_{22}R^2 + 5B_{22}R}{2\Sigma} \\
& + \frac{1}{2\Sigma}(\frac{A_{22}A_{44}R^4}{\overline{D}} + \frac{7A_{44}D_{22}R}{\overline{B}} + \frac{5A_{22}A_{44}R^3}{\overline{B}} + 6\frac{22A_{44}B_{22}R^2}{\overline{B}} \\
& + \frac{3A_{44}D_{22}R^2}{\overline{D}} + \frac{2A_{44}D_{22}^2}{\overline{D}A_{22}})]\} + \frac{\rho_{liquid}gR^3}{A_{22}}
\end{aligned}
\tag{2.37}
$$

$$
\begin{aligned}
v_2(s) = & C_{21} + C_{22}\theta + C_{23}\cos\theta + C_{24}\sin\theta + C_{25}\theta\cos\theta + C_{26}\theta\sin\theta \\
& - \rho_{liquid}gR^3\left[\frac{1}{8A_{44}} + \frac{R}{4\overline{B}} + \frac{R^2}{8\overline{D}} + \frac{D_{22}}{8(A_{22}D_{22} - B_{22}^2)}\right] \\
& \times(\theta^2\sin\theta + 6\theta\cos\theta - 12\sin\theta)
\end{aligned}
\tag{2.38}
$$

$$\beta_2(s)=\frac{1}{R}(C_{21}+C_{22}\theta)-2\frac{A_{44}(B_{22}+A_{22}R)}{\Sigma}(C_{25}\sin\theta-C_{26}\cos\theta)$$
$$-\frac{\rho_{liquid}gR^3}{4\Sigma}[2\theta\cos\theta(A_{22}R+B_{22}+\frac{A_{44}D_{22}+3R^2A_{22}A_{44}+2RA_{44}B_{22}}{\overline{B}}$$
$$+\frac{R^3A_{22}A_{44}+RA_{44}D_{22}}{\overline{D}})-\sin\theta(9A_{22}R+9B_{22}+\frac{5R^3A_{22}A_{44}+9RA_{44}D_{22}}{\overline{D}}$$
$$+\frac{9A_{44}D_{22}+19R^2A_{22}A_{44}+14RA_{44}B_{22}}{\overline{B}})] \quad (2.39)$$

where

$$\Sigma=D_{22}A_{22}+A_{44}R^2A_{22}+D_{22}A_{44}-B_{22}^2+2B_{22}A_{44}R \quad (2.40)$$

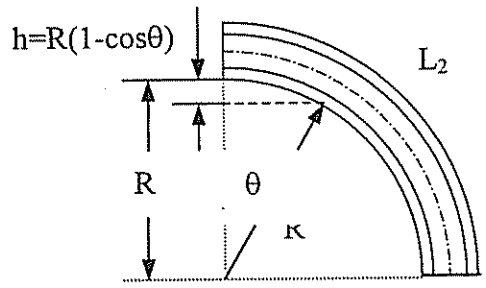

Figure 2.3 *h* of the Upper Curved Section

2.5.3 Vertical Section (L1+L2<s<L1+L2+L3)

The load in this section varies as a linear function of the coordinate s (between joint 2 and 3), $h=s+R$, and $p=p_0+\rho_{liquid}g(s+R)$. Since $\rho_{liquid}gR$ is a constant value, we can use $p_{01}=p_0+\rho_{liquid}gR$, and then $p=p_{01}+\rho_{liquid}gs$. By setting $R=\infty$ in the governing equations, the general solutions can be obtained as:

$$w_3(s) = C_{31} + C_{32}s + C_{33}s^2 + C_{34}s^3 + \frac{p_{01}s^4}{24\overline{D}} + \frac{\rho_{liquid}gs^5}{120\overline{D}} \tag{2.41}$$

$$v_3(s) = \frac{B_{22}}{A_{22}}(C_{32} + 2C_{33}s + 3C_{34}s^2) + C_{35} + C_{36}s + \frac{s^3}{24\overline{B}}[\rho gs + 4p_{01}] + \frac{\rho_{liquid}gs^2B_{22}}{2A_{22}A_{44}} \tag{2.42}$$

$$\beta_3(s) = -(C_{32} + 2C_{33}s + 3C_{34}s^2) - \frac{6\overline{D}}{A_{44}}C_{34} - \frac{p_{01}s^3}{6\overline{D}} - \frac{p_{01}s}{A_{44}} - \rho_{liquid}g\left(\frac{\overline{D}}{A_{44}^2} + \frac{s^2}{2A_{44}} + \frac{s^4}{24\overline{D}}\right) \tag{2.43}$$

2.5.4 Lower Curved Section (L1+L2+L3<s<L1+L2+L3+L4)

Similar to section 2, the pressure in this section varies with the depth, which can be approximated as $h = R + L_3 + R\sin\theta$, shown in Figure 2.4, where $\theta = \frac{s}{R}$, and so the pressure is $p = p_0 + \rho_{liquid}g(R + L_3 + R\sin\theta)$. Since here R and L_3 are known constants, so we can use $p_{02} = p_0 + \rho_{liquid}g(R + L_3)$, and so $p = p_{02} + \rho_{liquid}gR\sin\theta$. Then the general solutions are:

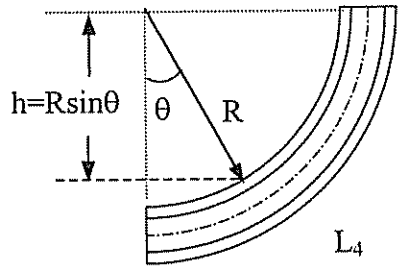

Figure 2.4 *h* of the Lower Curved Section

$$
\begin{aligned}
w_4(s) = & -\frac{B_{22}}{A_{22}R}C_{42} - C_{42} + C_{43}\sin\theta - C_{44}\cos\theta + C_{45}\theta\sin\theta - C_{46}\theta\cos\theta \\
& + [\frac{2}{A_{22}R\Sigma}(B_{22}^3 - 2B_{22}^2A_{44}R - B_{22}A_{44}D_{22}) + \frac{2D_{22}A_{44}}{\Sigma} - \frac{2D_{22}B_{22}}{R\Sigma} \\
& + \frac{B_{22}}{A_{22}R} - 1](C_{45}\cos\theta + C_{46}\sin\theta) + \frac{R^2p_0}{A_{22}} \\
& - \rho_{liquid}gR^3\{\theta^2\sin\theta[\frac{A_{22}D_{22} - B_{22}^2}{8A_{44}\Sigma} + \frac{D_{22} + A_{22}R^2 + 2B_{22}R}{4\Sigma} \\
& + \frac{1}{8\Sigma}(\frac{4A_{44}D_{22}R}{\overline{B}} + \frac{A_{22}A_{44}R^4}{\overline{D}} + \frac{4A_{22}A_{44}R^3}{\overline{B}} + \frac{2A_{44}D_{22}R^2}{\overline{D}} \\
& + \frac{4A_{44}B_{22}R^2}{\overline{B}} + \frac{A_{44}D_{22}^2}{\overline{D}A_{22}})] - \sin\theta[\frac{21(A_{22}D_{22} - B_{22}^2)}{32A_{44}\Sigma} \\
& + \frac{98D_{22} + 42A_{22}R^2 + 140B_{22}R}{32\Sigma} + \frac{1}{32\Sigma}(\frac{220A_{44}D_{22}R}{\overline{B}} + \frac{66A_{44}D_{22}R^2}{\overline{D}} \\
& + \frac{164A_{44}B_{22}R^2}{\overline{B}} + \frac{108A_{22}A_{44}R^3}{\overline{B}} + \frac{21A_{22}A_{44}R^4}{\overline{D}} + \frac{77A_{44}D_{22}^2}{\overline{D}A_{22}})] \\
& + \theta\cos\theta[\frac{A_{22}D_{22} - B_{22}^2}{2A_{44}\Sigma} + \frac{3D_{22} + 2A_{22}R^2 + 5B_{22}R}{2\Sigma} \\
& + \frac{1}{2\Sigma}(\frac{A_{22}A_{44}R^4}{\overline{D}} + \frac{7A_{44}D_{22}R}{\overline{B}} + \frac{5A_{22}A_{44}R^3}{\overline{B}} + \frac{6A_{44}B_{22}R^2}{\overline{B}} \\
& + \frac{3A_{44}D_{22}R^2}{\overline{D}} + \frac{2A_{44}D_{22}^2}{\overline{D}A_{22}})]\}
\end{aligned}
\tag{2.44}
$$

$$
\begin{aligned}
v_4(s) = & C_{41} + C_{42}\theta + C_{43}\cos\theta + C_{44}\sin\theta + C_{45}\theta\cos\theta + C_{46}\theta\sin\theta \\
& - \rho_{liquid}gR^3\left[\frac{1}{32A_{44}} + \frac{R}{16\overline{B}} + \frac{R^2}{32\overline{D}} + \frac{D_{22}}{32(A_{22}D_{22} - B_{22}^2)}\right] \\
& \times\left(4\theta^2\cos\theta - 24\theta\sin\theta - 45\cos\theta\right)
\end{aligned}
\tag{2.45}
$$

$$\beta_4(s)=\frac{1}{R}(C_{41}+C_{42}\theta)-2\frac{A_{44}(B_{22}+A_{22}R)}{\Sigma}(C_{45}\sin\theta-C_{46}\cos\theta)$$
$$+\frac{\rho_{liquid}gR^3}{4\Sigma}[2\theta\sin\theta(A_{22}R+B_{22}+\frac{A_{44}D_{22}+3R^2A_{22}A_{44}+2RA_{44}B_{22}}{\overline{B}}$$
$$+\frac{R^3A_{22}A_{44}+RA_{44}D_{22}}{\overline{D}})+\cos\theta(9A_{22}R+9B_{22}+\frac{5R^3A_{22}A_{44}+9RA_{44}D_{22}}{\overline{D}}$$
$$+\frac{9A_{44}D_{22}+19R^2A_{22}A_{44}+14RA_{44}B_{22}}{\overline{B}})] \quad (2.46)$$

where Σ has been specified in equation (2.40).

2.5.5 Lower Horizontal Section (L1+L2+L3+L4<s<L1+L2+L3+L4+L5)

In this section, the beam undergoes a constant loading, that is $p=p_0+\rho_{liquid}g(2R+L_3)$, so the general solutions will have the same format as those of section 1, except that the different constant value of p, i.e. $p=p_{03}=p_0+\rho_{liquid}g(2R+L_3)$.

$$w_5(s)=\frac{p_{03}}{24\overline{D}}s^4+C_{54}s^3+C_{53}s^2+C_{52}s+C_{51} \quad (2.47)$$

$$v_5(s)=\frac{p_{03}}{6\overline{B}}s^3+\frac{B_{22}(3C_{54}s^2+2C_{53}s+C_{52})}{A_{22}}+C_{56}s+C_{55} \quad (2.48)$$

$$\beta_5(s)=-\frac{p_{03}}{6\overline{D}}s^3-\frac{p_{03}}{A_{44}}s-\frac{6C_{54}\overline{D}}{A_{44}}-3C_{54}s^2-2C_{53}s-C_{52} \quad (2.49)$$

where $\overline{B}$ and $\overline{D}$ are the reduced stiffnesses and have been specified in (2.35) and (2.36).

The C_{ij} *(j=1..6, i=section/segment number)* values in the above solutions are constants that depend on the boundary conditions.

2.6 Solution for the Combined Beam

Now that analytic solutions for the curved and straight sections of the beam have been developed, they can be combined to describe the behavior of a beam made from a combination of curved and straight sections.

2.6.1 Boundary Conditions

Each section involves a set of equations with six unknown constants, which can be determined by the boundary conditions in the s, z plane, so the total number of unknowns for a beam made up of N sections is $6N$. To find the constants, three boundary conditions are needed at each end of each section of the beam. Thus, if the structure to be analyzed consists of the half cross section, the five beam segments will require three boundary conditions at each end of the beam (the planes of symmetry), six boundary conditions at each of the two junctions for a total of thirty boundary conditions and thirty unknown constants.

The boundary conditions at the ends of the beam are not the usual simple support or clamped support conditions used for elementary calculations. Instead, they are determined through the use of the symmetry of the cross section about the vertical planes. The 'ends' of the beam are not really the physical ends at all (there are no real ends since the cross section is closed) but are the planes of symmetry and treated as the ends of the beams for calculation purposes only. At these points, the lateral displacement w is not fixed. Due to the symmetry of the cross section, the slope of the beam must be zero and the transverse shear resultant must be zero. Due to the

requirement of continuity, the in-plane displacement v must be zero at each end of the half section of the truck tank.

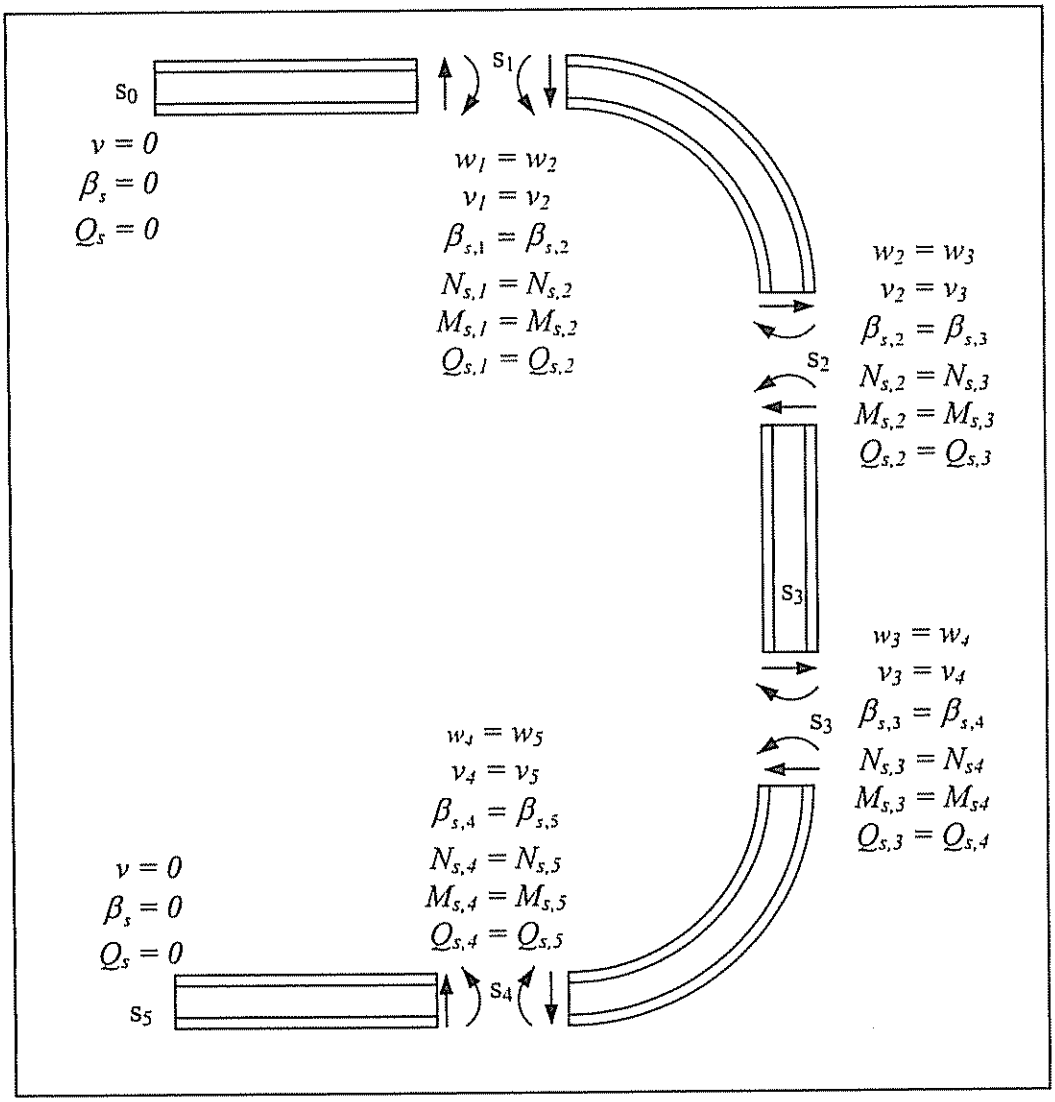

Figure 2.5 Boundary Conditions

At the junctions between sections, the boundary conditions take the form of matching conditions. At each junction, the in-plane resultants, moment resultants and transverse shear resultants must match. The displacements w and v must also match along with the angle of rotation β_s. Note that if transverse shear deformation is allowed, it is not required that the slopes of the beam sections must match at the junctions. It is perhaps a subtle point, but if the equations that account for transverse shear deformation are used, and if different materials or a different sandwich geometry are used in the sections on each side of the junction, the slopes could in fact differ even though β_s matches. Due to the symmetry about the vertical planes, this detail does not apply to the boundary conditions at the ends.

Now all the necessary boundary conditions have been determined and the unknown constants can be obtained. Figure 2.5 shows the boundary conditions for the five-segment beam from Figure 2.1. The total length of the five sections is L.

If the beam consists of more than the five sections discussed above, the boundary conditions are the same. At each end there are the conditions induced by symmetry: the in-plane displacement, transverse shear resultant and slope of the beam must be zero. At each junction between sections, the resultants, displacements and rotations must match. The boundary conditions for a beam consisting of N sections are summarized below.

At ends: $s = 0$ and $s = s_N$

$$\begin{aligned} v_0 &= 0 \\ \frac{\partial w}{\partial s} &= 0 \\ Q_s &= 0 \end{aligned} \tag{2.50}$$

At junctions: $s = s_i$ $(i=1..N-1)$

$$\begin{aligned} v_{0,i} &= v_{0,i+1} \\ w_i &= w_{i+1} \\ \beta_{s,i} &= \beta_{s,i+1} \\ N_{s,i} &= N_{s,i+1} \\ M_{s,i} &= M_{s,i+1} \\ Q_{s,i} &= Q_{s,i+1} \end{aligned} \tag{2.51}$$

2.6.3 General Solution for A Beam Composed Of *N* Sections

Now the boundary conditions can be applied to each section of the total beam. The solution for the general problem of *N* sections is obtained by applying the general solutions (2.32) through (2.49), or the appropriate simplifications, to each section in a piecewise fashion. In the i^{th} section, s should be replaced in the displacement equations by $(s-s_{i-1})$ where s_{i-1} is the value of s at the end of the previous (the $(i-1)^{th}$) section. The *6N* unknown constants are found by applying the *6N* boundary conditions using equations (2.50) and (2.51). The resulting problem is an algebraic system of *6N* equations in *6N* unknowns.

While the problem treated in the current research is one involving the cross sectional shape shown in Figure 1.3, the equations presented here could also be used for other shapes or cross sections made from symmetric or asymmetric sandwiches subject to a linearly varying internal pressure, provided that each segment is either straight or circular-cylindrically curved and that all of the assumptions we are using are valid. For the boundary conditions to be used, the cross section must be closed and symmetrical about the vertical planes.

2.6.4 Geometric Discontinuity

At points of geometric discontinuity such as the junction between straight and curved section or between sections composed of different materials or face thicknesses, etc. there will be discontinuous behavior exhibited by some of the problem parameters. For example, at the junction between a straight section and a curved section there will be a 'kink' in the plot of the in-plane resultant. Since the transition from an infinite to a finite radius of curvature is discontinuous, there is a discontinuity in the derivative of the in-plane resultant at the junction. The resultant must still be continuous but it is not a smooth function. Likewise, the stress will also exhibit a kink at the junction since stress is given by $\sigma_s = \overline{Q}_{12}\varepsilon_x + \overline{Q}_{22}\left[\varepsilon_s^0 + z\kappa_s\right]$ and ε_s^0 inherits the kink from the in-plane resultant. These effects may be less prominent in reality than in the mathematical model since there will be slight deviations from the mathematically perfect geometry that will likely lead to a smoothing effect on the actual stress distributions and displacements.

Chapter 3

IMPLEMENTATION OF THE SOLUTION USING *MAPLE V*

The displacement functions and boundary conditions developed above are used in a Maple worksheet to find the stresses, strains and displacements for a cross section compiled from user specified data.

3.1 Description of the Worksheet

The Maple software package uses an interface that is very similar to a computer programming language. Program structures such as If/Then logic tests and loops can be combined with symbolic algebraic manipulations to allow the analysis of complex problems. A worksheet/program was developed to allow the user to specify various input conditions and specify whether the sandwich should be subjected to a parametric optimization. The worksheet then determines the deflections, stresses, strains, etc. and, if required, modifies the thickness of the faces and core based on the optimization criteria.

The worksheet allows the user to specify the initial geometry and loading of the cross section including the number of segments; the thickness of the inner face, outer face and core, the material properties of each face and core for each segment; internal pressure and factor of safety for the allowable stresses. Once the inputs have been specified, the boundary conditions are applied and the unknown constants are determined. The displacements and stresses could be calculated. If desired, the core

thickness and face thicknesses can be adjusted in an automatic iterative process that optimizes the structure based on the specified criteria.

The optimization criterion is that the weight be minimized, subject to restrictions of the in-plane stress and the shear stress. The maximum allowable stress is the yield stress for a ductile material, or the ultimate strength for a material that displays brittle behavior (the stress/strain curve is linear to failure), divided by a suitable factor of safety. In areas of the faces that are subject to compressive stress an additional limit is imposed, such that the stress may not exceed the critical stress at which face wrinkling will occur.

When the optimization is to be performed with no restriction on the deflection, the determination of the face and core thicknesses both take place within the optimization loop. When a restriction is placed on the deflection, the optimization needs to be performed differently. A series of face thicknesses is specified; the corresponding core thickness that results in an acceptable deflection is determined through an iterative process, and the lightest combination chosen.

In Chapter 4, sandwich structures with geometric and material properties that are constant in the circumferential direction will be analyzed. Each component, the inner face, the outer face and the core, is made of the same material and has the same thickness throughout the circumferential length of the structure. The faces may differ in materials. With this restriction, only three materials and thickness need to be specified for the structure: one for the core and one for each face.

If the sandwich components are constant in thickness, the dimensions of each face and the core are determined for the entire structure by the thickness required at the point of maximum stress. Since the stress in the rest of the structure is lower

than this value, the strength of the material is under-utilized everywhere except at the point of maximum stress. Another way of looking at it is that the structure is overbuilt and therefore heavier than necessary.

The Maple worksheet is general enough to allow for any number of segments. The limitation is that the computational time required for large numbers of segments becomes extremely large since the system of equations that needs to be solved to determine the unknown constants is of order $6N$ where N is the number of segments.

3.2 Worksheet Algorithm

The general algorithm for the worksheet is as follows:

- Read input data file. Data file contains all geometric data and material selections for each element of the structure, as well as the internal pressure.
- Read the material property data files for the specified materials.
- Calculate the Q matrix for each segment of the structure.
- Calculate the A, B, D matrices for each segment of the structure.
- Define the expressions for the resultants, strains and stresses in terms of the displacements.
- Apply the boundary conditions and solve for the unknown constants.
- If the structure is to be optimized, continue with the following steps. If not, skip to the last step.
- Find the maximum in-plane and shear stress in each segment of the structure.
- Determine the optimum thickness for each component, subject to the maximum in-plane stress restriction (the determination of these values will be discussed below).

- Find the optimum core thickness, subject to the maximum deflection restriction.
- Determine the minimum core thickness to prevent core shear failure.
- If there is a face loaded in compression, determine the minimum face thickness of that face to prevent face wrinkling.
- Compare the face thicknesses obtained above with the specified minimum allowable face thickness.
- Modify the thickness of each face and the core using the greatest of the thickness values obtained from the last five steps as the new value.
- Return to the calculation of the A, B, D matrices and recalculate using the new values of the constants. Continue as before to this step for each iteration.
- After the specified number of times through the optimization loop, save the most recent data for use if further refinement is needed.
- Calculate the face and core thicknesses, and the weight of the full cross section per unit length.

3.3 Criteria for Optimization

3.3.1 Core Shear Failure

In order to determine the minimum allowable core thickness to prevent shear failure, the following assumptions are made by Zenkert [24]:

$$\begin{aligned} E_c &<< E_f \\ \left(t_{inner}, t_{outer}\right) &<< h_c \end{aligned} \tag{3.1}$$

The first assumption in (2.43) results in a constant shear stress across the core since the shear stress is given by

$$\tau_{sz} = \int \sigma_s dz \tag{3.2}$$

If the core is weak, the in-plane load carried by it will be negligible compared to that carried by the faces. The in-plane stress in the core is then approximated to zero and the transverse shear stress distribution will be constant through the thickness of the core. The second assumption is that the face thicknesses are much smaller than the core thickness. If this is the case, the linear distribution of the in-plane stress in the faces can be approximated as a constant stress, yielding a linear rather than parabolic distribution of the transverse shear stress in the faces. The effects of the assumptions are shown in Figure 3.1. With these approximations, the transverse shear stress in the core and the maximum in each face are given by

$$\tau_c = \tau_{f,\max} = \frac{Q_s}{h_c + \frac{t_i}{2} + \frac{t_o}{2}} \tag{3.3}$$

where Q_s is the transverse shear resultant.

It should be noted that the second approximation discussed above is conservative in that the predicted transverse shear stress in the core is slightly higher than if the parabolic distribution in the faces is used.

To find the minimum core thickness, substitute the allowable shear stress for τ_{sz} in equation (2.45) and solve for h_c.

$$h_{c,\min} = \frac{Q_s}{\tau_{c,allowable}} - \frac{t_i + t_o}{2} \tag{3.4}$$

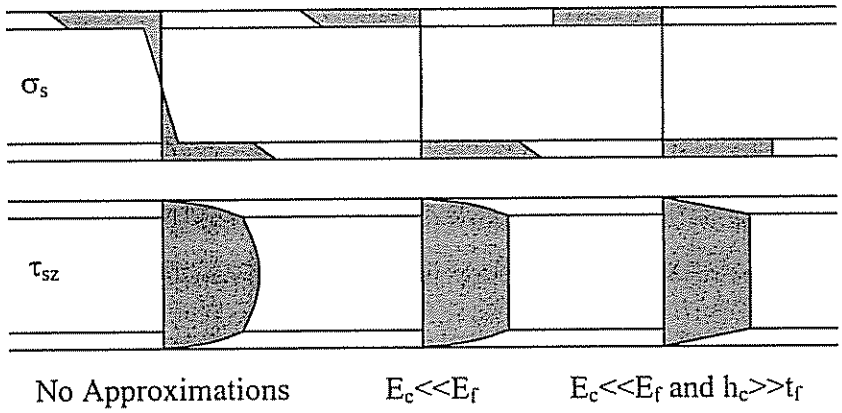

Figure 3.1 Approximations for The In-Plane And Transverse Shear Stress Distributions Through The Thickness Of The Sandwich

3.3.2 Face Wrinkling

Sandwiches with very thin faces can be subject to local instability phenomena known as face wrinkling. This occurs when the compressive load in a face is so great that the core is not stiff enough to prevent the face from buckling independently from the sandwich as a whole. Since this is a local rather than global action, the determination of the critical stress in the compressive face of a sandwich loaded in bending is performed in the same manner as for a sandwich loaded in in-plane compression.

There are two formulas that can be used to determine the critical wrinkling stress. The first is the equation developed by Hoff and Mautner [12]

$$\sigma_{s,cr} = -c\left(E_{s,face}E_{s,core}G_{sz,core}\right)^{1/3} \tag{3.5}$$

where c is a constant whose value has been taken by different researchers as being between 0.5 and 0.91. This equation implies that the effects of the behavior of one face are not felt by the other face since there is no geometric dependency.

The other formula for the critical stress is the one developed by Heath [11] for isotropic materials which includes geometric considerations. When the equation is modified for anisotropic materials, the critical wrinkling stress is given by

$$\sigma_{s,cr} = -\left[\frac{2}{3}\frac{t_f}{h_c}\frac{E_c\sqrt{E_{s,f}E_{x,f}}}{\left(1-\nu_{sx}\nu_{xs}\right)}\right]^{1/2} \tag{3.6}$$

As can be seen from the equation, the critical stress tends toward zero as the core to face thickness ratio becomes large.

Since the two equations often yield significantly different results, it is unclear which is the more appropriate one to use. The sandwich profiles in this study typically have large core to face thickness ratios and thus the critical wrinkling stress predicted by the Heath equation is often very small. While the effects of the geometry may be important for sandwiches that have cores that are thin enough for one face to influence the other, this author believes that since the h_c/t_f ratio is large for the sandwiches investigated here, the influence of one face on the other is negligible and as a result, the Hoff/Mautner equation should be used. Supporting this theory is the fact that even if the compressive face wrinkles, the structure is in bending so the other face is in tension and will not wrinkle. This effectively gives the core's response to the buckled face twice the distance (the full thickness of the core instead of the

distance from the face to the mid-surface) to decay without affecting or being affected by the other face.

For the investigation presented here, the Hoff/Mautner equation will therefore be used, with the value of the constant c taken to be 0.5, to be conservative.

3.3.3 Optimization the Structure for Lowest Weight

When determining the optimal face and core thicknesses for lowest weight, the same approximations regarding the stress distribution are made as for the shear stress calculation. They are repeated here:

$$\begin{aligned} E_c &<< E_f \\ \left(t_{inner}, t_{outer}\right) &<< h_c \end{aligned} \tag{3.7}$$

resulting in an approximately constant in-plane stress distribution through the face thickness. If one also makes the approximation that

$$\frac{h_c}{2} + t_f \approx \frac{h_c}{2} \tag{3.8}$$

then the in-plane and moment resultants can be written as

$$\begin{aligned} N_s &= t_i\sigma_i + t_o\sigma_o \\ M_s &= t_o\sigma_o \frac{h_c}{2} - t_i\sigma_i \frac{h_c}{2} \end{aligned} \tag{3.9}$$

The s subscript has been dropped from the stresses to simplify writing the equations. It is understood that the in-plane stresses are in the s direction. To find the

optimum face thicknesses, set the stresses equal to the maximum allowable values for the appropriate direction (tension or compression) and solve for t_i and t_o in terms of N_s, M_s, and h_c

$$t_{i,opt} = \frac{1}{\sigma_{i,allowable}}\left[\frac{N_s}{2} - \frac{M_s}{h_c}\right] \quad t_{o,opt} = \frac{1}{\sigma_{o,allowable}}\left[\frac{N_s}{2} + \frac{M_s}{h_c}\right] \tag{3.10}$$

The face thicknesses cannot be negative so the allowable stress will have the same sign as the quantity in the brackets. If the stress is negative (compressive), the allowable stress is the lesser of the maximum allowable due to overstressing or that which will induce face wrinkling. The resultants are known along with the allowable stresses, so all that remains is to find the optimum core thickness for the lowest weight. If there is no restriction on the deflection, the optimum core thickness can be found as follows. Writing the weight per unit platform area, with W equal to the weight of the components minus the weight of the adhesive (the adhesive is not included since it is not a known factor and does not influence the optimization results in any case) that holds them together

$$W = \rho_c h_c + \rho_i t_i + \rho_o t_o$$
$$W = \rho_c h_c + \frac{\rho_i}{\sigma_{i,allowable}}\left[\frac{N_s}{2} - \frac{M_s}{h_c}\right] + \frac{\rho_o}{\sigma_{o,allowable}}\left[\frac{N_s}{2} + \frac{M_s}{h_c}\right] \tag{3.11}$$

The weight is minimized when $\partial W/\partial h_c = 0$

$$\frac{\partial W}{\partial h_c} = \rho_c - \frac{M_s}{h_c^2}\left[\frac{\rho_o}{\sigma_{o,allowable}} - \frac{\rho_i}{\sigma_{i,allowable}}\right] = 0 \tag{3.12}$$

$$h_{c,opt} = \sqrt{\frac{M_s}{\rho_c}\left[\frac{\rho_o}{\sigma_{o,allowable}} - \frac{\rho_i}{\sigma_{i,allowable}}\right]} \tag{3.13}$$

If the quantity under the square root sign is negative, equation (3.13) yields no solution for h_c. For those cases, the weight continues to decrease as h_c becomes smaller with the minimum at h_c equals zero. In reality, there may be a minimum at a very small h_c, but the assumption of constant in-plane stress distribution in the faces eliminates the higher order terms that would allow the determination of this minimum. The optimal h_c in this region is unimportant for this problem anyway since there is a large enough transverse shear resultant in these regions that shear failure dominates the core thickness determination.

The core thickness must also be great enough that the shear stress in the core is below the maximum allowable value. The minimum core thickness that satisfies this constraint is calculated using Equation (3.4). Once the optimum thickness is obtained for each constraint; in-plane stress and shear stress, the greater of the two is used.

Changing t_i, t_o and h_c will change the bending/stretching coupling and therefore the moment resultant M, so the optimization is an iterative process. While the face thicknesses given by equation (3.10) are used for the calculation of $h_{c,opt}$, the assumption of uniform in-plane stress distribution in the faces can be eliminated from the optimum thickness calculation if the following iterative relation is used once the optimal core thickness has been determined

for the jth iteration: $$t_{k,j+1} = \frac{\sigma_{k,j,\max}}{\sigma_{k,allowable}} t_{k,j} \quad (k = inner, outer) \tag{3.14}$$

where σ_{max} is the maximum in-plane stress that occurs in the face, usually on the outer surface of the structure. This equation allows t_i and t_o to be refined a little more accurately than equation (3.14) does.

Chapter 4

PARAMETRIC ANALYSIS OF THE PROBLEM

Now the tools have been developed to analyze the rectangular cross section with rounded corners, the optimization of the cross section and sandwich geometry is then explored.

In general, plates and shells resist loads in different ways. Plates typically resist lateral loads through bending stresses while a well-designed shell under lateral loading minimizes the bending stresses and resists the load primarily through in-plane membrane stresses. Since the cross section in question is a combination of the two types of element, some level of compromise is inevitable. So the effect of the overall cross section geometry must be considered before the face and core thicknesses are optimized.

4.1 Analysis of the Cross Section Geometry

Since the cross section geometry is symmetric about the vertical and the horizontal axis, it is defined by three parameters: L_1, R, and L_3, which are shown in Figure 4.1. If the cross section is not to be any larger than necessary, i.e., larger than a specified pair of outer dimension limitations (L_{height} and L_{width}), then specifying one of the parameters (L_1, R and L_3) determines the other two. The length of circumference is readily available also.

The weight per unit length of the truck tank will be this circumferential length times the weight per unit platform area. The weight per unit area will be heavily

dependent on the cross sectional geometry since as L_1 and L_3 become larger, the greater bending and shear loads will require thicker faces and a thicker core to prevent over-stressing.

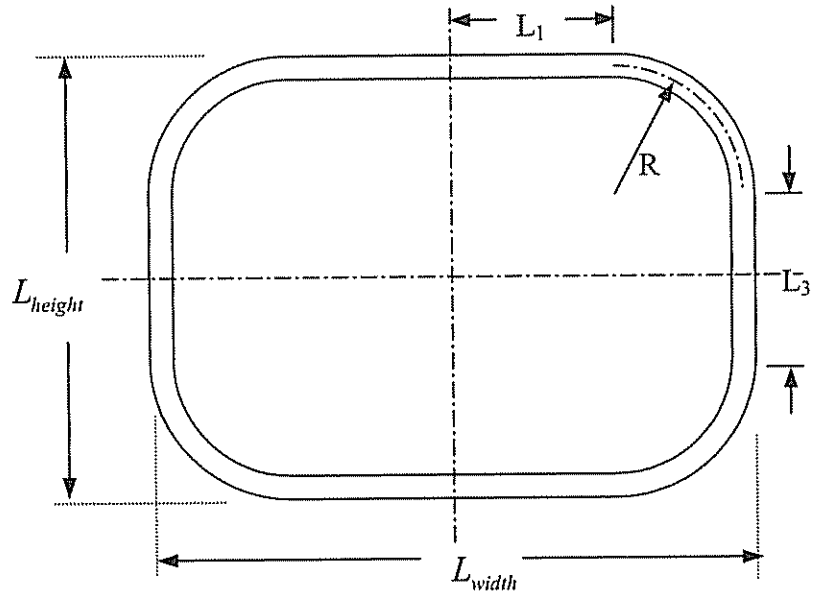

Figure 4.1 Definition of Geometric Parameters

In order to determine the effect of the cross section geometry on the weight of the structure, the sandwich will be optimized for different values of L_1 and L_3 and R, and the results will be compared.

4.2 Sample Cross Sections

The problem investigated in this thesis is a truck tank. Since there are limitations of 8 feet (2.43m) width and 14 feet (4.26m) height on outside dimensions on American highways, for comparison, we consider two cases, one is that the outside

dimensions of the tank is 8(ft. width) ×8(ft. height), which has a square cross section; another case is that the outside dimensions of the tank should be 8(ft. width) ×10(ft. height), which has a rectangular cross section.

As stated above, the cross section can be defined by three parameters: L_1, R, and L_3, which are shown in Figure 4.1. Since we have already known the outside dimension limitations L_{width} and L_{height}, as long as we specify one of the parameters (L_1, R and L_3), we can determine the other two. For example, if we specifies L_1, then $R = L_{width}/2 - L_1$ and $L_3 = L_{height} - 2R$.

In order to investigate the response of various cross sections, ten geometric configurations are selected for further studies, i.e. for both of the two cases described above, five radii—from small to large--are specified for the curved sections. Once the geometry is specified, the sandwich profile can be optimized for each sample cross section.

The cross sections consist of two groups. The square cross sections will be referred to as CS-S1 to CS-S5. The rectangular cross sections will be referred to as CS-R1 to CS-R5. Since R is the radius of the mid-plane of the sandwich and it is the outside face of the curved section that must clear the maximum exterior dimension, the radius used when specifying the cross section geometry will be the radius of the outer surface, R′, which is defined as

$$R' = R + \frac{(t_i + h_c + t_o)}{2} \tag{4.1}$$

The values for R′, L_1 and L_3 for each cross section are listed in Table 4.1.

Table 4.1 Geometric Specifications for Sample Cross Sections

Unit (ft/m)	L_1	R′	L_3
CS-S1	1.5/0.4572	2.5/0.762	3/0.9144
CS-S2	1.8/0.5486	2.2/0.6706	3.6/1.097
CS-S3	2.2/0.6706	1.8/0.5486	4.4/1.341
CS-S4	2.5/0.762	1.5/0.4572	5/1.524
CS-S5	3/0.9144	1/0.3048	6/1.829
CS-R1	1.5/0.4572	2.5/0.762	5/1.524
CS-R2	1.8/0.5486	2.2/0.6706	5.6/1.707
CS-R3	2.2/0.6706	1.8/0.5486	6.4/1.951
CS-R4	2.5/0.762	1.5/0.4572	7/2.134
CS-R5	3/0.9144	1/0.3048	8/2.438

4.3 Sample Materials and Loadings

As a sample problem, Aluminum 6061-T6 is used as the face material, and a foam core that has a density of 75Kg/m^3 is used in this sample problem. The property values are listed in Table 4.2.

Table 4.2 Material Properties for the Sample Problem

		Aluminum 6061-T6	Foam Core
E_{11}	GPa	72	79.091e-3
E_{22}	GPa	72	79.091e-3
G_{12}	GPa	26	28.247e-3
ν		0.33	0.4
σ_comp	MPa	-290	-69
σ_tens	MPa	290	69
τ	MPa	193	1.022
ρ	kg/m^3	2700	75

E_{11}: modulus of elasticity in the fiber direction

E_{22}: modulus of elasticity perpendicular to the fiber direction

G_{12}: In-plane shear modulus (for transversely isotropic composites, $G_{13} = G_{12}$)

ν: Poisson's ratio

σ_comp: Compressive strength

τ: In-plane shear strength

ρ: Density in kg/m^3

4.4 Loadings

Water (ρ=1000Kg/m^3) is used as the sample linearly varying load. The results are calculated for two situations:

- **Sample Loading I**

In this case, only the liquid loading is considered but exclude the effect of the constant internal pressure, i.e., the truck tank is filled with water, so there is no inner air pressure. The loading profile is shown in Figure 4.2.

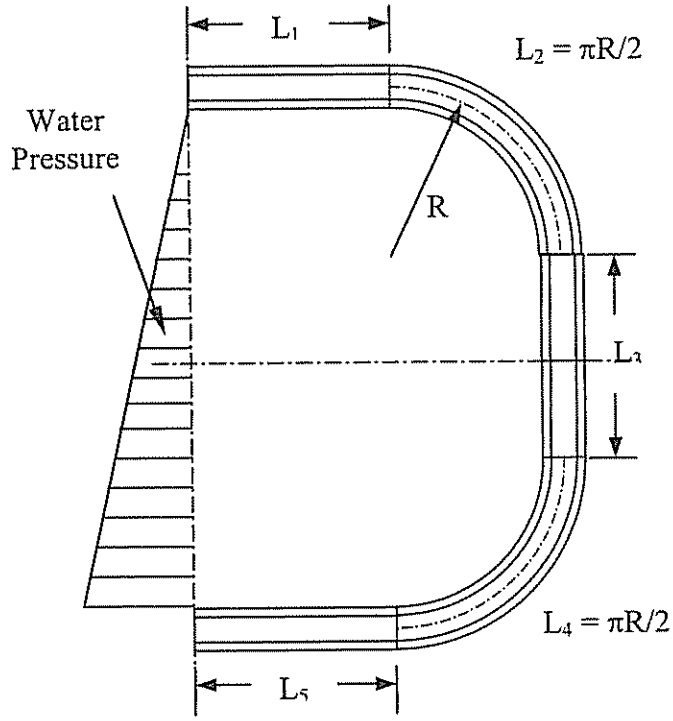

Figure 4.2 Loading Profile of Sample Loading I

- **Sample Loading II**

In this case, the truck tank is not filled, so the loading of the idealized truck tank CS shown in Fig. 4.3 consists of two parts: the first is the hydraulic head loading exerted by the fluid contained in the tank, arbitrarily the fluid level is assumed to coincide with the intersection between the curved panel in the top and the vertical sandwich panel (side panel); and the second loading the constant inner pressure, which has the value of 100Mpa.

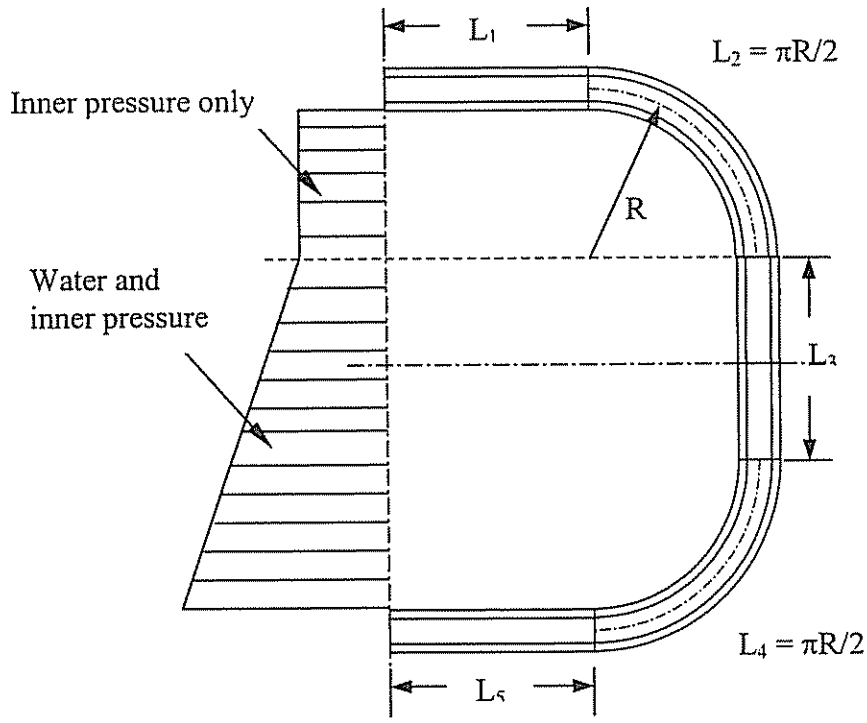

Figure 4.3 Loading Profile of Sample Loading I

4.5 Results for the Sample Problem

In order to find the lightest construction for a given material combination, an initial range is chosen for the thickness of each face. The thickness of each face is then varied over this initial range. For each combination of face thicknesses, the thickness of the core is modified such that the stresses are less than the allowable stresses. The weight is then calculated for each final combination.

In order to automatically determine the optimum face thicknesses, a range of face thicknesses that is broad enough to include the minimum is established. Within this range, a three by three grid of points is calculated: one at the top, middle and

bottom of the range for each face for a total of nine data points. The point resulting in the lowest weight structure is designated as the new center of the range for the $(i+1)^{th}$ iteration and the magnitude of the range is reduced. The process is repeated until the resolution of the data points is sufficiently accurate.

The allowable stress is the strength of the material divided by the factor of safety. Tentatively a factor of safety 2 is used for both faces and core in this sample problem. Since the problem studied here in this thesis is a rather practical one, the transportation truck tank is a frequently used, heavy duty vehicle, greater values of the factor of safety may be required in reality, the effect of the factor of safety on the optimal structure and weight will be discussed in Chapter 5.

4.5.1 Results for Case I — (No Constant Internal Pressure)

Since the thickness of the sandwich is not yet known, the outer surface is specified and the mid-plane radius, R is adjusted within the worksheet using equation (4.1) to keep the outer surface constant each time the thickness of the sandwich is changed.

After running the Maple program described in the previous chapter, the optimized values of the faces and core thicknesses and weight can be obtained and are listed in Table 4.3. Also in this table, the ratios of the inner cross section area to weight are listed, since we assumed that there is no variation of any geometry parameter in the axial direction, these ratios are equivalent to the truck tank volume to weight ratio.

Table 4.3 Optimized Geometry and Weight for Sample Case I, Subject to Maximum Allowable Stresses and Lightest Weight Criteria

	t_i (mm)	t_o (mm)	h_c (mm)	W (Kg/m)	Cross section inner area A (m^2)	R=A/W
CS-S1	0.619	0.563	43.15	53.40	5.079	0.0952
CS-S2	0.663	0.599	46.04	57.99	5.159	0.0890
CS-S3	0.711	0.676	49.30	64.39	5.248	0.0815
CS-S4	0.740	0.759	51.36	69.55	5.301	0.0762
CS-S5	0.813	0.910	54.19	78.94	5.360	0.0679
CS-R1	0.933	0.879	42.32	76.83	6.513	0.0848
CS-R2	0.980	0.987	42.46	82.27	6.617	0.0804
CS-R3	1.069	1.189	43.87	92.79	6.718	0.0724
CS-R4	1.127	1.247	48.25	100.57	6.746	0.0671
CS-R5	1.095	1.203	61.50	110.86	6.698	0.0604

From this table, it is seen that the square cross sections are comparatively lighter, the reason is that the moment resultants generated by the pressure on the straight sides act to balance each other out and are most effective at doing so when they are of the same magnitude. This occurs when the straight sections are of the same length. In this case, each one reduces the maximum moment in the adjacent side by the same amount and as a result, neither side is overbuilt with respect to the other for the constant thickness sandwich construction due to the fact that the maximum bending moments are smaller.

In a rectangular configuration where one side is longer and the other shorter than in the square case, the moment generated in the longer side by the pressure on that side is larger since the moment increases with the length of the straight section. The pressure on the shorter side helps to counteract this moment

(through the matching conditions at the junctions between sections) but when there is a differential in the lengths, this effect of counteracting the moment is reduced and the maximum net moment resultant in the longer side is of greater magnitude for the rectangular case, resulting in the need for a heavier sandwich to handle the increased moment. Likewise, the net moment resultant in the shorter side is smaller in magnitude, so the sandwich will be overbuilt in that section.

The volume to weight ratio of both the square and rectangular cross sections shows a decreasing trend as the radius decreases. So if the only consideration is the volume to weight ratio, then a tank with a circular cross section should be the best choice, but in that case, it results in very thin faces and a non-existent core. To illustrate this trend, three additional rectangular cross sections with very large corner radii are examined and the results are listed in Table 4.4.

Table 4.4 Optimized Geometry and Weight for Sample Loading I, Extra-Large Corner Radii, Subject to Maximum Allowable Stresses and Lightest Weight Criteria

	R(ft/m)	t_i (mm)	t_o (mm)	h_c (mm)	W (Kg/m)	Cross section inner area A (m^2)	R=A/W
CS-RA	3/0.9144	0.530	0.489	37.19	44.68	4.920	0.1101
CS-RB	3.5/1.067	0.408	0.387	28.99	33.81	4.737	0.1401
CS-SC	3.8/1.158	0.303	0.321	21.95	25.63	4.621	0.1803

But this weight saving cannot be fully realized, in actual use, there will be many other loads and factors such as durability, vibration, etc. that will not permit the

use of a shell that is as thin as that predicted using membrane analysis. When considering the additional loadings, it would be unreasonable to assume that it is possible to transfer the weight of the loadings to the shell and maintain a state of membrane stress. Furthermore, a truck tank with a round cross section cannot be loaded as efficiently as one that is more rectangular, since not all of the space is usable space. So a circular cross section is not very feasible

Plots of the in-plane stress in the faces, shear stresses in the cores and the bending moment resultant as functions of the circumferential coordinate, s for the sample cross sections are shown in Figure 4.4 through 4.9, along with the maximum allowable in-plane and shear stresses and critical stresses at which the faces will wrinkle. In the plots for CS-R1,CS-R3 and CS-R5, the profile of lateral deflection are included also. For simplicity, the plots for cross section CS-S2, CS-S4, CS-R2 and CS-R4 are listed.

And only the right half of the cross section is shown on the plots since the response of the other half is identical due to the symmetry about the vertical axis.

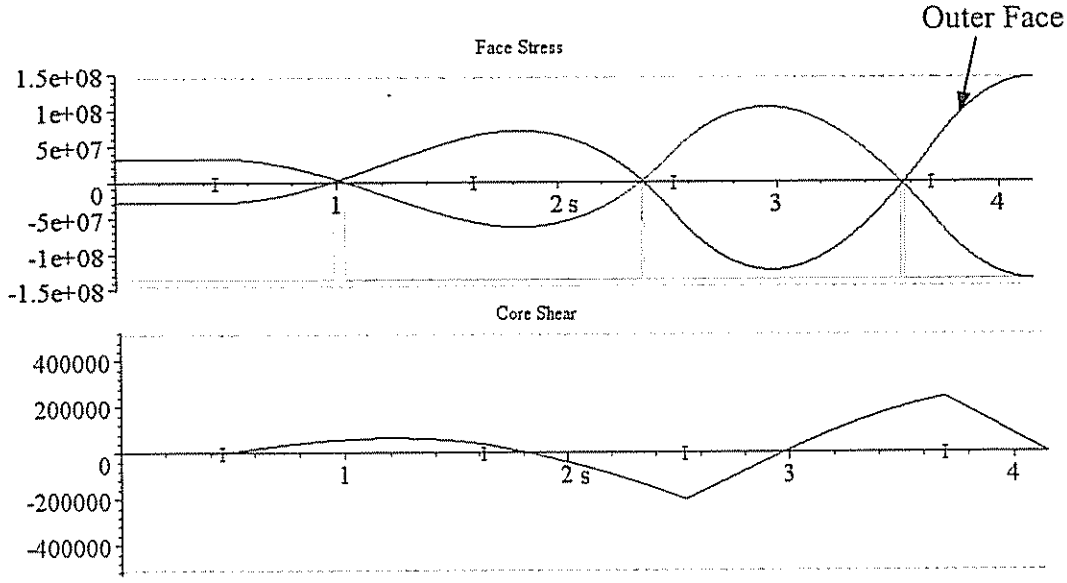

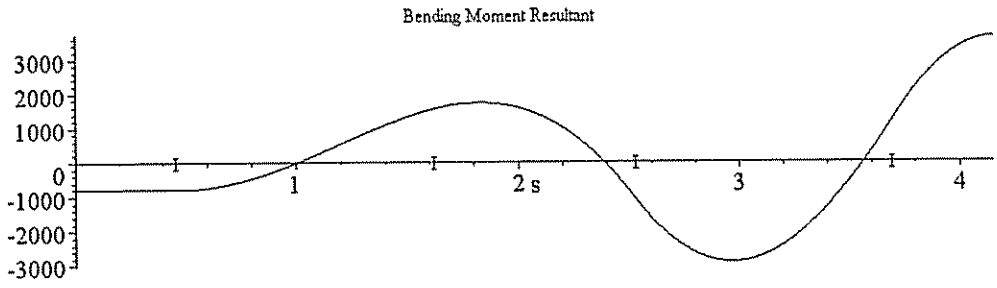

Figure 4.4 Stresses and Moment Resultant of CS-S1 (Sample Case I)

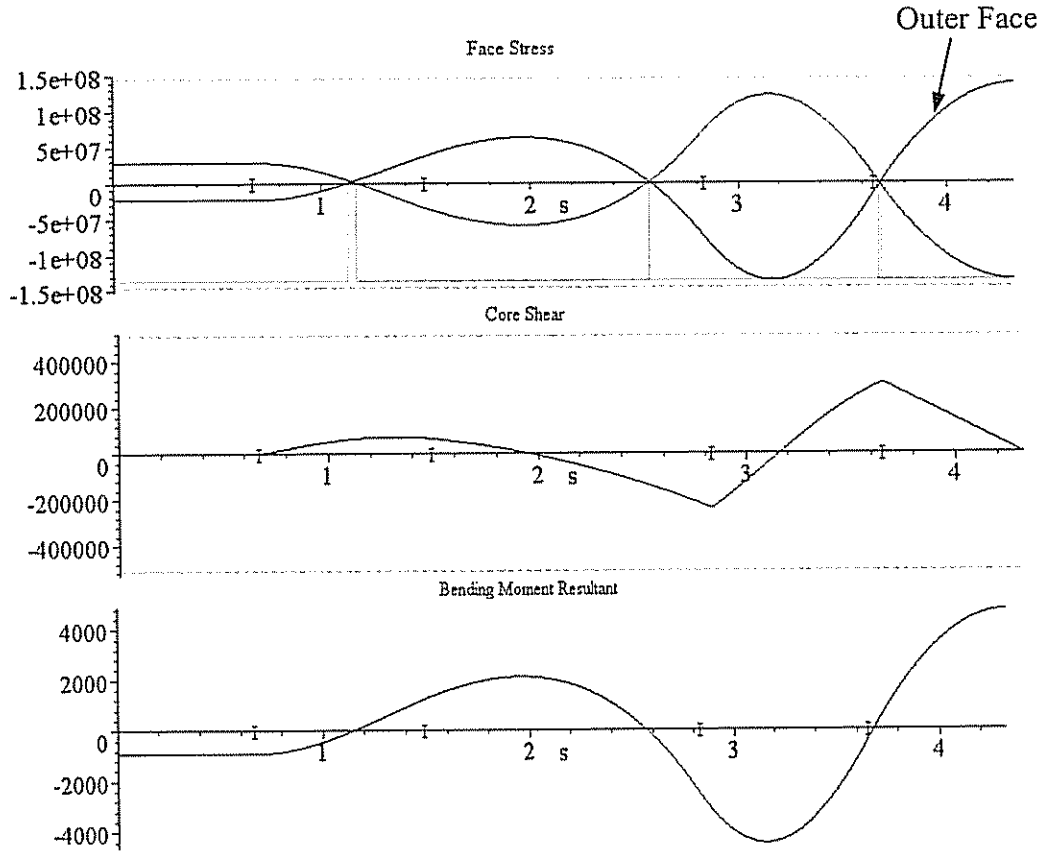

Figure 4.5 Stresses and Moment Resultant of CS-S3 (Sample Case I)

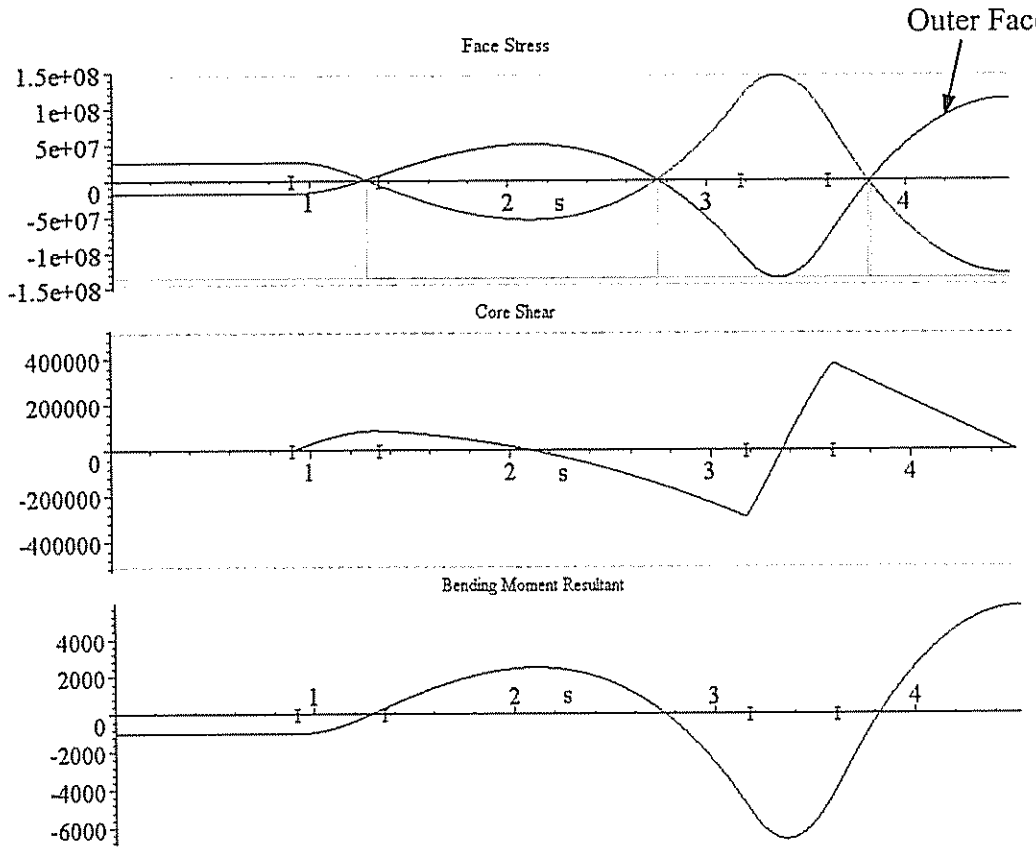

Figure 4.6 Stresses and Moment Resultant of CS-S5 (Sample Case I)

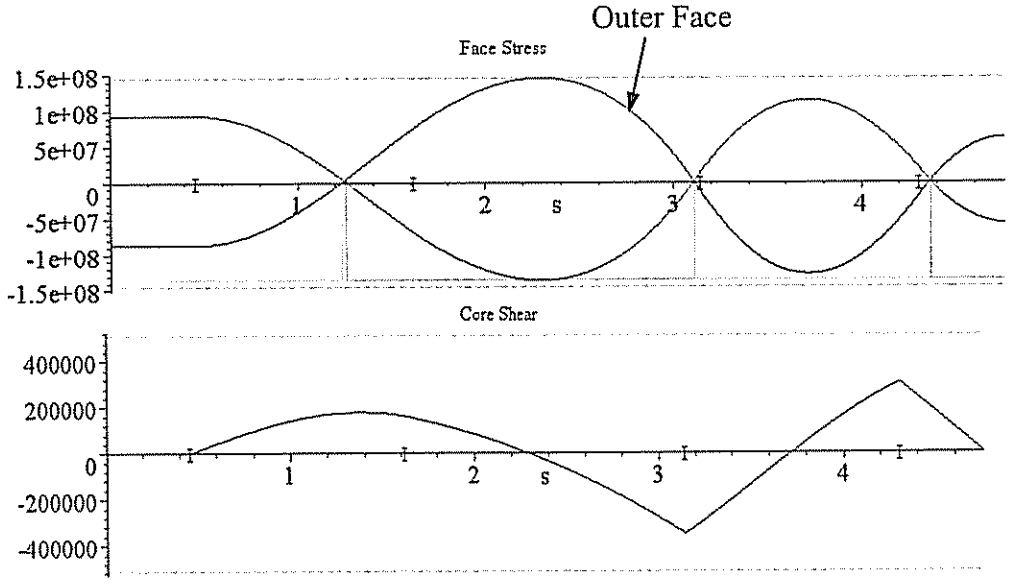

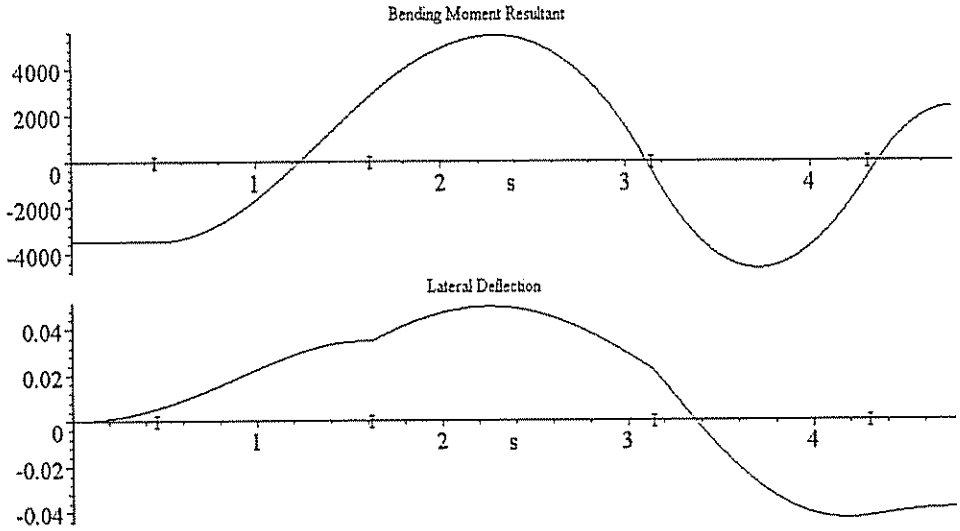

Figure 4.7 Stresses, Moment Resultant and Later Deflection of CS-R1 (Sample Case I)

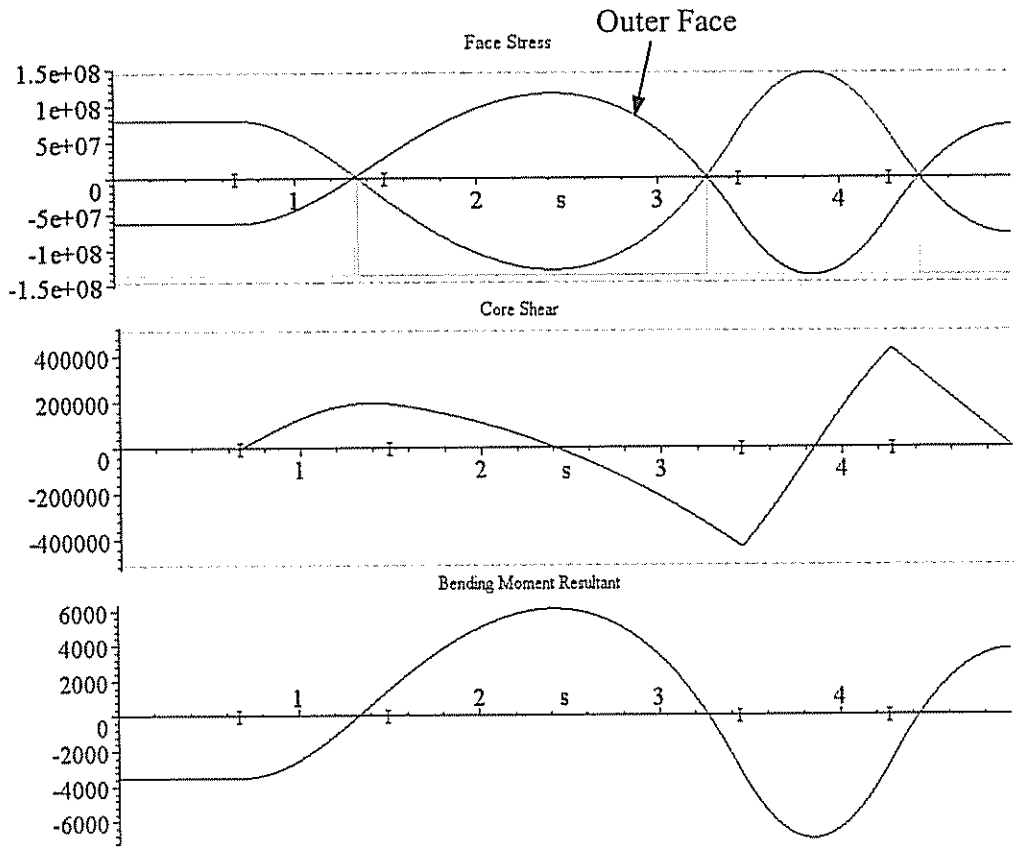

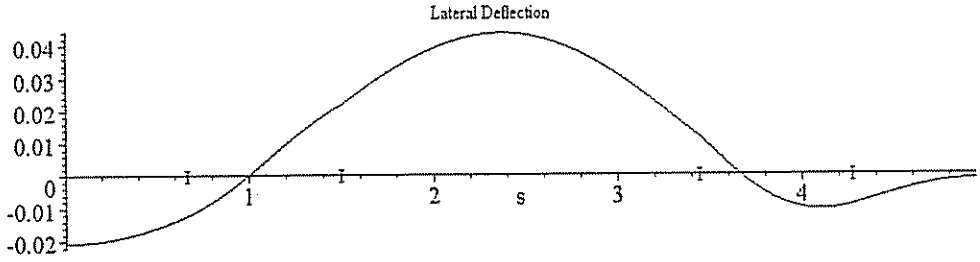

Figure 4.8 Stresses, Moment Resultant and Later Deflection of CS-R3 (Sample Case I)

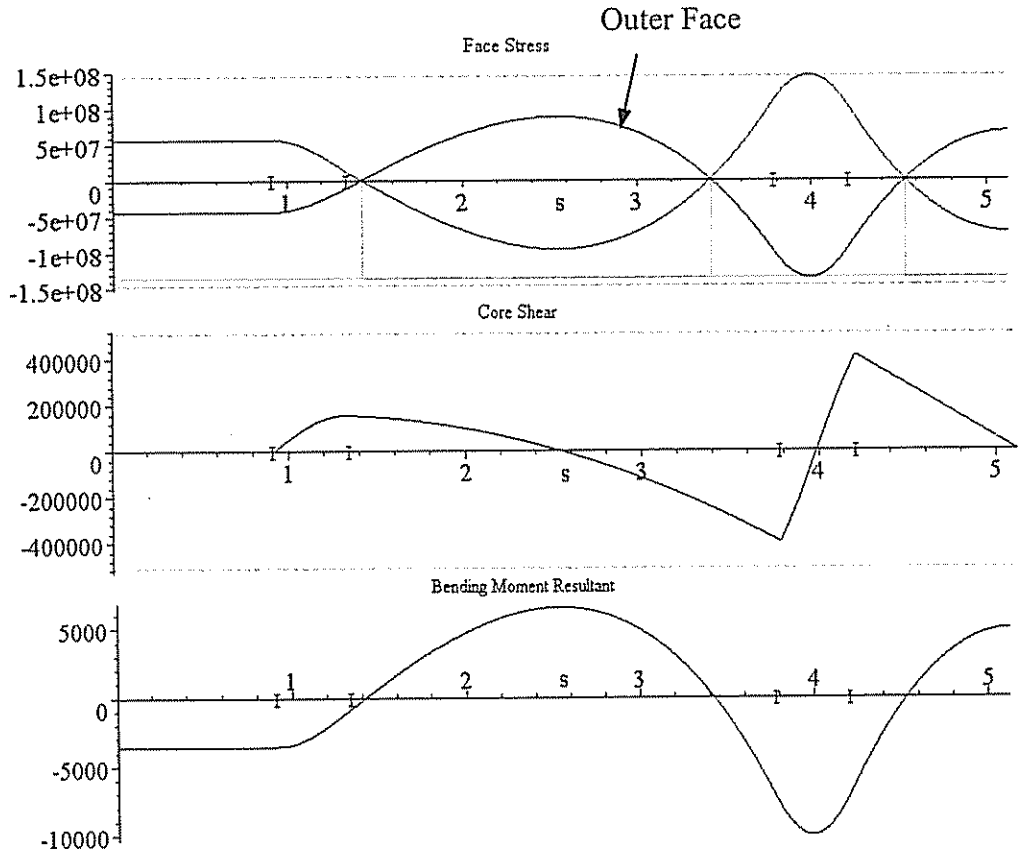

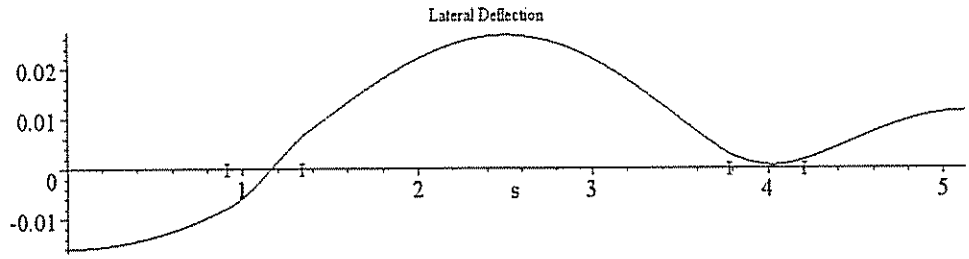

Figure 4.9 Stresses, Moment Resultant and Later Deflection of CS-R5 (Sample Case I)

From these plots, one can see that the core shear stresses did not reach the maximum core shear limits. This is because both of the lightest weight and the stress limitations were used as the optimization criteria, if one optimized the structure only under the criterion of the stress limitations, as an example, for CS-S3, the results would be:

$$t_i = 1.217mm \qquad t_o = 1.146mm \qquad h_c = 29.36mm \qquad W = 74.78Kg/m \qquad (4.2)$$

Compared to the value in Table 4.2, there is a 16.14% increase on the optimized weight, since one must use thicker faces in compensation for the thinner core in which the maximum shear stress reaches the core shear limitation. The plot of this situation is shown below in Figure 4.10.

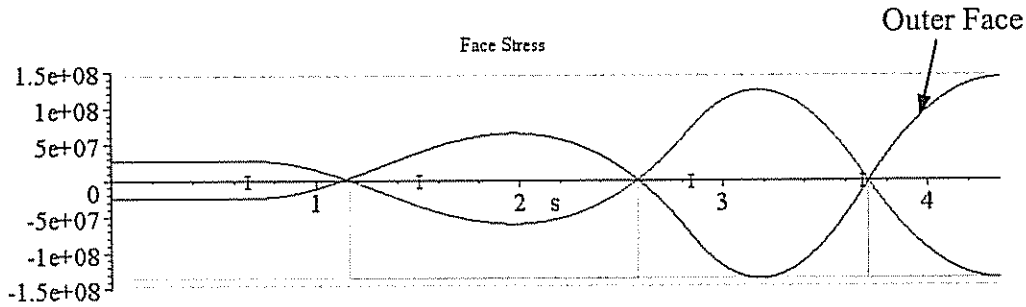

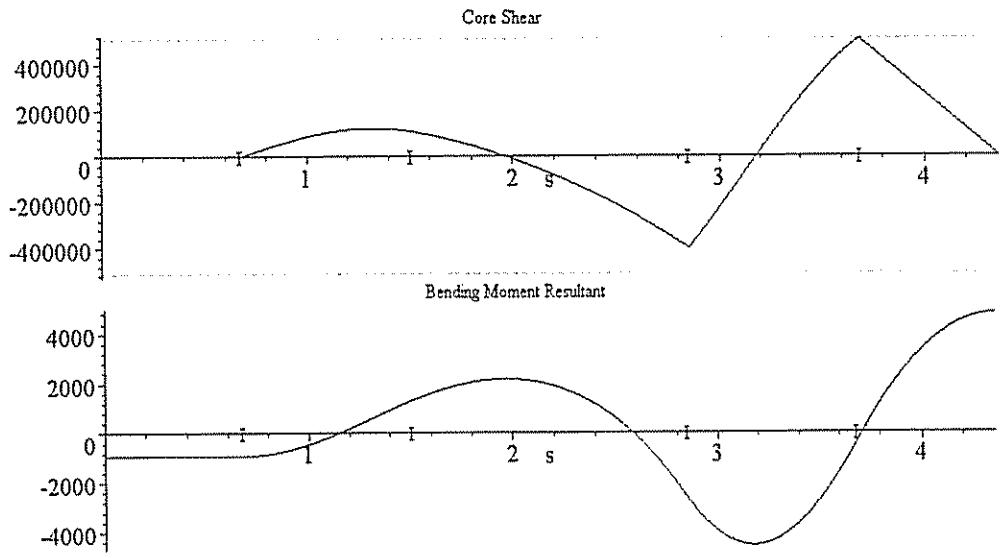

Figure 4.10 Stresses and Moment Resultant of CS-S3 (Sample Loading I, Using the Stress Limitations Only for Optimization)

4.5.2 Results for Case II—(with constant internal pressure)

The optimized values of the faces and core thicknesses and weight can be obtained and are listed in Table 4.5.

Table 4.5 Optimized Geometry and Weight for Sample Case II, Subject to Maximum Allowable Stresses and Lightest Weight Criteria

	t_i (mm)	t_o (mm)	h_c (mm)	W (Kg/m)	Cross section area A (m^2)	R=A/W
CS-S1	1.293	1.410	101.90	121.26	4.598	0.0379
CS-S2	1.377	1.304	123.29	135.27	4.526	0.0335
CS-S3	1.487	1.177	152.21	154.91	4.398	0.0284
CS-S4	1.568	1.090	174.16	170.27	4.279	0.0251
CS-S5	1.700	0.9570	211.28	197.01	4.036	0.0205

CS-R1	1.440	2.006	164.40	197.67	5.400	0.0273
CS-R2	1.506	1.857	186.29	212.69	5.297	0.0249
CS-R3	1.602	1.679	216.20	234.23	5.124	0.0219
CS-R4	1.676	1.557	239.17	251.39	4.969	0.0198
CS-R5	1.800	1.370	278.33	281.49	4.659	0.0166

Also, plots of the in-plane stress in the faces, shear stresses in the cores and the bending moment resultant as functions of the circumferential coordinate, s for the sample geometries are shown in Figure 4.11 through 4.16, along with the maximum allowable in-plane and shear stresses and critical stresses at which the faces will wrinkle.

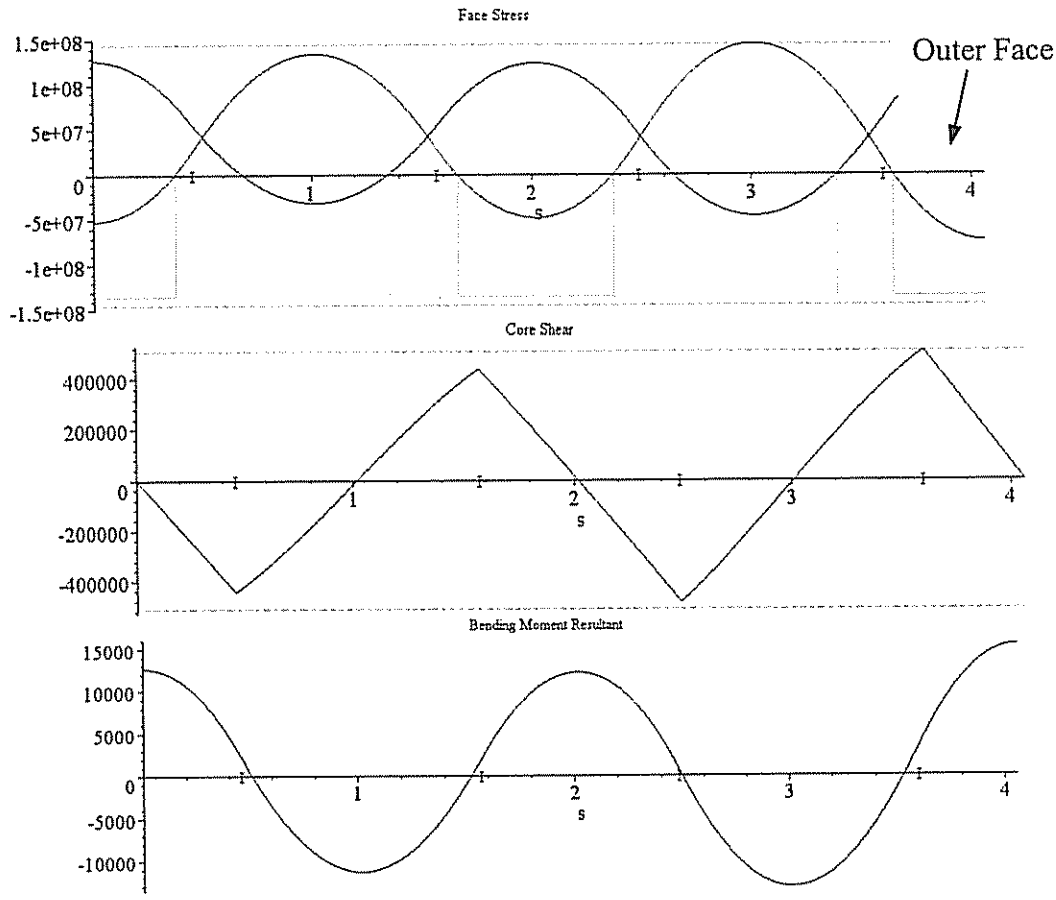

Figure 4.11 Stresses and Moment Resultant of CS-S1 (Sample Case II)

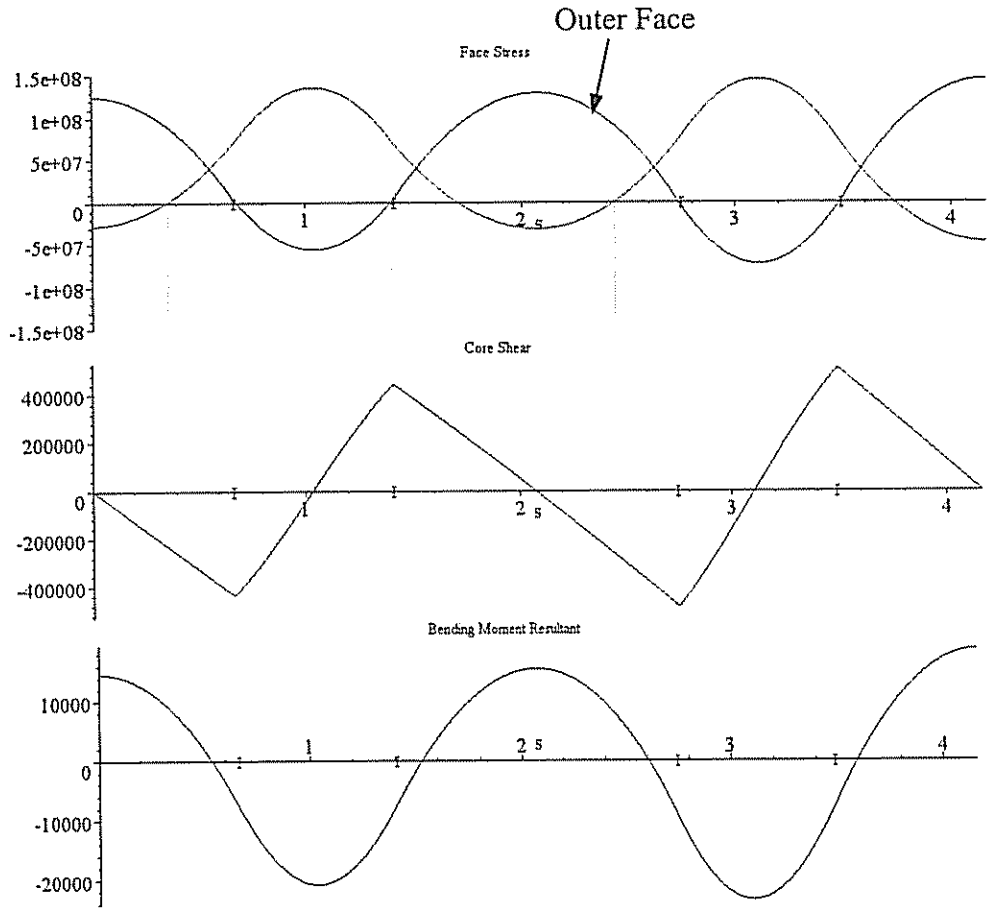

Figure 4.12 Stresses and Moment Resultant of CS-S3 (Sample Case II)

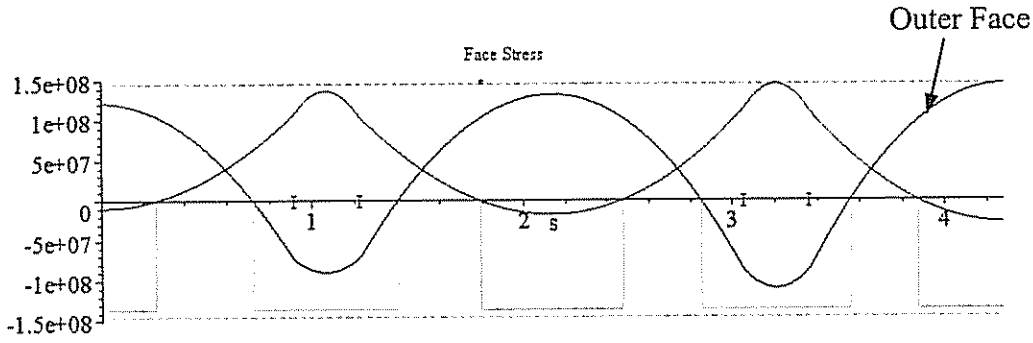

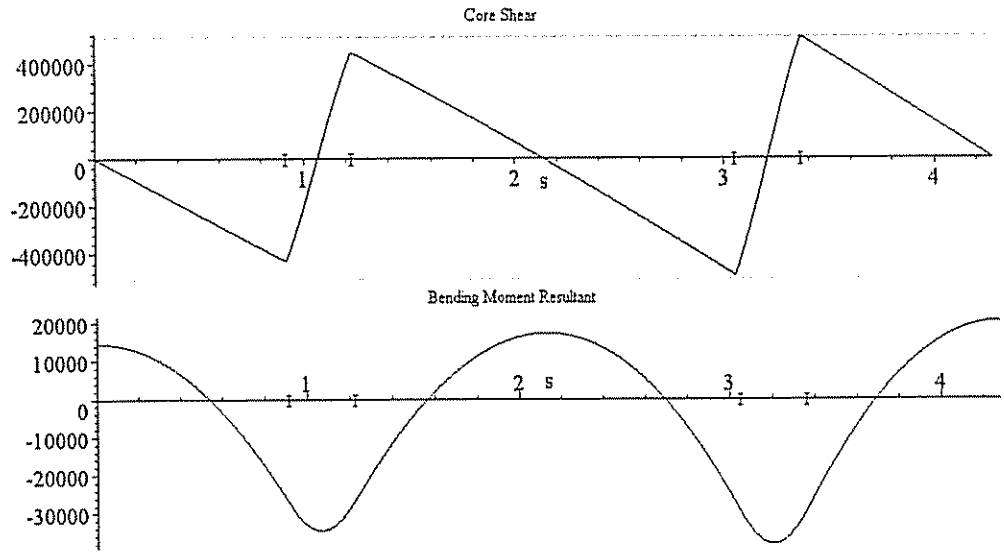

Figure 4.13 Stresses and Moment Resultant of CS-S5 (Sample Case II)

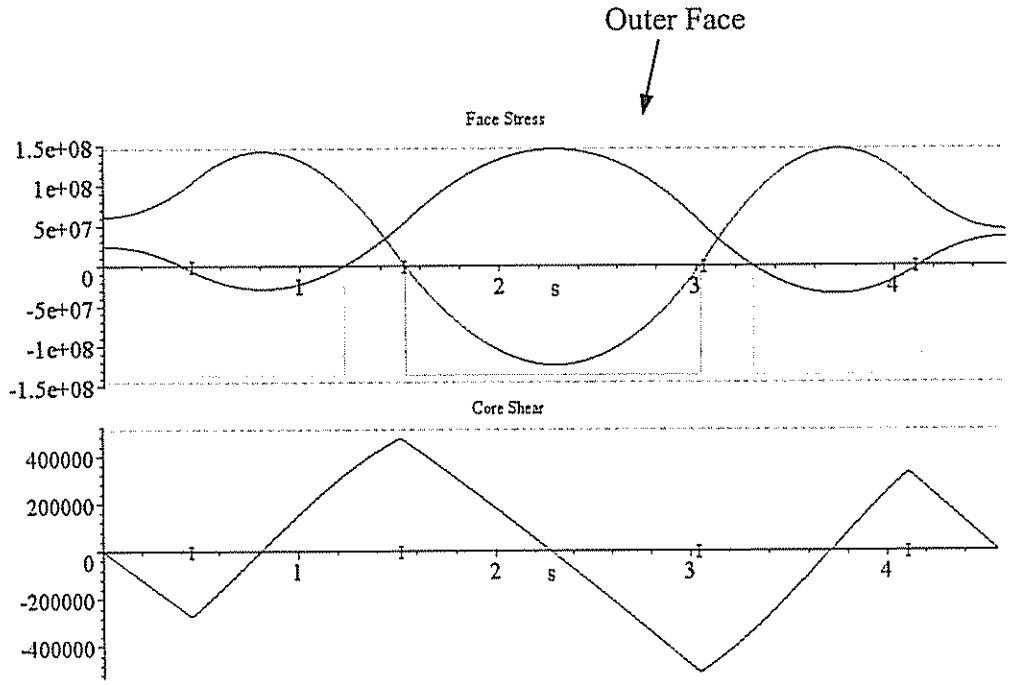

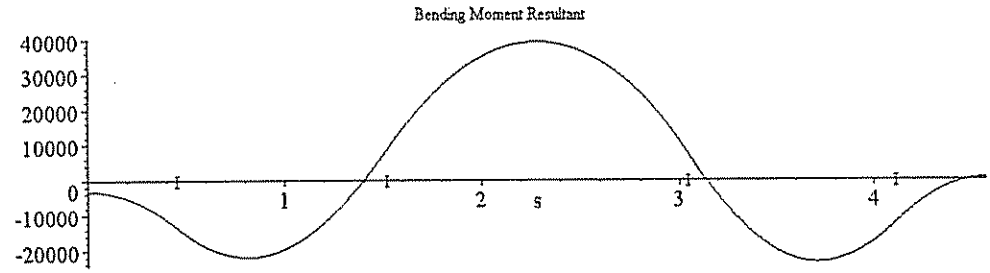

Figure 4.14 Stresses and Moment Resultant of CS-R1 (Sample Case II)

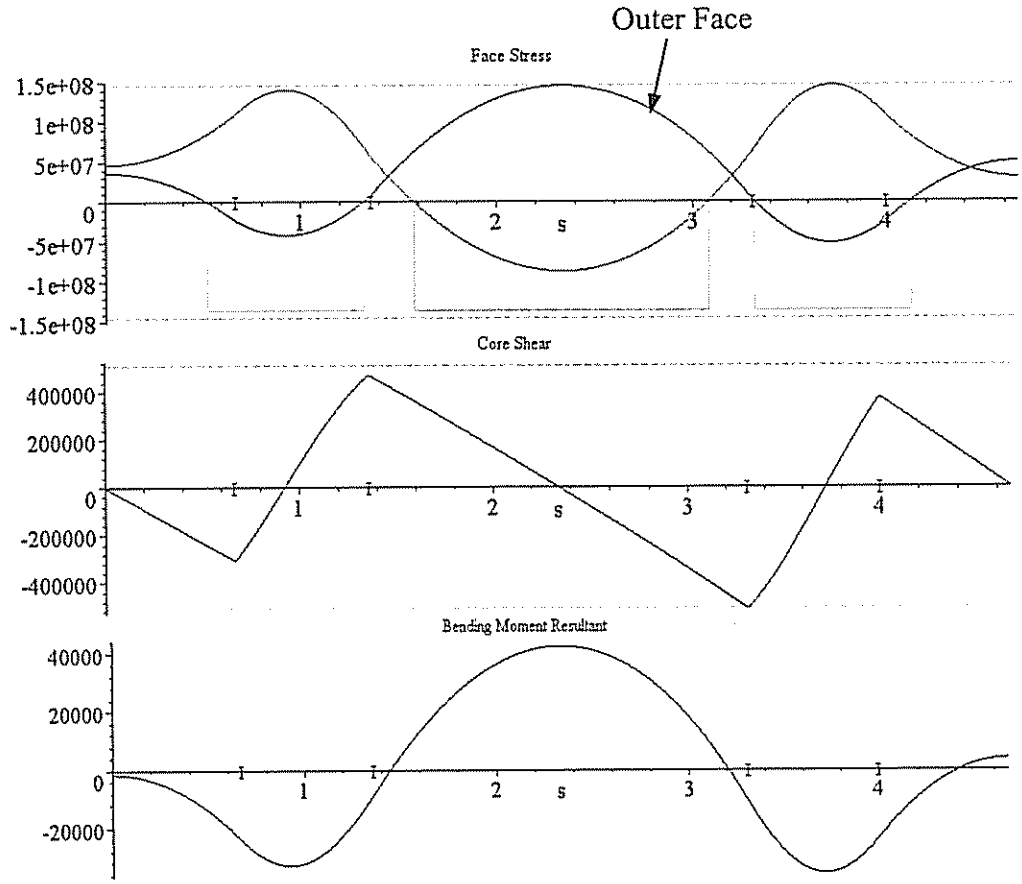

Figure 4.15 Stresses and Moment Resultant of CS-R3 (Sample Case II)

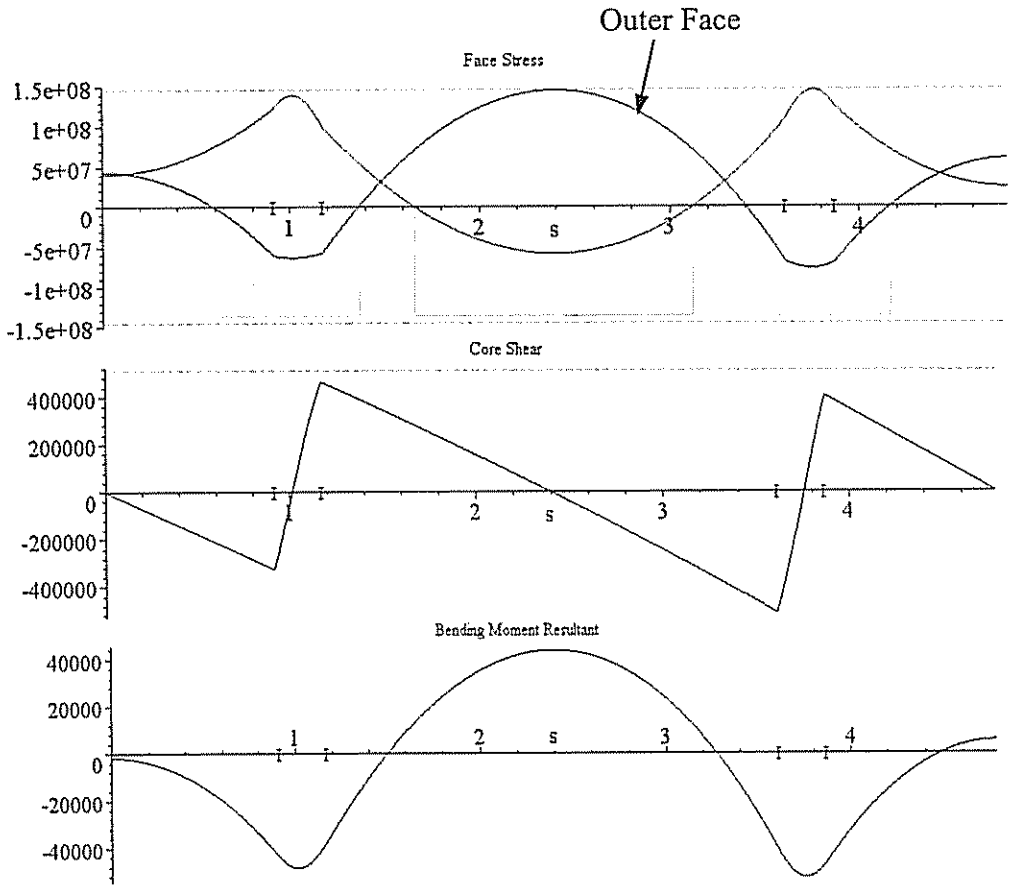

Figure 4.16 Stresses and Moment Resultant of CS-R5 (Sample Case II)

4.6 Critical Failure Points

The points in the structure that experience the greatest stress are the points where the moment resultant and the shear resultant are largest, and can be referred to as Critical Failure Points.

For different geometries of the cross section and the loadings, the locations of the Critical Failure Points are not the same:

- The possible locations where the moment resultant can have the greatest magnitude are at either the middle of one (both, in the case of a square cross

section) of the straight sections or one of the curved sections. Sometimes, the critical points at the curved sections are shifted a bit away from the middle of the corner, and can be designated such as $s_{1.5+}$, $s_{3.5-}$, etc.

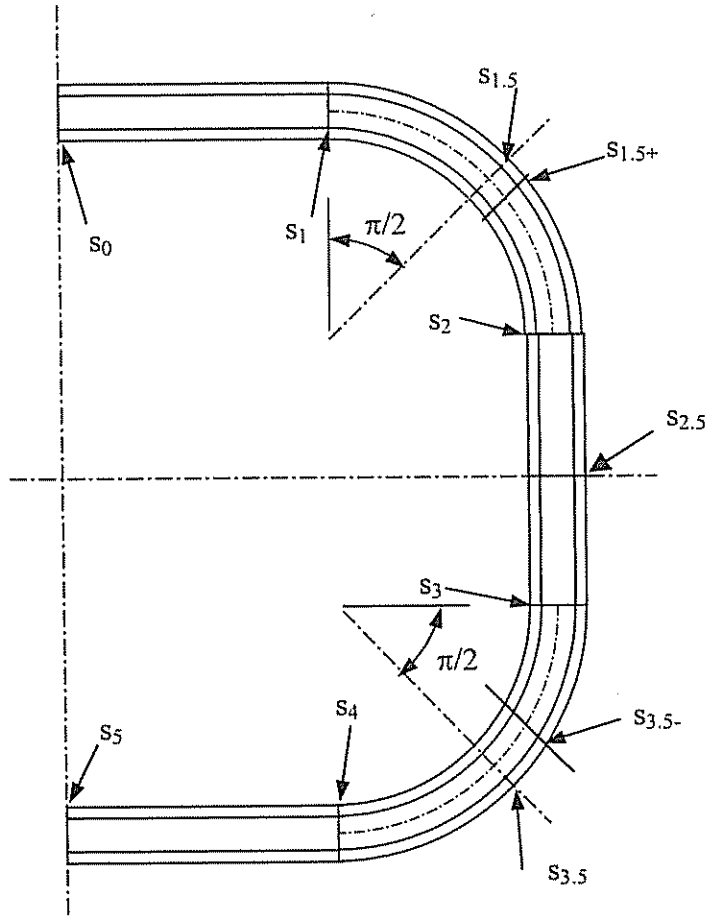

Figure 4.17 Critical Points Where Stresses Are Maximized

- The extreme magnitudes of the shear resultant occur at the joints between the straight and curved sections, say s_1, s_2, s_3, s_4 or s_5, normally the greatest shear critical point is the joint between the vertical and lower curved sections, s_3.

4.7 Discussion of Optimized Geometry

When optimized for the least weight, subject to the restrictions on the stress, the resulting structure has very thin faces and a very thick core. These values for the optimum construction may be useful only in the academic sense. While they do result in the lightest weight construction, they are not practical from an application point of view. In some cases, the optimized geometry also fails to adhere to one of the assumptions posed in the development of the theory: $h << R$. When optimized for lowest weight, h is on the same order as R and h/R may not be small enough to neglect. Also, transverse flexibility of the core is not considered. When 'soft' cores, such as the polymer foams considered here are used, the faces can often deflect relative to one another. This will be most noticeable in the curved section where the transverse normal stresses will try to pull the faces away from each other, stretching the core in the z direction. As such, it must be recognized that there will be a certain amount of associated error in the results, underscoring the preliminary nature of this investigation. These results also show that, under these conditions, the limiting considerations are not the basic in-plane and shear stresses only, but rather are other factors that affect the functional usefulness of the structure. For example, a sandwich face that is less than one millimeter thick may resist the in-plane loads without failure but will not be able to tolerate any concentrated transverse loading from sources such as cargo, fittings, internal structure, etc. The structure would be very susceptible to damage and would not be sufficiently durable.

In the interest of gaining more insight into the effects that various parameters or limitations have on the geometry and weight of the structure, several possibilities are examined in the following Chapter.

4.8 Summary

In this chapter, the overall geometry of the cross section and the geometry of the sandwich were considered. The geometric and material properties of the sandwich were constant in the circumferential direction. Ten different cross sections and two loading cases were selected to be optimized for comparison.

In the next chapter, several factors/parameters were varied to examine their effect on the optimized geometry and the weight of the structure. Also, a preliminary exploration of the situation of varied sandwich geometry in the circumferential direction will be included.

Chapter 5

ANALYSIS OF VARIOUS PARAMETERS INFLUENCING ON THE OPTIMAL STRUCTURE

Further from the baseline study in the previous chapter, here, several parameters will be varied to determine their influence on the optimal truck tank construction.

5.1 Face Wrinkling

One possible mode of failure for a sandwich face loaded in compression is face wrinkling. Face wrinkling is a local elastic instability of the face and is described in more detail by Zenkert [24] and Vinson [22]. When the effects of face wrinkling are considered, the magnitude of the compressive stress in either face must be less than the critical face wrinkling stress. The expression for the critical face wrinkling stress is given by equation (2.56), and will be repeated here with the value of c taken as 0.5.

$$\sigma_{cr} = -0.5\left(E_{f,s} E_c G_{c,sz}\right)^{1/3} \tag{5.1}$$

For the sample loading I described in Chapter 4, when the sandwich profile is optimized for cross section CS-R3 without considering face wrinkling, using the 75 kg/m^3 foam core material and Aluminum 6061-T6 faces, the resulting face and core thicknesses are:

$$t_i = 1.088mm \quad h_c = 43.18mm \quad t_o = 1.129mm \tag{5.2}$$

and the weight per unit length of the structure is 91.21kg/m.

A plot of the in-plane stress in the faces as a function of the circumferential coordinate, s is shown in Figure 5.1 along with the critical stress at which the faces will wrinkle.

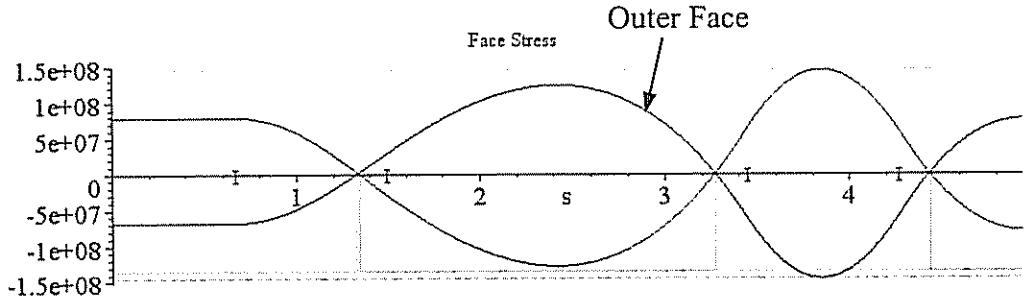

Figure 5.1 In-Plane Stress in the Faces of CS-R3 without Considering Face Wrinkling (Sample Loading I)

As can be seen in Figure 5.1, the compressive stress in the outer face exceeds the critical face wrinkling stress in the lower curved section. When face wrinkling is considered, the outer face must be thickened such that the maximum compressive stress does not exceed either the critical face wrinkling stress or the maximum allowable stress.

When the optimization is performed with face wrinkling included, the resulting sandwich geometry is

$$t_i = 1.069mm \quad h_c = 43.87mm \quad t_o = 1.189mm \tag{5.3}$$

and the weight per unit length of the structure is 92.79kg/m, that have been listed in Table 4.3. The corresponding plot of the in-plane stresses is shown in Figure 4.8.

The weight per unit length of the structure after adjusting the face thicknesses to prevent face wrinkling has an increase of 1.732% in the overall weight.

The increase is so small because the maximum allowable stress of the Aluminum face is very closed to the critical face wrinkling stress calculated. If we use quasi-isotropic Carbon/Epoxy (properties are listed in Table 5.2) is used, there is a larger difference between the maximum allowable stress and the critical face wrinkling stress as the face material, one sees the significance of how the criterion of face wrinkling affects the optimal weight. The results calculated for the cross section CS-R3 with 75 kg/m^3 core under sample loading I are listed in Table 5.1.

Table 5.1 Optimized Construction for CS-R3, Using Quasi-Isotropic Carbon/Epoxy Faces, Sample Loading I, with/without Consideration of Face Wrinkling

	t_i (mm)	t_o (mm)	h_c (mm)	W (Kg/m)
Face Wrinkling	1.238	1.480	37.05	68.88
w/o Face Wrinkling	1.035	0.903	37.43	57.31

One can see that there is a 20.188% weight increase after adding the factor of face wrinkling. Plots of the in-plane stresses with/without Face Wrinkling are shown in Figure 5.2 and Figure 5.3.

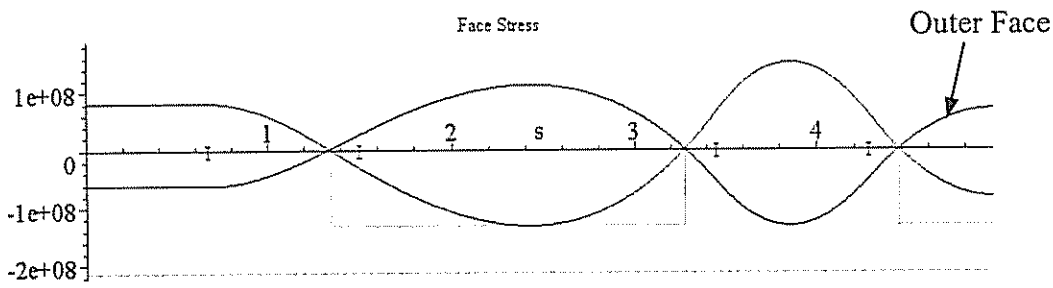

Figure 5.2 In-Plane Stress in the Faces of CS-R3 Considering Face Wrinkling (Sample Case I, Quasi-Isotropic Carbon/Epoxy Faces)

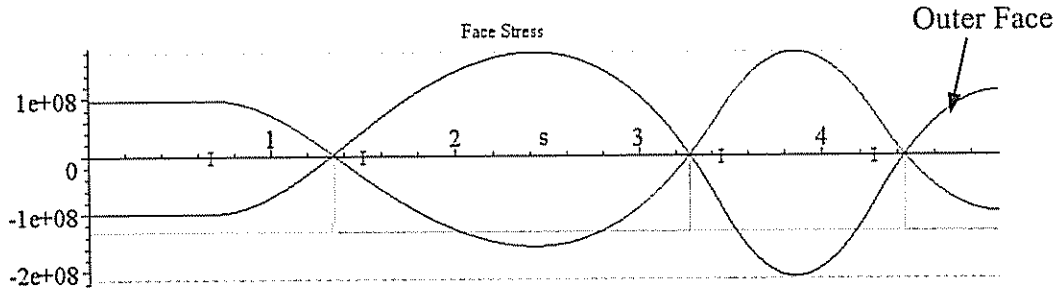

Figure 5.3 In-Plane Stress in the Faces of CS-R3 without Considering Face Wrinkling (Sample Case I, Quasi-Isotropic Carbon/Epoxy Faces)

In some cases, the critical stress will be above the maximum allowable stress for the face in question. In these cases, the weight will not change since face wrinkling will not be the limiting failure mode.

5.2 Minimum Allowable Face Thickness

The face thicknesses that correspond to the lightest weight construction are often too thin to be practical. If a minimum face thickness is prescribed, the optimum construction can be determined subject to this additional constraint. This minimum thickness may be dependent on the face material manufacturer's guidelines,

the concentrated loading that may occur, or any other factor that may apply. For example, consider the sample problem under the sample loading case I, if one defines a minimum face thickness of 1 mm, it will be active for several of the 10 sample cross section geometries. Table 5.2 then lists the optimized core thickness and weight corresponding given this additional restriction.

Table 5.2 Optimized Construction Subject to a Minimum Allowed Face Thickness Dimension

	No Restriction on Face Thickness		Minimum Face Thickness Equal to 1mm				Weight increase by Adding the Restriction (%)
	W (Kg/m)		t_i (mm)	t_o (mm)	h_c (mm)	W (Kg/m)	
CS-S1	53.40		1	1	43.06	71.66	34.195
CS-S2	57.99		1	1	45.98	74.78	28.953
CS-S3	64.39		1	1	49.25	78.67	22.177
CS-S4	69.55		1	1	51.33	81.41	17.052
CS-S5	78.94		1	1	54.20	85.70	8.563
CS-R1	76.83		1	1	42.28	81.65	6.274
CS-R2	82.27		1	1	42.47	83.12	1.033
CS-R3	92.79		1.069	1.189	43.87	92.79	0
CS-R4	100.57		1.127	1.247	48.25	100.57	0
CS-R5	110.86		1.095	1.203	61.50	110.86	0

When both faces are restricted by the minimum thickness, a symmetric sandwich with both faces equal to the minimum allowed thickness results.

The restriction of minimum thickness will substantially affect the durability of the structure, as well as its ability to resist concentrated loads.

5.3 Factor of Safety

When designing structures, an empirical safety factor is often used when determining the allowable stresses. Material properties are not exact values in reality, but rather stochastic variables and a factor of safety helps to allow for any lower-than-expected material properties and/or higher-than-expected loading conditions. Although a stochastic approach is occasionally used where each parameter is given a distribution function (often either a normal distribution or a Weibull distribution) rather than a distinct value and the likelihood of failure calculated, traditionally an empirical safety factor is used. The factor of safety that is used for the allowable stresses in the faces and core can strongly influence the optimized geometry in many cases. Any increase in the factor of safety will result in a heavier structure.

As a baseline for comparison, consider still the cross section geometry CS-R3 which has Aluminum 6061-T6 faces and a 75Kg/m^3 core, under the sample loading case I, i.e., the pure hydraulic loading without constant inner pressure. Table 5.4 shows the effect of increasing the factor of safety for the stresses in the faces and/or the core.

Table 5.3 Effect of the Factor of Safety on Geometry and Weight

$F.S._{face}$	1	2	3	4	5	6	7
$F.S._{core}$	1	2	2	2	2	2	2
t_i (mm)	0.763	1.069	1.299	1.491	1.658	1.806	1.942
h_c (mm)	31.28	43.87	53.40	61.36	68.31	74.54	80.24
t_o (mm)	0.840	1.189	1.457	1.682	1.881	2.060	2.225
W (kg/m)	66.24	92.79	112.81	129.45	143.92	156.86	168.63

$F.S._{face}$	1	2	2	2	2	2	2
$F.S._{core}$	1	3	4	4.5	5	6	7
ti (mm)	0.763	0.821	0.597	0.522	0.462	0.371	0.305
hc (mm)	31.28	56.10	74.43	83.41	92.28	109.73	126.79
to (mm)	0.840	0.922	0.680	0.600	0.535	43.75	0.367
W (kg/m)	66.24	87.79	88.44	90.67	93.61	100.83	109.05

In this table, two series of Factor of Safety are examined: one keeps the F.S. of the core unchanged and varies the F.S. of the faces; the other involves a constant value of F.S. of the faces and a series of varying F.S. of the core. From the table, one can see that the F.S. of the faces has much greater influence on the optimized weight of the structure.

5.4 Studies for the Different Core and Face Materials

For the purpose of comparison, the cross section CS-S3 and CS-R3 are used in this section and the rest of this chapter, also, the sample loading in use will be the sample case I, i.e., the purely hydraulic loading.

First, in parametrically examining the effect of different core density on the optimal structure, three core materials will be used with the same face material Aluminum 6061-T6. The core properties are listed in Table 5.5, and the optimized geometry and weight for both CS-S3 and CS-R3 are listed in Table 5.6.

Table 5.4 Optimized Geometry and Weight for Three Different Cores with Aluminum 6061-T6 Faces

		t_i (mm)	t_o (mm)	h_c (mm)	W (Kg/m)
CS-S3	Foam #1 (75 kg/m^3)	0.711	0.676	49.30	64.39
	Foam #2 (100 kg/m^3)	0.782	0.757	42.14	72.61
	Foam #3 (125 kg/m^3)	0.875	0.849	37.77	81.45
CS-R3	Foam #1 (75 kg/m^3)	1.069	1.189	43.87	92.79
	Foam #2 (100 kg/m^3)	1.258	1.300	37.45	105.50
	Foam #3 (125 kg/m^3)	1.406	1.448	33.52	117.97

It is clear that the lowest weight results when the lightest core material is used.

Then, the optimized weight and sandwich profile for cross sections CS-S3 and CS-R3 with all combination of face materials are compiled in tables 5.6 – 5.9. The core material used is the 75 kg/m^3 foam because this provides the minimum weight construction. The face material abbreviations CE, KE, EG and AL correspond to carbon/epoxy, Kevlar/epoxy, E-glass/epoxy and aluminum. The material properties are listed in Table 5.5. The parametric optimization is based on the criteria that the sandwich must not be over-stressed.

Table 5.5 Properties for Isotropic and Quasi-Isotropic Face Materials

		Quasi-Isotropic Carbon/Epoxy T300/5208	Quasi-Isotropic Kevlar 49/Epoxy	Quasi-Isotropic E Glass/Epoxy	Aluminum 6061 T6
E	GPa	65.48	32.44	40.22	72.0
	psi $\times 10^6$	9.50	4.71	5.83	10.01
G_{12}	GPa	22.60	10.95	15.46	26.0
	psi $\times 10^6$	3.28	1.59	2.24	3.77
G_{23}	GPa	5.60	2.30	11.99	26.0
	psi $\times 10^6$	0.81	0.33	1.74	3.77
ν		0.31	.32	.23	0.33
σ_c	MPa	427.5	144.0	497.5	290.0
	psi $\times 10^3$	62.0	20.9	72.2	37.0
σ_t	MPa	358.6	760.0	667.7	290.0
	psi $\times 10^3$	52.0	110.2	96.8	37.0
V_f	-	0.70	0.60	0.72	NA
ρ	kg/m^3	1536.2	1397.8	1965.0	2700
	lb/ft^3	95.9	87.3	122.7	169.3.

The weight penalty listed in the following tables is the increase in weight for a given material combination compared to the lightest case.

Table 5.6 Optimized Constructions for Cross Section CS-R3 Sorted by Face Material, Core Is 75 kg/m^3 Foam

Materials		Geometry			Weight
Inner face	Outer face	t_i (m)	h_c (m)	t_o (m)	W (kg/m)
CE	CE	1.238	37.05	1.480	68.88
CE	KE	1.232	36.52	2.777	84.32
CE	EG	1.244	36.94	1.705	79.58
CE	AL	1.169	39.07	1.353	82.96
KE	CE	2.239	37.70	1.435	80.81
KE	KE	2.316	35.83	2.796	97.37

KE	EG	2.340	36.39	1.706	92.63
KE	AL	1.912	43.67	1.197	90.74
EG	CE	1.448	36.97	1.501	78.50
EG	KE	1.446	36.28	2.853	94.58
EG	EG	1.453	36.87	1.720	89.14
EG	AL	1.248	42.54	1.255	89.32
AL	CE	1.249	37.96	1.425	83.28
AL	KE	1.094	42.47	2.336	92.98
AL	EG	1.129	41.52	1.495	90.03
AL	AL	1.069	43.87	1.189	92.79

Table 5.7 Optimized Constructions for Cross Section CS-R3, Sorted By Weight.

Materials		Weight W (kg/m)	Weight Penalty (% increase comparative to the lightest combination)
Inner face	Outer face		
CE	CE	68.88	0
EG	CE	78.50	13.966
CE	EG	79.58	15.534
KE	CE	80.81	17.320
CE	AL	82.96	20.441
AL	CE	83.28	20.906
CE	KE	84.32	22.416
EG	EG	89.14	29.413
EG	AL	89.32	29.675
AL	EG	90.03	30.706
KE	AL	90.74	31.736
KE	EG	92.63	34.480
AL	AL	92.79	34.713
AL	KE	92.98	34.988
EG	KE	94.58	37.311
KE	KE	97.37	41.363

Table 5.8 Optimized Constructions for Cross Section CS-S3 Sorted by Face Material, Core Is 75 kg/m^3 Foam

Materials		Geometry			Weight
Inner face	Outer face	t_i (m)	h_c (m)	t_o (m)	W (kg/m)
CE	CE	1.024	36.14	0.971	50.19
CE	KE	1.161	31.51	2.058	61.11
CE	EG	1.108	33.63	1.203	57.30
CE	AL	0.829	43.92	0.768	57.58
KE	CE	1.593	42.29	0.818	57.71
KE	KE	1.745	38.47	1.653	66.28
KE	EG	1.697	40.20	0.988	63.59
KE	AL	1.351	49.02	0.682	64.06
EG	CE	1.042	40.82	0.866	55.87
EG	KE	1.147	36.85	1.772	65.09
EG	EG	1.108	38.64	1.048	61.95
EG	AL	0.875	47.76	0.715	62.59
AL	CE	0.833	42.59	0.812	58.04
AL	KE	0.910	38.81	1.640	66.49
AL	EG	0.883	40.52	0.981	63.80
AL	AL	0.711	49.30	0.676	64.39

Table 5.9 Optimized Constructions for Cross Section CS-S3, Sorted by Weight.

Materials		Weight W (kg/m)	Weight Penalty (% increase comparative to the lightest combination)
Inner face	Outer face		
CE	CE	50.19	0
EG	CE	55.87	11.317
CE	EG	57.30	14.166
CE	AL	57.58	14.724
KE	CE	57.71	14.983
AL	CE	58.04	15.641
CE	KE	61.11	21.757
EG	EG	61.95	23.431

EG	AL	62.59	24.706
KE	EG	63.59	26.699
AL	EG	63.80	27.117
KE	AL	64.06	27.635
AL	AL	64.39	28.292
EG	KE	65.09	29.687
KE	KE	66.28	32.058
AL	KE	66.49	32.477

5.5 Preliminary Study for the Cross Sections with Variable Geometry in the Circumferential Direction

All of the truck-tank cross sections discussed so far have constant geometry in the circumferential direction. The material and sandwich profile were the same at all points in the cross section. Now a more efficient construction will be investigated that would allow the material properties or/and geometry of the sandwich to vary in the circumferential direction to better accommodate stresses that vary with the s coordinate.

5.5.1 Variable Core Thickness

In this section, the core will have a constant thickness and the face thicknesses will vary in a discrete fashion.

As in the previous chapter, the structure will be optimized based on the criteria of obtaining the lowest weight possible without over-stressing the faces or the core, and without allowing face wrinkling.

Using core with a constant thickness, the face thicknesses are adjusted to prevent overstressing or wrinkling of the faces due to the bending load or overstressing of the core due to shear load. The point where the bending load is the lowest is very close to the point where the shear load is greatest so the two requirements have a tendency to work against each other. As a sample case, the exploration using the cross

section CS-R3 with Aluminum 6061-T6 faces and a varied-thickness core has a density of 75 kg/m^3, under sample loading I will be illustrated.

The sandwich face profile and the plots of in-plane and shear stress for the sample structure are shown in Figures 5.4 to 5.6. In each section, the thicknesses of the faces are optimized to be as thin as possible without allowing face wrinkling or over-stressing. In every iteration, the optimal core thickness is calculated for each segment and the thickest value used for the entire face.

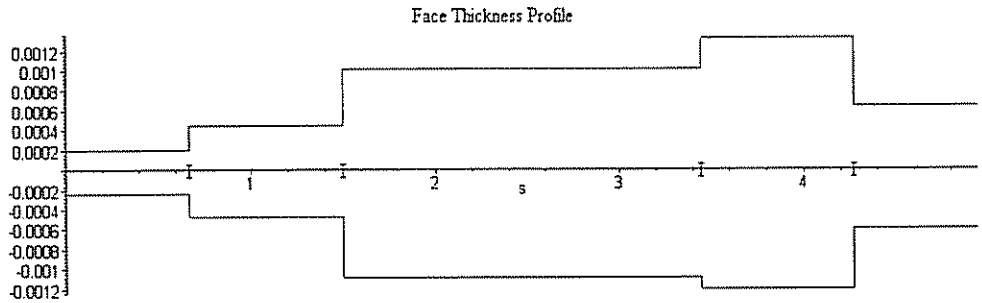

Figure 5.4 Sandwich Faces Profile for the Case of Variable Face Thicknesses

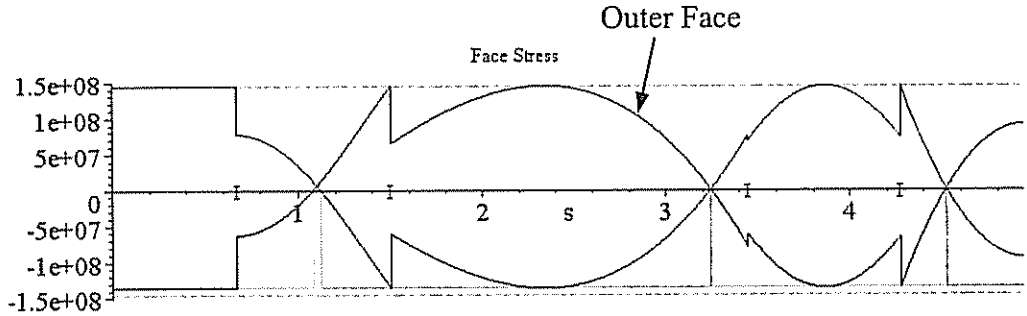

Figure 5.5 In-Plane Stresses Plots for Sandwich with Variable Face Thicknesses

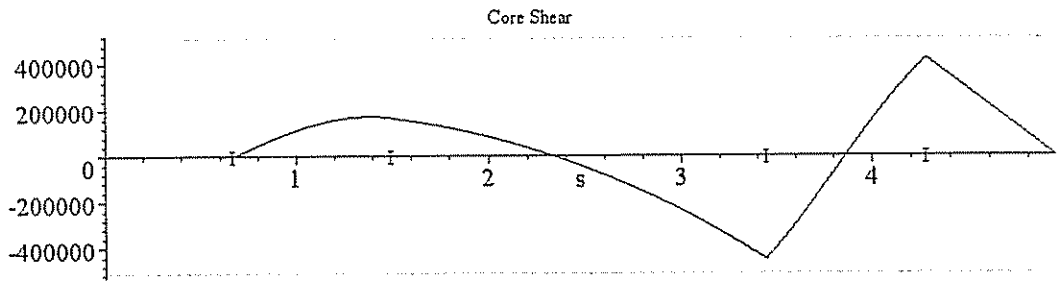

Figure 5.6 Stress Plots for Sandwich with Variable Face Thicknesses

The resulting face thicknesses and optimal weight are:

$$h_c = 44.85mm \qquad W = 76.70kg/m \tag{5.1}$$

It can be seen from Figure 5.4 that if the entire faces were as thick as the thickest part, the structure would be significantly over-built in other areas. The stress plots show that the faces and core are being utilized with greater efficiency when the thicknesses of the faces are allowed to vary in the circumferential direction. Compared to the result from the constant-geometry sandwich of the same cross section that has a weight value of 92.79kg/m, there is a 17.34 percent decrease in weight.

Obviously when a greater number of segments are used, a closer approximation to a smooth variation of the thickness will be obtained, but in this preliminary study, only five segments are used to show the general trend.

Although the efficiency of the sandwich has been improved by using variable face thicknesses, greater weight savings can be achieved by allowing both the core and the faces to vary in the circumferential direction.

5.5.2 Sandwich with Variable Face and Core Thickness

If the thickness of the faces of the sandwich are allowed to vary in the circumferential direction, the material can be utilized more efficiently than when they are of constant thickness. The limiting case would be when the entire face is at the maximum allowable in-plane stress and the core is at the maximum allowable shear stress over the entire cross section. Since this does not leave any extra capacity for additional loading conditions, the results only serve to demonstrate that greater weight savings can be achieved by allowing as many properties as possible to vary according to the local stress levels. For comparison, the cross section CS-R3 with Aluminum 6061-T6 faces and the core that has a density of 75 kg/m^3 are again used. The optimized profile of faces and the whole sandwich profile are shown separately in Figure 5.7 and Figure 5.8, since if the same scale is used and put them into a single picture, the variation of the face thicknesses is too small to be noticed. In these two figures, the interface between the faces and the core is the z = 0 plane. Figure 5.9 to Figure 5.11 are the plots of in-plane stresses in faces, shear stress in the core and the bending moment resultant.

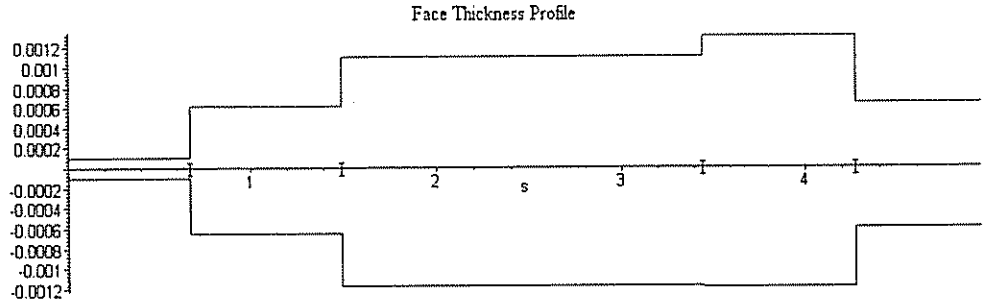

Figure 5.7 Plot of the Face Thickness with the Core Excluded for the Case of Variable Face and Core Thicknesses

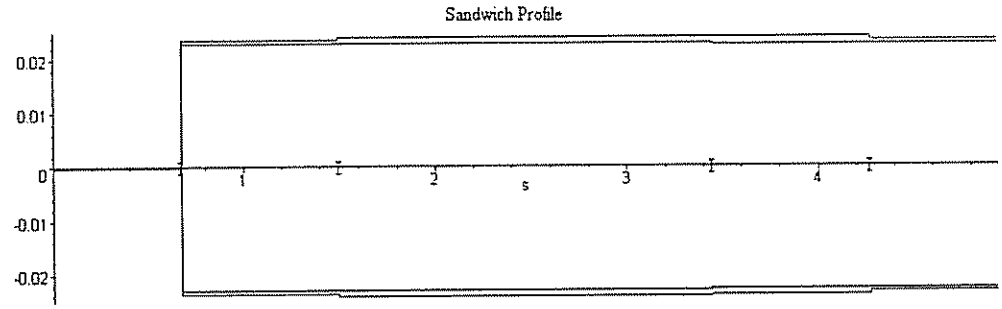

Figure 5.8 Plot of Sandwich Profile for the Case of Variable Face and Core Thicknesses

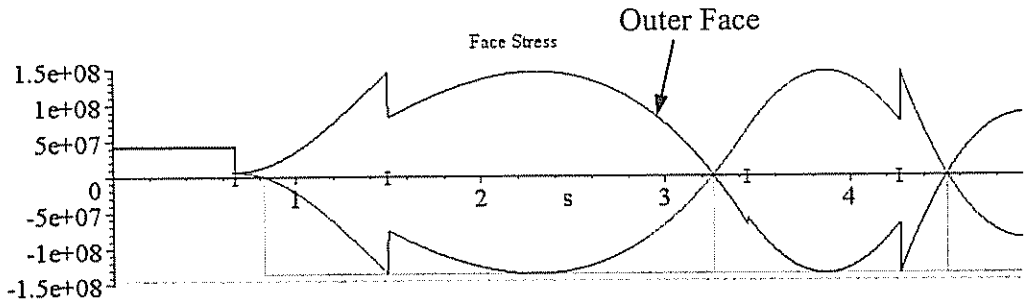

Figure 5.9 In-Plane Stresses Plots for Sandwich with Variable Face and Core Thickness

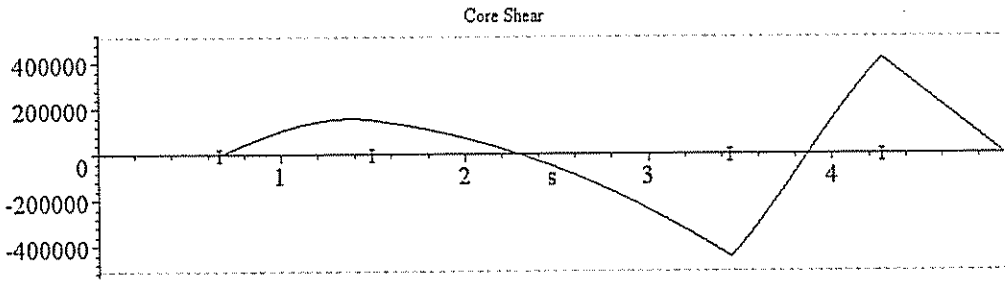

Figure 5.10 Stress Plots for Sandwich with Variable Face and Core Thickness

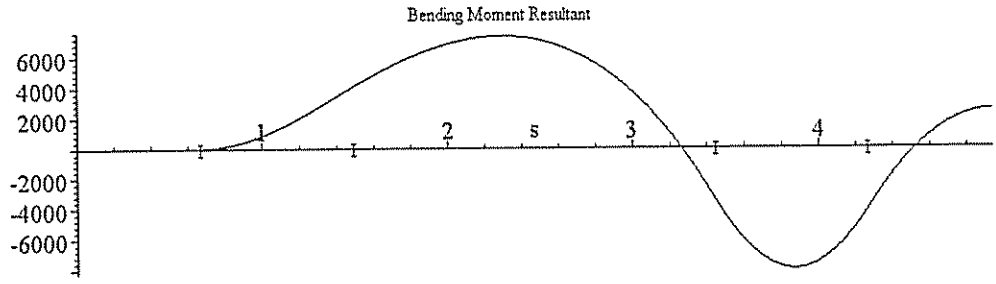

Figure 5.11 Bending Moment Resultant Plots for Sandwich with Variable Face and Core Thickness

The weight per unit length of the optimized structure is 45.86kg/m. Compared to the constant-geometry sandwich, there is a significant reduction of 50.58 percent.

If the structure is to be able to withstand any other types of loading, such as beam bending or torsion, the faces will need to be limited to a minimum thickness.

5.6 Summary

In this chapter, the effects of several parameters, such as face wrinkling, core density, factor of safety and minimum face thickness on the optimal structure and weight were examined. Optimal weights for different face material combinations were calculated for comparison. Also, a preliminary study for the case of varied cross section geometries in the circumferential direction was conducted.

Chapter 6

CONCLUSIONS AND RECOMMENDATIONS FOR FURTHER RESEARCH

In this thesis, the use of sandwich construction for a truck tank structure has been investigated. In order to improve the efficiency of the structure, the sandwich was allowed to take on a mid-plane asymmetric configuration where one face could be thicker than the other, involve different materials or different stacking sequences. Different material combinations for the faces were investigated to determine the choice that results in the lightest structure. The loading considered was mainly concentrated in a linear-varied loading to accommodate the purpose of liquid transportation, and the mathematical formulation did not include in-plane shear loads or bending loads in the axial direction of the shell. This is consistent with the analysis of a cross section that is sufficiently far from the ends of the shell, reinforcing bulkheads, etc. as to be outside of the bending boundary layers induced by those restraints, allowing the assumption of a plane-strain condition in the axial direction.

The shape of the cross section was that of a rectangle with rounded corners. In the region outside the bending boundary layers, this was modeled as a combination of straight beams and circular ring sections. Analytical solutions were obtained for the response by solving the governing differential equations and applying the appropriate boundary and matching conditions.

6.1 Conclusions from Chapter Four

In Chapter Four, the effects of the overall geometry of the cross section were examined. It was found that, because of the large bending loads introduced by the straight beam sections, a circular cross section, i.e. no straight sections, results in the lightest construction possible. This was expected since a circular shell handles all of the internal pressure loadings as in-plane membrane stresses. There are many reasons why this may not be the ideal construction, such as cost and manufacturability, efficiency of the geometry of the cargo bay in terms of usable space, etc. In order to further explore the axially asymmetric possibilities, ten cross section geometries were chosen for additional analysis. All of the cross sections were specified to fulfill the outside dimension limitations on the American highway system.

It was found that a square cross section resulted in a lighter structure than a rectangular cross section with the same corner radius. This is because the bending loads in the horizontal sections (the top and bottom of the shell) are more completely counteracted by the bending loads in the vertical sections when they are of the same length. In the rectangular cross sections, the greatest bending moment occurs in the middle of the longer straight section, while in the square cross sections it is in the middle of the corner section. In both the square and rectangular cross sections there was a trend of decreasing weight with increased corner radius.

It was noticed that the core shear stresses is not necessary to reach the maximum core shear limits for the overall structure to achieve the lightest weight.

When the thickness of the core and faces remain constant in the circumferential direction, the faces experience the greatest in-plane stresses either at the middle of one of the straight sections or near (or at) the 45 degree point in one of

the curved sections. The core experiences the greatest shear stress at the junction between the vertical straight section and the lower corner section.

6.2 Conclusions from Chapter Five

In Chapter Five, several factors that may affect the optimized structure and weight were examined. Cross section CS-R3 and sample loading I were used as a baseline to investigate the sensitivity of the results to those factors.

It was found that in many cases, the critical face wrinkling stress was lower than the allowable compressive stress for the faces, so it must be taken into account as an optimization criterion.

The optimum face thicknesses are very thin, and in practical applications the faces may need to be thicker than the optimum value for lowest weight to account for durability concerns, localized loading, etc. The effect of specifying a minimum face thickness sometimes may significantly increase the weight of the structure.

The optimal weight of the structure is more sensitive to the factor of safety of the face than that of the core.

Three core materials were compared, and it was concluded that the with the lightest density the lowest sandwich weight results.

The optimum construction was determined for each combination of materials. The carbon/epoxy composite proved to be the lightest choice of materials when used for both faces.

A preliminary investigation was performed for the situation of variable geometry in the circumferential direction. With the thickness of the core and faces allowed to vary in the circumferential direction, a more efficient utilization of the materials can be achieved.

6.3 Summary

In brief, the conclusions that can be drawn from this investigation are that under the loading and restrictions included here:

- The best overall geometry will depend on factors other than the internal volume to weight ratio.
- The weight of the structure increases as the radius of the corner decreases.
- For a given corner radius, a square cross section will be lighter than a rectangular one that has the same outer or dimensions.
- Of the materials analyzed here, the 75 kg/m^3 foam core and quasi-isotropic carbon/epoxy composite faces are the best choice of materials for the structure.
- When the geometry of the sandwich is allowed to vary in the circumferential direction, significant weight savings can be achieved.

6.4 Recommendations for Further Research

In future research, other loading conditions such as solid cargo loads can be analyzed. These include, but are not limited to, beam action bending of the tank, torsion loading, vibration and the response within the bending boundary layers.

In addition to allowing the thickness of the sandwich components to vary in the circumferential direction, the material properties themselves may be varied. For example, a layer of stiffer foam could be introduced just under the face in areas of high compressive stresses to increase the critical face wrinkling stress. The density of the core could be allowed to vary in the circumferential direction. The faces could include additional layers of Kevlar in areas of high tensile stress. Web stiffeners could be introduced into the core in the areas of high shear stress. Finite element solutions could be used to gain insight into the behavior near bulkheads and other restrictive supports.

Since the deflection are often greater than those which can be considered small, the effects of the geometric non-linearity should be studied using a theory based on a class of medium deflections that will encompass those experienced by the structure.

REFERENCES

1. Aiello, M. A. and Ombres, L., 1997. "Local Buckling Loads of Sandwich Panels Made With Laminated Faces," *Composite Structures*, Vol. 38, 1997, pp. 191 – 201.

2. Bau-Madsen, N. K., Svendsen, K. H., and Kildegaard, A., 1993. "Large Deflections of Sandwich Plates – An Experimental Investigation," *Composite Structures*, Vol. 23, 1993, pp. 47 – 52.

3. Beer, F. P., and Johnston, R. E., Jr., 1981. "Mechanics of Materials," McGraw Hill, Inc., New York, NY, 1981.

4. Bozhevolnaya, E. and Frostig, Y., 1997. "Nonlinear Closed – Form High – Order Analysis of Curved Sandwich Panels," *Composite Structures*, Vol. 38, 1997, pp. 383 – 394.

5. Caisheng, Z., Heller, M. and Lam, Y. C., 1993. "Analytical Formulae For Calculating Stresses In Unidirectional / Cross-Ply Unbalanced Composites," *Composite Structures*, Vol. 24, 1993, pp. 333 – 343.

6. Flanagan, G., 1993. "A Sublaminate Analysis Method For Predicting Disbond and Delamination Loads In Composite Structures," *Journal of Reinforced Plastics and Composites*, Vol. 12, August, 1993, pp. 876 – 887.

7. Fox, R. W., and McDonald, A. T., 1992. "Introduction to Fluid Mechanics, Fourth Edition," John Wiley & Sons, New York, NY, 1992.

8. Frostig, Y. and Shenhar, Y., 1995. "High – Order Bending of Sandwich Beams With A Transversely Flexible Core and Unsymmetrical Laminated Composite Skins," *Composite Engineering*, Vol. 5, No. 4, 1995, pp. 405 – 414.

9. Frostig, Y., Baruch, M., Vilnay, O. and Sheinman, I., 1991. "Bending of Nonsymmetric Sandwich Beams With Transversely Flexible Core," *Journal of Engineering Mechanics*, Vol. 117, No. 9, September, 1991, pp. 1931 – 1952.

10. Frostig, Y. and Rabinovitch, O., "Behavior of Unidirectional Sandwich Panels with a Multi-Skin Construction or a Multi-Layered Core Layout—High-Order Approach," *Journal of Sandwich Structures and Materials*, Vol.2, July 2000, pp. 181-213.

11. Heath, W. G., 1960. "Sandwich Construction Part 2: The Optimum Design of Flat Sandwich Panels," *Aircraft Engineering*, August, Vol. 32, 1960, pp. 230 – 235.

12. Hoff, N. J. and Mautner, S. E., 1945. "Buckling of Sandwich Type Panels," *Journal of the Aeronautical Sciences*, Vol. 12, No. 3, 1945, pp. 245 – 297.

13. Kwon, Y. W. and Fuller, L. B., 1994. "Compressive Failure of Sandwich Composites After Impact Loading," *Recent Advances In Structural Mechanics*, PVP-Vol. 295/NE-Vol. 16, 1994, pp. 53 – 63.

14. Monforton, G. R., and Ibrahim, I. M., 1975. "Analysis of Sandwich Plates With Unbalanced Cross – Ply Faces," *International Journal of Mechanical Science*, Vol. 17, 1975, pp. 227 – 238.

15. Qatu, M. S., 1993. "Theories and Analysis of Thin and Moderately Thick Laminated Composite Beams," *International Journal of Solids Structures*, Vol. 30, No. 20, 1993, pp. 2743 – 2756.

16. Satapathy, N.R. and Vinson, J.R., "Sandwich Beam with mid-plane Asymmetry Subjected to Lateral Loads", Journal of Sandwich Structures and Materials, Vol. 3, No. 4, October 2000, pp. 379-390

17. Shenhar, Y., Frostig, Y., and Altus, E., 1996. "Stresses and Failure Patterns In the Bending of Sandwich Beams With Transversely Flexible Cores and Laminated Composite Skins," *Composite Structures*, Vol. 35, 1996, pp. 143 – 152.

18. Singh, G. and Rao, G. V., 1998. "Nonlinear Oscillations of Thick Asymmetric Cross – Ply Beams," *Acta Mechanica*, Vol. 127, 1998, pp. 135 – 146.

19. Sun, C. T., and Chin, H., 1987. "Analysis of Asymmetric Composite Laminates," *AIAA Journal*, Vol. 26, No. 6, 1987, pp. 714 – 718.

20. Tanov, R., and Tabiei, A., 1999. "Finite Element Implementation of a New Sandwich Homogenization Procedure," *Proceedings of the American Society for Composites*, Fourteenth Technical Conference, 1999, pp. 693 – 703.

21. Thomsen, O. T., "Modeling of Multi-Layer Sandwich Type Structures Using a High-Order Plate Formulation," *Journal of Sandwich Structures and Materials*, Vol.2, October 2000, pp. 331-349.

22. Vinson, J. R., 1999. "The Behavior of Sandwich Structures of Isotropic and Composite Materials," Technomic Publishing Company, Inc., Lancaster, PA, 1999.

23. Vinson, J. R., and Sierakowski, R. L., 1987. "The Behavior of Structures Composed of Composite Materials," Kluwer Academic Publishers, Dordrecht, Netherlands, 1987.

24. Zenkert, D., 1995. "An Introduction to Sandwich Construction," Engineering Materials Advisory Services, Ltd., London, United Kingdom, 1995

Appendix A

MAPLE WORKSHEET

```
> restart:
```

Input Section

Any system of units may be used as long as there is consistency between all of the entries (don't forget material properties)

```
> Digits:=12:
```

file containing the input data

```
> input_data_file:="C:/thesis/cs.txt";
```

file for storing the output data

```
> output_data_file:="C:/the/temp_output.txt";
```

Include effects of transverse shear deformation?

```
> tsd:="yes";
```

Optimize faces and core?

```
> opt_face:="yes";  opt_core:="yes";
```

will the faces and core have constant geometric and material properties?

```
> constant_face_properties:="yes": constant_core_properties:="yes";
```

Check for face wrinkling?

```
> face_wrinkle:="yes";
> read input_data_file;
```

Factor of safety for allowable in-plane stresses in the faces

```
> FS1:=2;
```

Factor of safety for allowable shear stresses in the core

```
> FS2:=2;
```

constant c in face wrinkling equation

```
> fw_const:=1/FS1*0.5e+0;
```

n is the maximum number of times the face and core thicknesses will be varied in the optimization loop

```
> n:=16;
```

set allowable deflection as a fraction of the total thickness of the sandwich

```
> d_fraction:=1/10;
```

Loading Properties and RHO is the mass density of the hydraulic load

```
> RHO:=1000;
> g:=9.8;
> p[0]:=pressure;
```

Assign Lengths and check for errors

internal pressure must be renamed since the subscript can't be saved, nseg is the total number of segments in beam (half cross section)

```
> nseg:=h1seg+c1seg+vseg+c2seg+h2seg;
```

Assign lengths for the upper horizontal section

```
> for i from 1 to h1seg do
> L[i]:=hLengths[i];
> od;
```

Assign lengths for the vertical section

```
> for i from 1 to vseg do
> L[i+h1seg+c1seg]:=vLengths[i];
> od;
```

Assign lengths for the upper curved section

```
> corner_seg:=2:
> for i from 1 to c1seg do
> L[i+h1seg]:=R*Angle[i];
> od;
> outer_R:=R;
Assign lengths for the lower curved section
> for i from 1 to c2seg do
> L[i+h1seg+c1seg+vseg]:=R*Angle[i];
> od;
Assign lengths for the lower horizontal section
> for i from 1 to h2seg do
> L[i+h1seg+c1seg+vseg+c2seg]:=hLengths[i];
> od;
```

Error Checking

```
> Asum:=0:
> for i from 1 to c1seg do
> Asum:=Asum+Angle[i];
> od;
> if Asum <> Pi/2 then print ("ERROR!  angles must total Pi/2"); fi:
> Asum:=0:
> for i from 1 to c2seg do
> Asum:=Asum+Angle[i];
> od;
> if Asum <> Pi/2 then print ("ERROR!  angles must total Pi/2"); fi:
```

Materials

Specify the materials for the inner face, outer face and core

If it is desired to specify different materials for different segments, simply define the material matrix with i as the segment and 1, 2 or 3 to indicate the inner face, core or outer face

```
> for i from 1 to nseg do
> material[i,3]:=outerface_material;
> material[i,2]:=core_material;
> material[i,1]:=innerface_material:
> od:
```

Read Material Properties
note: the 1 direction is the axial direction.
If fibers are aligned in the hoop direction, the 2 direction is the fiber direction

```
> for i from 1 to nseg do
> for j from 1 to 3 do
> read material[i,j];
> E[11][i,j]:=E11;
> E[22][i,j]:=E22;
> G[12][i,j]:=G12;
> G[23][i,j]:=G23;
> nu[12][i,j]:=nu12;
> nu[21][i,j]:=nu[12][i,j]*E[22][i,j]/E[11][i,j];
> sigma_allow_compressive[1][i,j]:=yield_stress_compression1/FS1;
> sigma_allow_compressive[2][i,j]:=yield_stress_compression2/FS1;
> sigma_allow_tensile[1][i,j]:=yield_stress_tension1/FS1;
> sigma_allow_tensile[2][i,j]:=yield_stress_tension2/FS1;
> sigma_allow_shear[i,j]:=yield_stress_shear/FS2;
> rho.i.j:=rho;
> od;
> od;
```

Calculate the Q matrix for each section

```
> for i from 1 to nseg do
> for j from 1 to 3 do
> Q[11][i,j]:=E[11][i,j]/(1-nu[12][i,j]*nu[21][i,j]);
> Q[12][i,j]:=nu[12][i,j]*E[22][i,j]/(1-nu[12][i,j]*nu[21][i,j]);
> Q[22][i,j]:=E[22][i,j]/(1-nu[12][i,j]*nu[21][i,j]);
> Q[44][i,j]:=G[23][i,j];
> Q[66][i,j]:=G[12][i,j];
> od;
> od:
```

Optimization loop

```
> inner_max:=array(1..nseg,1..n):
> inner_min:=array(1..nseg,1..n):
> outer_max:=array(1..nseg,1..n):
> outer_min:=array(1..nseg,1..n):
```

> t1:=array(1..nseg,1..n+1):
> t3:=array(1..nseg,1..n+1):
> hc:=array(1..nseg,1..n+1):

initialize the face and core thicknesses to those specified by the user

> for i from 1 to nseg do
> t1[i,1], hc[i,1], t3[i,1]:=t_i[i], h[i], t_o[i]:
> od:

Main optimization loop

> for j from 1 to n do

Reset the dependent variables for each iteration

> for i from 1 to nseg do
> t_i[i]:=t1[i,j]:t_o[i]:=t3[i,j]:h[i]:=hc[i,j]:
> C.i[1]:=evaln(C.i[1]);C.i[2]:=evaln(C.i[2]);C.i[3]:=evaln(C.i[3]):
> C.i[4]:=evaln(C.i[4]);C.i[5]:=evaln(C.i[5]);C.i[6]:=evaln(C.i[6]):
> od:
> Const:=evaln(Const):Boundary:=evaln(Boundary):
> R:=outer_R-(t_i[corner_seg]/2+h[corner_seg]/2+t_o[corner_seg]/2):
> inner_R:=R-(t_i[corner_seg]/2+h[corner_seg]/2+t_o[corner_seg]/2):

Re-assign lengths for the curved section to adjust for the thickness of the sandwich

> for i from 1 to c1seg do
*> L[i+h1seg]:=R*Angle[i]:*
> od:
> for i from 1 to c2seg do
*> L[i+h1seg+c1seg+vseg]:=R*Angle[i]:*
> od:

A, B, D Matrix

> for i from 1 to nseg do
> z.i[3]:=(h[i]+t_i[i]+t_o[i])/2: distance from mid-plane of sandwich to top of outer face
> z.i[2]:=(h[i]+t_i[i]-t_o[i])/2: distance from mid-plane of sandwich to top of core
> z.i[1]:=(t_i[i]-h[i]-t_o[i])/2: distance from mid-plane of sandwich to top of inner face
> z.i[0]:=(-h[i]-t_i[i]-t_o[i])/2: distance from mid-plane of sandwich to bottom of inner face

Calculate the A, B, D stiffnesses.
note: DD[22]] is used instead of D[22] since Maple reserves D as the symbol for a partial derivative

```
> A.i[11]:=Q[11][i,1]*(z.i[1]-z.i[0])+Q[11][i,2]*(z.i[2]-z.i[1])+Q[11][i,3]*(z.i[3]-
z.i[2]):
> A.i[12]:=Q[12][i,1]*(z.i[1]-z.i[0])+Q[12][i,2]*(z.i[2]-z.i[1])+Q[12][i,3]*(z.i[3]-
z.i[2]):
> A.i[22]:=Q[22][i,1]*(z.i[1]-z.i[0])+Q[22][i,2]*(z.i[2]-z.i[1])+Q[22][i,3]*(z.i[3]-
z.i[2]):
> A.i[44]:=5/4*(Q[44][i,1]*(z.i[1]-z.i[0]-4/3*(z.i[1]^3-
z.i[0]^3)/(h[i]+t_i[i]+t_o[i])^2)+Q[44][i,2]*(z.i[2]-z.i[1]-4/3*(z.i[2]^3-
z.i[1]^3)/(h[i]+t_i[i]+t_o[i])^2)+Q[44][i,3]*(z.i[3]-z.i[2]-4/3*(z.i[3]^3-
z.i[2]^3)/(h[i]+t_i[i]+t_o[i])^2)):
> B.i[12]:=1/2*(Q[12][i,1]*(z.i[1]^2-z.i[0]^2)+Q[12][i,2]*(z.i[2]^2-
z.i[1]^2)+Q[12][i,3]*(z.i[3]^2-z.i[2]^2)):
> B.i[22]:=1/2*(Q[22][i,1]*(z.i[1]^2-z.i[0]^2)+Q[22][i,2]*(z.i[2]^2-
z.i[1]^2)+Q[22][i,3]*(z.i[3]^2-z.i[2]^2)):
> DD.i[22]:=1/3*(Q[22][i,1]*(z.i[1]^3-z.i[0]^3)+Q[22][i,2]*(z.i[2]^3-
z.i[1]^3)+Q[22][i,3]*(z.i[3]^3-z.i[2]^3)):
> od:
```

Define functions for in-plane, lateral and shear displacements
All calculations are done for half part of the cross section and mirrored due to the symmetry about the vertical and horizontal axes.

```
> s0:=0:
> for i from 1 to nseg do
> s.i:=(s.(i-1)+L[i]):        position of ith  junction
> od:
```

For Each Section (Upper Horizontal, Upper Curved, Vertical, Lower Curved and Lower Horizontal):
Define Displacement functions for v(s), w(s) and beta(s). Displacements are in terms of theta for the Upper Curved section, alpha for the Lower Curved section, and are converted to s using formulae given.
Define Strain functions: epsilon[2] and epsilon[23], and the curvature kappa.
Define Stress and Moment Resultants.

Note: The BBar and DBar formulas have been inverted from the normal form. This prevents 'division by zero' errors when analyzing symmetric sandwiches. To account for this inversion, BBar and DBar are used where 1/BBar and 1/DBar are ordinarily used.

Upper Horizontal Section

```
> for i from 1 to h1seg do
```

Define Displacement functions

```
> DBar.i:=A.i[22]/(DD.i[22]*A.i[22]-B.i[22]^2):
```

```
> BBar.i:=B.i[22]/(DD.i[22]*A.i[22]-B.i[22]^2):
> w.i:=s*C.i[2]+s^3*C.i[4]+C.i[1]+s^2*C.i[3]+1/24*p[0]*s^4*DBar.i:
>
v.i:=(2*s*C.i[3]+C.i[2]+3*s^2*C.i[4])*B.i[22]/A.i[22]+s*C.i[6]+C.i[5]+1/6*p[0]*
s^3*BBar.i:
> beta.i:=-C.i[2]-3*s^2*C.i[4]-2*s*C.i[3]-p[0]*s/A.i[44]-6*C.i[4]/(A.i[44]*DBar.i)-
p[0]*s^3/6*DBar.i:
```

Calculate epsilon and kappa. epsilon[2] is the s-direction in-plane strain at the mid-plane and epsilon[23] is the s,z shear strain, kappa is the curvature.

```
> epsilon.i[2]:=diff(v.i,s):
> epsilon.i[23]:=1/2*(beta.i+diff(w.i,s)):
> kappa.i[2]:=diff(beta.i,s):
```

Calculate the Moment resultants

```
> Moment.i[2]:=B.i[22]*epsilon.i[2]+DD.i[22]*kappa.i[2]:
```

Calculate Shear resultants

```
> Shear.i[23]:=A.i[44]*(beta.i+diff(w.i,s)):
> od:
```

Upper Curved Section

```
> for i from h1seg+1 to h1seg+c1seg do
```

Define Displacement functions

```
> theta:=(s-s.h1seg)/R:
```

positional angle in the curved section. s.hseg is the value of s at the end of the horizontal section.

```
> sigma.i:=DD.i[22]*A.i[22]+A.i[44]*R^2*A.i[22]+DD.i[22]*A.i[44]-
B.i[22]^2+2*B.i[22]*A.i[44]*R:
> DBar.i:=A.i[22]/(DD.i[22]*A.i[22]-B.i[22]^2):
> BBar.i:=B.i[22]/(DD.i[22]*A.i[22]-B.i[22]^2):
> w.i:=-B.i[22]*C.i[2]/(R*A.i[22])-C.i[2]+C.i[3]*sin(theta)-
C.i[4]*cos(theta)+(C.i[5]*sin(theta)-C.i[6]*cos(theta))*theta+(-1-
4*A.i[44]*B.i[22]^2/(A.i[22]*sigma.i)+2*DD.i[22]*A.i[44]/sigma.i+2*B.i[22]^3/(A.
i[22]*R*sigma.i)-2*B.i[22]*A.i[44]*DD.i[22]/(A.i[22]*R*sigma.i)-
2*B.i[22]*DD.i[22]/(R*sigma.i)+B.i[22]/(A.i[22]*R))*(C.i[6]*sin(theta)+C.i[5]*cos
(theta))+R^2*p[0]/A.i[22]+RHO*g*R^3*(theta^2*cos(theta)*((A.i[22]*DD.i[22]-
B.i[22]^2)/(8*A.i[44]*sigma.i)+(DD.i[22]+A.i[22]*R^2+2*B.i[22]*R)/(4*sigma.i)+(
4*A.i[44]*DD.i[22]*R*BBar.i+A.i[22]*A.i[44]*R^4*DBar.i+4*A.i[22]*A.i[44]*R^3
*BBar.i+2*A.i[44]*DD.i[22]*R^2*DBar.i+4*A.i[44]*B.i[22]*R^2*BBar.i+A.i[44]*
DD.i[22]^2*DBar.i/A.i[22])/(8*sigma.i))-cos(theta)*(3*(A.i[22]*DD.i[22]-
B.i[22]^2)/(4*A.i[44]*sigma.i)+(13*DD.i[22]+6*A.i[22]*R^2+19*B.i[22]*R)/(4*sig
ma.i)+(29*A.i[44]*DD.i[22]*R*BBar.i+3*A.i[22]*A.i[44]*R^4*DBar.i+15*A.i[22]
*A.i[44]*R^3*BBar.i+9*A.i[44]*DD.i[22]*R^2*DBar.i+22*A.i[44]*B.i[22]*R^2*B
Bar.i+10*A.i[44]*DD.i[22]^2*DBar.i/A.i[22])/(4*sigma.i))-
theta*sin(theta)*((A.i[22]*DD.i[22]-
B.i[22]^2)/(2*A.i[44]*sigma.i)+(3*DD.i[22]+2*A.i[22]*R^2+5*B.i[22]*R)/(2*sigm
```

```
a.i)+(7*A.i[44]*DD.i[22]*R*BBar.i+A.i[22]*A.i[44]*R^4*DBar.i+5*A.i[22]*A.i[44
]*R^3*BBar.i+3*A.i[44]*DD.i[22]*R^2*DBar.i+6*A.i[44]*B.i[22]*R^2*BBar.i+2*
A.i[44]*DD.i[22]^2*DBar.i/A.i[22])/(2*sigma.i))+1/A.i[22]):
>
v.i:=C.i[1]+theta*C.i[2]+cos(theta)*C.i[3]+sin(theta)*C.i[4]+cos(theta)*theta*C.i[
5]+sin(theta)*theta*C.i[6]-
RHO*g*R^3*(1/(8*A.i[44])+R*BBar.i/4+R^2*DBar.i/8+DD.i[22]/(8*(A.i[22]*DD.i
[22]-B.i[22]^2)))*(theta^2*sin(theta)+6*theta*cos(theta)-12*sin(theta)):
> beta.i:=-2*A.i[44]*(B.i[22]+A.i[22]*R)*(sin(theta)*C.i[5]-
cos(theta)*C.i[6])/sigma.i+(C.i[1]+theta*C.i[2])/R-
RHO*g*R^3/(4*sigma.i)*(2*theta*cos(theta)*(A.i[22]*R+B.i[22]+(A.i[44]*DD.i[22
]+3*R^2*A.i[22]*A.i[44]+2*R*A.i[44]*B.i[22])*BBar.i+(R^3*A.i[22]*A.i[44]+R*A
.i[44]*DD.i[22])*DBar.i)-
sin(theta)*(9*A.i[22]*R+9*B.i[22]+(9*A.i[44]*DD.i[22]+19*R^2*A.i[22]*A.i[44]+
14*R*A.i[44]*B.i[22])*BBar.i+(5*R^3*A.i[22]*A.i[44]+9*R*A.i[44]*DD.i[22])*D
Bar.i)):
```

Calculate epsilon and kappa

```
> epsilon.i[2]:=diff(v.i,s)+w.i/R:
> epsilon.i[23]:=1/2*(beta.i+diff(w.i,s)-v.i/R):
> kappa.i[2]:=diff(beta.i,s):
Calculate the Moment resultant
> Moment.i[2]:=B.i[22]*epsilon.i[2]+DD.i[22]*kappa.i[2]:
```

Calculate Shear resultant

```
> Shear.i[23]:=A.i[44]*(beta.i+diff(w.i,s)-v.i/R):
> od:
```

Vertical Section

```
> for i from h1seg+c1seg+1 to h1seg+c1seg+vseg do
```

Define Displacement functions

```
> sb:=s-s.(h1seg+c1seg):
> DBar.i:=A.i[22]/(DD.i[22]*A.i[22]-B.i[22]^2):
> BBar.i:=B.i[22]/(DD.i[22]*A.i[22]-B.i[22]^2):
> p[1]:=p[0]+RHO*g*inner_R:
>
w.i:=sb*C.i[2]+sb^3*C.i[4]+C.i[1]+sb^2*C.i[3]+sb^4*DBar.i*p[1]/24+RHO*g*sb
^5*DBar.i/120:
>
v.i:=(2*sb*C.i[3]+C.i[2]+3*sb^2*C.i[4])*B.i[22]/A.i[22]+sb*C.i[6]+C.i[5]+sb^3*
BBar.i*(RHO*g*sb+4*p[1])/24+RHO*g*sb^2*B.i[22]/(2*A.i[44]*A.i[22]):
> beta.i:=-C.i[2]-2*sb*C.i[3]-3*sb^2*C.i[4]-6*C.i[4]/(A.i[44]*DBar.i)-
p[1]*sb^3*DBar.i/6-p[1]*sb/A.i[44]-
RHO*g*(1/(A.i[44]^2*DBar.i)+sb^2/(2*A.i[44])+sb^4*DBar.i/24):
```

Calculate epsilon and kappa

```
> epsilon.i[2]:=diff(v.i,s):
> epsilon.i[23]:=1/2*(beta.i+diff(w.i,s)):
> kappa.i[2]:=diff(beta.i,s):
```

Calculate the Moment resultants

```
> Moment.i[2]:=B.i[22]*epsilon.i[2]+DD.i[22]*kappa.i[2]:
```

Calculate Shear resultants

```
> Shear.i[23]:=A.i[44]*(beta.i+diff(w.i,s)):
> od:
```

Lower Curved Section

```
> for i from h1seg+c1seg+vseg+1 to h1seg+c1seg+vseg+c2seg do
```

Define Displacement functions

```
> alpha:=(s-s.(h1seg+c1seg+vseg))/R:
```

positional angle in the curved section. s.hseg is the value of s at the end of the horizontal section.

```
> sigma.i:=DD.i[22]*A.i[22]+A.i[44]*R^2*A.i[22]+DD.i[22]*A.i[44]-
B.i[22]^2+2*B.i[22]*A.i[44]*R:
> DBar.i:=A.i[22]/(DD.i[22]*A.i[22]-B.i[22]^2):
> BBar.i:=B.i[22]/(DD.i[22]*A.i[22]-B.i[22]^2):
> p[2]:=p[0]+RHO*g*(inner_R+L[3]):
> w.i:=-B.i[22]*C.i[2]/(R*A.i[22])-C.i[2]+C.i[3]*sin(alpha)-
C.i[4]*cos(alpha)+(C.i[5]*sin(alpha)-C.i[6]*cos(alpha))*alpha+(-1-
4*A.i[44]*B.i[22]^2/(A.i[22]*sigma.i)+2*DD.i[22]*A.i[44]/sigma.i+2*B.i[22]^3/(A.
i[22]*R*sigma.i)-B.i[22]*A.i[44]*DD.i[22]/(A.i[22]*R*sigma.i)-
2*B.i[22]*DD.i[22]/(R*sigma.i)+2*B.i[22]/(A.i[22]*R))*(C.i[6]*sin(alpha)+C.i[5]*
cos(alpha))+R^2*p[2]/A.i[22]-
RHO*g*R^3*(alpha^2*sin(alpha)*((A.i[22]*DD.i[22]-
B.i[22]^2)/(8*A.i[44]*sigma.i)+(DD.i[22]+A.i[22]*R^2+2*B.i[22]*R)/(4*sigma.i)+(
4*A.i[44]*DD.i[22]*R*BBar.i+A.i[22]*A.i[44]*R^4*DBar.i+4*A.i[22]*A.i[44]*R^3
*BBar.i+2*A.i[44]*DD.i[22]*R^2*DBar.i+4*A.i[44]*B.i[22]*R^2*BBar.i+A.i[44]*
DD.i[22]^2*DBar.i/A.i[22])/(8*sigma.i))-sin(alpha)*(21*(A.i[22]*DD.i[22]-
B.i[22]^2)/(32*A.i[44]*sigma.i)+(98*DD.i[22]+42*A.i[22]*R^2+140*B.i[22]*R)/(3
2*sigma.i)+(220*A.i[44]*DD.i[22]*R*BBar.i+21*A.i[22]*A.i[44]*R^4*DBar.i+108
*A.i[22]*A.i[44]*R^3*BBar.i+66*A.i[44]*DD.i[22]*R^2*DBar.i+164*A.i[44]*B.i[2
2]*R^2*BBar.i+77*A.i[44]*DD.i[22]^2*DBar.i/A.i[22])/(32*sigma.i))+alpha*cos(al
pha)*((A.i[22]*DD.i[22]-
B.i[22]^2)/(2*A.i[44]*sigma.i)+(3*DD.i[22]+2*A.i[22]*R^2+5*B.i[22]*R)/(2*sigm
a.i)+(7*A.i[44]*DD.i[22]*R*BBar.i+A.i[22]*A.i[44]*R^4*DBar.i+5*A.i[22]*A.i[44
]*R^3*BBar.i+3*A.i[44]*DD.i[22]*R^2*DBar.i+6*A.i[44]*B.i[22]*R^2*BBar.i+2*
A.i[44]*DD.i[22]^2*DBar.i/A.i[22])/(2*sigma.i))):
>
v.i:=C.i[1]+alpha*C.i[2]+cos(alpha)*C.i[3]+sin(alpha)*C.i[4]+cos(alpha)*alpha*
C.i[5]+sin(alpha)*alpha*C.i[6]-
```

```
RHO*g*R^3*(1/(32*A.i[44])+R*BBar.i/16+R^2*DBar.i/32+DD.i[22]/(32*(A.i[22]*
DD.i[22]-B.i[22]^2)))*(4*alpha^2*cos(alpha)-24*alpha*sin(alpha)-45*cos(alpha)):
> beta.i:=-2*A.i[44]*(B.i[22]+A.i[22]*R)*(sin(alpha)*C.i[5]-
cos(alpha)*C.i[6])/sigma.i+(C.i[1]+alpha*C.i[2])/R+RHO*g*R^3/(4*sigma.i)*(2*al
pha*sin(alpha)*(A.i[22]*R+B.i[22]+(A.i[44]*DD.i[22]+3*R^2*A.i[22]*A.i[44]+2*
R*A.i[44]*B.i[22])*BBar.i+(R^3*A.i[22]*A.i[44]+R*A.i[44]*DD.i[22])*DBar.i)+co
s(alpha)*(9*A.i[22]*R+9*B.i[22]+(9*A.i[44]*DD.i[22]+19*R^2*A.i[22]*A.i[44]+1
4*R*A.i[44]*B.i[22])*BBar.i+(5*R^3*A.i[22]*A.i[44]+9*R*A.i[44]*DD.i[22])*DB
ar.i)):
```

Calculate epsilon and kappa

```
> epsilon.i[2]:=diff(v.i,s)+w.i/R:
> epsilon.i[23]:=1/2*(beta.i+diff(w.i,s)-v.i/R):
> kappa.i[2]:=diff(beta.i,s):
```

Calculate the Moment resultant

```
> Moment.i[2]:=B.i[22]*epsilon.i[2]+DD.i[22]*kappa.i[2]:
```

Calculate Shear resultant

```
> Shear.i[23]:=A.i[44]*(beta.i+diff(w.i,s)-v.i/R):
> od:
```

Lower Horizontal Section

```
> for i from h1seg+c1seg+vseg+c2seg+1 to nseg do
```

Define Displacement functions

```
> sd:=s-s.(h1seg+c1seg+vseg+c2seg):
> DBar.i:=A.i[22]/(DD.i[22]*A.i[22]-B.i[22]^2):
> BBar.i:=B.i[22]/(DD.i[22]*A.i[22]-B.i[22]^2):
> p[3]:=p[0]+RHO*g*(2*inner_R+L[3]):
> w.i:=sd*C.i[2]+sd^3*C.i[4]+C.i[1]+sd^2*C.i[3]+1/24*p[3]*sd^4*DBar.i:
>
v.i:=(2*sd*C.i[3]+C.i[2]+3*sd^2*C.i[4])*B.i[22]/A.i[22]+sd*C.i[6]+C.i[5]+1/6*p[
3]*sd^3*BBar.i:
> beta.i:=-C.i[2]-3*sd^2*C.i[4]-2*sd*C.i[3]-p[3]*sd/A.i[44]-
6*C.i[4]/(A.i[44]*DBar.i)-p[3]*sd^3/6*DBar.i:
```

Calculate epsilon and kappa. epsilon[2] is the s-direction in-plane strain at the mid-plane and epsilon[23] is the s,z shear strain, kappa is the curvature.

```
> epsilon.i[2]:=diff(v.i,s):
> epsilon.i[23]:=1/2*(beta.i+diff(w.i,s)):
> kappa.i[2]:=diff(beta.i,s):
```

Calculate the Moment resultants

```
> Moment.i[2]:=B.i[22]*epsilon.i[2]+DD.i[22]*kappa.i[2]:
```

Calculate Shear resultants

```
> Shear.i[23]:=A.i[44]*(beta.i+diff(w.i,s)):
> od:
```

For All Segments:

> *for i from 1 to nseg do*

Calculate the In-Plane resultants

> *In_plane.i[2]:=A.i[22]*epsilon.i[2]+B.i[22]*kappa.i[2]:*

> *In_plane.i[1]:=A.i[12]*epsilon.i[2]+B.i[12]*kappa.i[2]:*

Define equations for the face stresses (calculated at the distal surface of the face, i.e. max stress)

> *sigma_inner.i[2]:=Q[22][i,1]*(epsilon.i[2]+z.i[0]*kappa.i[2]):*

> *sigma_outer.i[2]:=Q[22][i,3]*(epsilon.i[2]+z.i[3]*kappa.i[2]):*

> *od:*

Boundary Conditions

Set the Boundary conditions

At s=0

shear force is zero at s=0 (due to symmetry)

> *BC1:=eval(Shear1[23],s=0)=0:*

beta is zero at left end

> *BC2:=eval(beta1,s=0)=0:*

in-plane displacement is zero at left end

> *BC3:=eval(v1,s=0)=0:*

At s=s.nseg

shear force is zero at s=L (due to symmetry)

> *BC4:=eval(Shear.nseg[23],s=s.nseg)=0:*

beta is zero at right end

> *BC5:=eval(beta.nseg,s=s.nseg)=0:*

in-plane displacement is zero at right end

BC6:=eval(v.nseg,s=s.nseg)=0:

At junctions

> *for i from 1 to nseg-1 do*

in-plane displacements match at junctions

> *BC.(6*(i-1)+7):=eval(v.i,s=s.i)=eval(v.(i+1),s=s.i):*

lateral displacements must match at junctions

> *BC.(6*(i-1)+8):=eval(w.i,s=s.i)=eval(w.(i+1),s=s.i):*

betas must match at junctions

> *BC.(6*(i-1)+9):=eval(beta.i,s=s.i)=eval(beta.(i+1),s=s.i):*

shear resultants must match at junctions

> *BC.(6*(i-1)+10):=eval(Shear.i[23],s=s.i)=eval(Shear.(i+1)[23],s=s.i):*

moments must match at junctions

> *BC.(6*(i-1)+11):=eval(Moment.i[2],s=s.i)=eval(Moment.(i+1)[2],s=s.i):*

resultants must match at junctions

```
> BC.(6*(i-1)+12):=evalf(eval(In_plane.i[2],s=s.i)=eval(In_plane.(i+1)[2],s=s.i)):
> od:
```

Combine Boundary Conditions and Unknown Constants in to sets

```
> Boundary:={BC.(1..(6*(nseg-2)+12))}:
> Const:={ }:
> for i from 1 to nseg do
> Const:=Const union {C.i[1],C.i[2],C.i[3],C.i[4],C.i[5],C.i[6]}:
> od:
```

Using the boundary conditions, solve for the unknown coefficients

```
> Csolution1:=fsolve(Boundary,Const):assign(Csolution1):
> indets(Csolution1):
```

Optimize Face and Core Thicknesses

```
> for i from 1 to nseg do
```

Find the maximum and minimum stresses in the faces for each segment.
If there is no sign change in the slope of the stress plot, the extrema will be at one of the ends.

```
>
inner_max[i,j]:=max(evalf(eval(sigma_inner.i[2],s=s.(i1))),evalf(eval(sigma_inner.i[
2],s=s.i)));
> inner_min[i,j]:=min(evalf(eval(sigma_inner.i[2],s=s.(i-
1))),evalf(eval(sigma_inner.i[2],s=s.i)));
> outer_max[i,j]:=max(evalf(eval(sigma_outer.i[2],s=s.(i-
1))),evalf(eval(sigma_outer.i[2],s=s.i)));
> outer_min[i,j]:=min(evalf(eval(sigma_outer.i[2],s=s.(i-
1))),evalf(eval(sigma_outer.i[2],s=s.i)));
```

If there is a sign change in the slope of the stress plot, the extrema will be at the point where the slope is zero.

```
> signchange_test_inner:=evalf(eval(diff(sigma_inner.i[2],s),s=s.(i-
1)+.00001)*eval(diff(sigma_inner.i[2],s),s=s.i-.00001)):
> if signchange_test_inner < 0 then
> critical_point_inner:=fsolve(diff(sigma_inner.i[2],s)=0,s, s.(i-1)..s.i):
> critical_value_inner:=evalf(eval(sigma_inner.i[2],s=critical_point_inner)):
> if critical_value_inner > inner_max[i,j] then
> inner_max[i,j]:=critical_value_inner:
> else inner_min[i,j]:=critical_value_inner: fi:
> fi:
> signchange_test_outer:=evalf(eval(diff(sigma_outer.i[2],s),s=s.(i-
1)+.00001)*eval(diff(sigma_outer.i[2],s),s=s.i-.00001)):
> if signchange_test_outer < 0 then
> critical_point_outer:=fsolve(diff(sigma_outer.i[2],s)=0,s, s.(i-1)..s.i):
> critical_value_outer:=evalf(eval(sigma_outer.i[2],s=critical_point_outer)):
```

```
> if critical_value_outer > outer_max[i,j] then
> outer_max[i,j]:=critical_value_outer:
> else outer_min[i,j]:=critical_value_outer: fi:
> fi:
```

Shear stress

```
> Shear_max[i,j]:=max(evalf(eval(abs(Shear.i[23]),s=s.(i-
1))),evalf(eval(abs(Shear.i[23]),s=s.i)));
```

Determine the critical stress that will induce face wrinkling.
(Hoff/Mautner equation)

```
> if face_wrinkle = "yes" then
> sigma_crit_inner.i:=-fw_const*(E[22][i,1]*E[22][i,2]*G[23][i,2])^(1/3):
> sigma_crit_outer.i:=-fw_const*(E[22][i,3]*E[22][i,2]*G[23][i,2])^(1/3):
> else
> sigma_crit_inner.i:=-10e+20:
> sigma_crit_outer.i:=-10e+20:
> fi:
```

Vary the face thicknesses to bring the stress up to the allowable level in both faces in each segment
Determine whether each face is in tension or compression and use the appropriate allowable stress.
If a face segment has tensile AND compressive stresses, determine the thickness to handle each and use the greater of the two

```
> if inner_min[i,j] > 0 then
> sigma_allow_inner[i]:=sigma_allow_tensile[2][i,1]:
> t1[i,j+1]:=t1[i,j]*inner_max[i,j]/sigma_allow_inner[i]:
> elif inner_max[i,j] < 0 then
> sigma_allow_inner[i]:=max(sigma_allow_compressive[2][i,1],sigma_crit_inner.i):
> t1[i,j+1]:=t1[i,j]*inner_min[i,j]/sigma_allow_inner[i]:
> else
> t1a:=t1[i,j]*inner_max[i,j]/sigma_allow_tensile[2][i,1]:
>
t1b:=t1[i,j]*inner_min[i,j]/max(sigma_allow_compressive[2][i,1],sigma_crit_inner.i)
:
> if t1a > t1b then t1[i,j+1]:=t1a:
sigma_allow_inner[i]:=sigma_allow_tensile[2][i,1]:
> else t1[i,j+1]:=t1b:
sigma_allow_inner[i]:=max(sigma_allow_compressive[2][i,1],sigma_crit_inner.i):
fi:
> fi:
>  if outer_min[i,j] > 0 then
> sigma_allow_outer[i]:=sigma_allow_tensile[2][i,3]:
> t3[i,j+1]:=t3[i,j]*outer_max[i,j]/sigma_allow_outer[i]:
```

```
> elif outer_max[i,j] < 0 then
> sigma_allow_outer[i]:=max(sigma_allow_compressive[2][i,3],sigma_crit_outer.i):
> t3[i,j+1]:=t3[i,j]*outer_min[i,j]/sigma_allow_outer[i]:
> else
> t3a:=t3[i,j]*outer_max[i,j]/sigma_allow_tensile[2][i,3]:
>
t3b:=t3[i,j]*outer_min[i,j]/max(sigma_allow_compressive[2][i,3],sigma_crit_outer.i)
:
> if t3a > t3b then t3[i,j+1]:=t3a:
sigma_allow_outer[i]:=sigma_allow_tensile[2][i,3]:
> else t3[i,j+1]:=t3b:
> sigma_allow_outer[i]:=max(sigma_allow_compressive[2][i,3],sigma_crit_outer.i):
fi:
> fi:
```

set a minimum allowable face thicknesses

```
> min_thickness:=0.0001:
> if t1[i,j+1] < min_thickness then t1[i,j+1]:=min_thickness: fi:
> if t3[i,j+1] < min_thickness then t3[i,j+1]:=min_thickness: fi:
```

If faces are not to be optimized, restore original thicknesses

```
> if opt_face <> "yes" then
> t1[i,j+1],t3[i,j+1]:=t1[i,j],t3[i,j]:
> fi:
> od:
```

end of i loop (iterate through all of the segments)

If properties are constant in s, set all face thicknesses to max value.

```
> if constant_face_properties="yes" and opt_face="yes" then
> t1max:=0:t3max:=0:
> for i from 1 to nseg do
> if t1[i,j+1] > t1max then t1max:=t1[i,j+1]: fi:
> if t3[i,j+1] > t3max then t3max:=t3[i,j+1]: fi:
> od:
> for i from 1 to nseg do
> t1[i,j+1]:=t1max:
> t3[i,j+1]:=t3max:
> od:
> fi: end of constant property case.
```

End face optimization procedure

Core optimization

```
> for i from 1 to nseg do
> if opt_core="yes" then
```

set a minimum allowable core thickness - this is determined by the max allowable core shear stress

```
> h_min:=Shear_max[i,j]/sigma_allow_shear[i,2]-(t1[i,j+1]+t3[i,j+1])/2:
```

determine the optimum core thickness for the lowest weight

```
> if opt_face = "yes" then
```

Determine the optimal core thickness if the faces will also be optimized.

```
> Fa:=evalf(eval(Moment.i[2]/rho.i.2*(rho.i.3/sigma_allow_outer[i]-
rho.i.1/sigma_allow_inner[i]),s=s.(i-1))):
> Fb:=evalf(eval(Moment.i[2]/rho.i.2*(rho.i.3/sigma_allow_outer[i]-
rho.i.1/sigma_allow_inner[i]),s=s.i)):
> if Fa > Fb then
> if Fa > 0 then opt_h:=sqrt(Fa): else opt_h:=0: fi:
> else
> if Fb > 0 then opt_h:=sqrt(Fb): else opt_h:=0: fi:
> fi:
> hc[i,j+1]:=max(opt_h,h_min):
> else
```

Determine the optimal core thickness if the faces will not be changed. (the thinner, the lighter)

```
> hc[i,j+1]:=evalf(max(eval(-Moment.i[2]/(t1[i,j]*sigma_allow_inner[i]-
In_plane.i[2]/2),s=s.(i-1)),eval(-Moment.i[2]/(t1[i,j]*sigma_allow_inner[i]-
In_plane.i[2]/2),s=s.i),eval(Moment.i[2]/(t3[i,j]*sigma_allow_outer[i]-
In_plane.i[2]/2),s=s.(i-1)),eval(Moment.i[2]/(t3[i,j]*sigma_allow_outer[i]-
In_plane.i[2]/2),s=s.i),h_min)):
> fi:
> else
> hc[i,j+1]:=hc[i,j]:
> fi:
> od:
```

end of i loop (iterate through all of the segments)

If properties are constant in s, set all core thicknesses to max value.

```
> if constant_core_properties="yes" and opt_core="yes" then
> hmax:=0:
> for i from 1 to nseg do
> if hc[i,j+1] > hmax then hmax:=hc[i,j+1]:
> fi:
> od:
> for i from 1 to nseg do
> hc[i,j+1]:=hmax:
> od:
> fi:
```

end of constant property case

End of core optimization procedure

```
> od:  end of j loop (optimization loop)
>
W:=evalf(eval((L[1]*(t_i[1]*rho11+h[1]*rho12+t_o[1]*rho13)+L[2]*(t_i[2]*rho21
+h[1]*rho22+t_o[2]*rho23)+L[3]*(t_i[3]*rho31+h[1]*rho32+t_o[3]*rho33)+L[4]
*(t_i[4]*rho41+h[1]*rho42+t_o[4]*rho43)+L[5]*(t_i[5]*rho51+h[1]*rho52+t_o[5
]*rho53))*2)):
> A:=evalf(eval((L[1]*L[3]+inner_R*(L[1]+L[3]+L[5])+inner_R^2*Pi/2)*2)):
> Ratio:=A/W:
> print("t_i = ",t_i[1],"hc = ",h[1],"t_o = ", t_o[1],"W = ",W,"A =",A, "Ratio
=",Ratio);
```

Save updated Geometric data
record the last values for the optimized thicknesses for later use

```
> save h1seg, c1seg, vseg, c2seg, h2seg, pressure, R, Angle, hLengths, vLengths, t_o,
t_i, h, outerface_material, core_material, innerface_material, output_data_file:
```

Plots

All plots are over one half of the complete cross section, i.e. right half.

Calculate functions for plotting

```
> with(plots):
```

Combined functions for the stresses, displacements, strains and resultants

```
> facestress_inner:=sigma_inner1[2]*(1-Heaviside(s-s1)):
> facestress_outer:=sigma_outer1[2]*(1-Heaviside(s-s1)):
> w:=w1*(1-Heaviside(s-s1)):
> v:=v1*(1-Heaviside(s-s1)):
>
CoreMaxShearStress1:=Shear1[23]/DD1[22]*E[22][1,1]*t_i[1]*E[22][1,3]*t_o[1]
*(h[1]+t_i[1]/2+t_o[1]/2)/(E[22][1,1]*t_i[1]+E[22][1,3]*t_o[1])*(1-Heaviside(s-
s1)):
> CoreMaxShearStress2:=Shear1[23]/(h[1]+t_i[1]/2+t_o[1]/2)*(1-Heaviside(s-s1)):
Sigma_wrinkle_i/o stresses calculated using the Hoff equation
> sigma_wrinkle_i:=-fw_const*(E[22][1,1]*E[22][1,2]*G[23][1,2])^(1/3)*(1-
Heaviside(s-s1)):
> sigma_wrinkle_o:=-fw_const*(E[22][1,3]*E[22][1,2]*G[23][1,2])^(1/3)*(1-
Heaviside(s-s1)):
Sigma_wrinkle_i/o stresses  calculated using the Heath equation
> sigma_wrinkle_i:=-
sqrt(2/3*t_i[1]/h[1]*E[22][1,2]*sqrt(E[11][1,1]*E[22][1,1])/(1-
nu[12][1,1]*nu[21][1,1]))*(1-Heaviside(s-s1)):
> sigma_wrinkle_o:=-
sqrt(2/3*t_o[1]/h[1]*E[22][1,2]*sqrt(E[11][1,3]*E[22][1,3])/(1-
nu[12][1,3]*nu[21][1,3]))*(1-Heaviside(s-s1)):
> stresslimit_comp_inner:=sigma_allow_compressive[2][1,1]*(1-Heaviside(s-s1)):
```

```
> stresslimit_tens_inner:=sigma_allow_tensile[2][1,1]*(1-Heaviside(s-s1)):
> stresslimit_comp_outer:=sigma_allow_compressive[2][1,3]*(1-Heaviside(s-s1)):
> stresslimit_tens_outer:=sigma_allow_tensile[2][1,3]*(1-Heaviside(s-s1)):
> stresslimit_shear_core:=sigma_allow_shear[1,2]*(1-Heaviside(s-s1)):
> epsilon[2]:=epsilon1[2]*(1-Heaviside(s-s1)):
> Moment[2]:=Moment1[2]*(1-Heaviside(s-s1)):
> Shear[23]:=Shear1[23]*(1-Heaviside(s-s1)):
> In_plane[2]:=In_plane1[2]*(1-Heaviside(s-s1)):
> iface:=-(h[1]/2+t_i[1])*(1-Heaviside(s-s1)):oface:=(h[1]/2+t_o[1])*(1-
Heaviside(s-s1)):
> coretop:=h[1]/2*(1-Heaviside(s-s1)):corebottom:=-(h[1]/2)*(1-Heaviside(s-s1)):
> for i from 2 to nseg do
> facestress_inner:=facestress_inner+sigma_inner.i[2]*Heaviside(s-s.(i-1))*(1-
Heaviside(s-s.i)):
> facestress_outer:=facestress_outer+sigma_outer.i[2]*Heaviside(s-s.(i-1))*(1-
Heaviside(s-s.i)):
> w:=w+w.i*Heaviside(s-s.(i-1))*(1-Heaviside(s-s.i)):
> v:=v+v.i*Heaviside(s-s.(i-1))*(1-Heaviside(s-s.i)):
>
CoreMaxShearStress1:=CoreMaxShearStress1+Shear.i[23]/DD.i[22]*E[22][i,1]*t_i
[i]*E[22][i,3]*t_o[i]*(h[i]+t_i[i]/2+t_o[i]/2)/(E[22][i,1]*t_i[i]+E[22][i,3]*t_o[i])*
Heaviside(s-s.(i-1))*(1-Heaviside(s-s.i)):
>
CoreMaxShearStress2:=CoreMaxShearStress2+Shear.i[23]/(h[i]+t_i[i]/2+t_o[i]/2)*
Heaviside(s-s.(i-1))*(1-Heaviside(s-s.i)):
```

Using the Hoff equation

```
> sigma_wrinkle_i:=sigma_wrinkle_i-
fw_const*(E[22][i,1]*E[22][i,2]*G[23][i,2])^(1/3)*Heaviside(s-s.(i-1))*(1-
Heaviside(s-s.i)):
> sigma_wrinkle_o:=sigma_wrinkle_o-
fw_const*(E[22][i,3]*E[22][i,2]*G[23][i,2])^(1/3)*Heaviside(s-s.(i-1))*(1-
Heaviside(s-s.i)):
>
stresslimit_comp_inner:=stresslimit_comp_inner+sigma_allow_compressive[2][i,1]*
Heaviside(s-s.(i-1))*(1-Heaviside(s-s.i)):
>
stresslimit_tens_inner:=stresslimit_tens_inner+sigma_allow_tensile[2][i,1]*Heavisid
e(s-s.(i-1))*(1-Heaviside(s-s.i)):
>
stresslimit_comp_outer:=stresslimit_comp_outer+sigma_allow_compressive[2][i,3]*
Heaviside(s-s.(i-1))*(1-Heaviside(s-s.i)):
```

```
>
stresslimit_tens_outer:=stresslimit_tens_outer+sigma_allow_tensile[2][i,3]*Heavisid
e(s-s.(i-1))*(1-Heaviside(s-s.i)):
>
stresslimit_shear_core:=stresslimit_shear_core+sigma_allow_shear[i,2]*Heaviside(s
-s.(i-1))*(1-Heaviside(s-s.i)):
> epsilon[2]:=epsilon[2]+epsilon.i[2]*Heaviside(s-s.(i-1))*(1-Heaviside(s-s.i)):
> Moment[2]:=Moment[2]+Moment.i[2]*Heaviside(s-s.(i-1))*(1-Heaviside(s-s.i)):
> Shear[23]:=Shear[23]+Shear.i[23]*Heaviside(s-s.(i-1))*(1-Heaviside(s-s.i)):
> In_plane[2]:=In_plane[2]+In_plane.i[2]*Heaviside(s-s.(i-1))*(1-Heaviside(s-s.i)):
> oface:=oface+(h[i]/2+t_o[i])*Heaviside(s-s.(i-1))*(1-Heaviside(s-s.i)):
> iface:=iface-(h[i]/2+t_i[i])*Heaviside(s-s.(i-1))*(1-Heaviside(s-s.i)):
> coretop:=coretop+h[i]/2*Heaviside(s-s.(i-1))*(1-Heaviside(s-s.i)):
> corebottom:=corebottom-(h[i]/2)*Heaviside(s-s.(i-1))*(1-Heaviside(s-s.i)):
> od:
```

Develop Plots

```
> Digits:=10:
> CoreShearplot:=plot([CoreMaxShearStress2],s=0..s.nseg,title="Core Shear",
color=[black], titlefont=[TIMES,ROMAN,12], numpoints=300):
> wrinkleplot:=plot([sigma_wrinkle_i*Heaviside(-
facestress_inner),sigma_wrinkle_o*Heaviside(-facestress_outer)],s=0..s.nseg,
color=[grey,pink],numpoints=200):
> wplot:=plot(w,s=0..s.nseg, color=[black], title="Lateral
Deflection",titlefont=[TIMES,ROMAN,12], numpoints=100):
> vplot:=plot(v,s=0..s.nseg, title="In-Plane Displacement",
titlefont=[TIMES,ROMAN,12], numpoints=50):
> eplot:=plot(epsilon[2],s=0..s.nseg, title="In-Plane Strain",
titlefont=[TIMES,ROMAN,12], numpoints=50):
> Nplot:=plot(In_plane[2],s=0..s.nseg, title="In-Plane
Resultant",titlefont=[TIMES,ROMAN,12], numpoints=50):
> Mplot:=plot(Moment[2],s=0..s.nseg, color=[black],title="Bending Moment
Resultant", titlefont=[TIMES,ROMAN,12], numpoints=100):
> Qplot:=plot(Shear[23],s=0..s.nseg, title="Shear Resultant",
titlefont=[TIMES,ROMAN,12], numpoints=100):
> Stress_Plot:=plot([facestress_outer,facestress_inner], s=0..s.nseg, title="Face
Stress", linestyle=[1,1], color=[black,blue], titlefont=[TIMES,ROMAN,12],
numpoints=300):
>
stresslimit_plot:=plot([stresslimit_comp_inner,stresslimit_tens_inner,stresslimit_com
p_outer,stresslimit_tens_outer],s=0..s.nseg,linestyle=[3,3,3,3],color=[grey,grey,grey,
grey]):
```

```
> shearlimit_plot:=plot([stresslimit_shear_core,-
stresslimit_shear_core],s=0..s.nseg,linestyle=[3,3],color=[grey,grey]):
>
> Profile:=plot([iface,corebottom,coretop,oface], s=0..s.nseg, linestyle=[1,1,1,1],
color=[blue,black,black,red], title="Sandwich Profile",
titlefont=[TIMES,ROMAN,12], numpoints=300):
> Profile2:=plot([iface-corebottom,oface-coretop], s=0..s.nseg, linestyle=[1,1],
color=[blue,red], title="Face Thickness Profile", titlefont=[TIMES,ROMAN,12],
numpoints=400):
Markers at the junctions between segments
> jmark:={}:
> for i from 1 to nseg-1 do
> jmark:=jmark union {[s.i,0,"I"]};
> od:
> junctions:=textplot(jmark,color=black,font=[TIMES,ROMAN,12]):
```

Profile 2 shows just the faces with the core removed, Profile shows the whole sandwich

```
> display([Profile2,junctions]);
> display([Profile,junctions]);
> display([wplot,junctions],font=[TIMES,ROMAN,16]);
>
display([Stress_Plot,junctions,wrinkleplot,stresslimit_plot],font=[TIMES,ROMAN,16]
);
> display([CoreShearplot,junctions,shearlimit_plot],font=[TIMES,ROMAN,16]);
> display([Qplot,junctions]);
> display([Mplot,junctions],font=[TIMES,ROMAN,16]);
> display([eplot,junctions]);
> display([vplot,junctions]);
> display([Nplot,junctions]);
```

Delaware Center for Transportation University of Delaware Newark, Delaware 19716

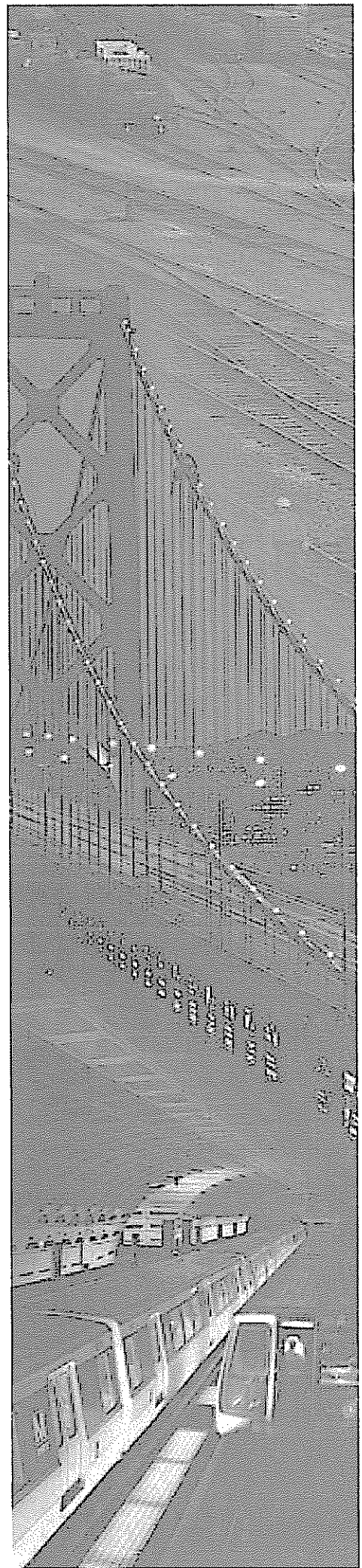

AN EQUAL OPPORTUNITY/AFFIRMATIVE ACTION EMPLOYER

To the extent permitted by applicable State and Federal laws, the University of Delaware is committed to assuring equal opportunity to all persons and does not discriminate on the basis of race, creed, color, sex, age, religion, national origin, veteran or handicapped status, or gender identity and expression, or sexual orientation in its educational programs, activities, admissions, or employment practices as required by Title IX of the Educational Amendments of 1972, Section 504 of the Rehabilitation Act of 1973, Title VII of the Civil Rights Act of 1964, and other applicable statutes. The University of Delaware has designated Karen Mancini, Director of the Office of Disabilities Support Services, as its ADA/Section 504 Coordinator under Federal law. Inquiries concerning Americans with Disabilities Act compliance, Section 504 compliance, campus accessibility, and related issues should be referred to Karen Mancini (302-831-4643) in the Office of Disabilities Support Services. Inquiries concerning Title VII and Title IX compliance and related issues should be referred to the Director of the Office of Equity and Inclusion, Becki Fogerty (302-831-8063).